A Noble Approach for Noise Removal from Brain Image using Region Filling

Daizy Deb[1] ,Bahnishikha Dutta[2], Sudipta Roy[3]
[1,2,3]Department of Information Technology,Assam University, Silchar,Assam, India
[1]daizydeb@rediffmail.com[2]Bahnishikha.dutta@yahoo.com

Abstract — **In today's world, one of the reason in rise of mortality among the people is brain cancer. Brain tumour is the main cause of brain cancer. A tumour can be defined as any mass caused by abnormal or uncontrolled growth of cells. This mass of tumour grows within the skull, due to which normal brain activity is hampered. Which is if not detected in earlier stage, can take away the person's life. Hence, it is very important to detect the brain tumour as early as possible. For detection of brain tumour, first we have to read the MRI image of brain and then we can apply segmentation on the image. But in the MRI brain image, some confidential information of patient's is always there. To apply segmentation, this unnecessary information has to be removed, as it can be considered as noise. Here we present an efficient method for removing noise from the MRI image of brain using Region Filling method.**

Keywords — Brain tumour; Noise; Filtering; Region of Interest; Region Filling.

I. INTRODUCTION

Brain cancer is one of the leading causes of death in the world now days. An uncontrolled growth of cancer cells in the brain leads to brain cancer, which is a very serious type of malignancy. A malignant brain tumour is the main cause of brain cancer. All brain tumours are not malignant, some are benign also. Brain cancer is also called glioma and meningioma [1].

According to the National Brain Tumour Society, US, over 600,000 people are living with the primary brain tumour. Among these 600,000 people, 28,000 are children under the age of 20. Metastatic brain tumours (cancer that spreads from other parts of the body to the brain) are the most common type of brain tumour, which is the reason of cancer for 20% to 40% of persons. Over 7% of all the primary brain tumours reported in the United States are diagnosed among children under the age of 20. 210,000 people in the United States are diagnosed with a primary or metastatic brain tumour every year i.e. over 575 people a day.

In general, the risk of developing a malignant CNS or brain tumour over the course of one's lifetime is less than 1%. But the risk increases with the age. 4.5 per 100,000 persons under the age of 20 will be diagnosed with a malignant brain tumour. After the age of 75, this rate rises to 57 per 100,000 persons. Among the people over the age of85, the risk stops increasing. The risk for developing brain cancer is very high among the people with a family history of brain cancer and those who had radiation therapy of the head.

II. RELATED WORKS IN NOISE REMOVAL

T. Logeswari and M. Karnan [1] applied weighted median filter for removing the noise presented in the MRI image of the brain. Weighted median filter is a type of nonlinear filters. It retains the robustness and edge preserving capacity of the image. Dr. Samir Kumar Bandyopadhyay [3] removed noise based on Maximum Difference Threshold value, which is constant threshold value determined by observation. Pratibha Sharma and co-authors [4] applied spatial noise filter for removing noise from the MRI image of a brain. Sudipta Roy, Samir K. Bandyopadhyay [5] first used high pass filter and then finally used median filter for removing noise. Here a high pass filter is used in matlab, by which each pixel of the image is replaced by weighted average of the surrounding pixels. Then merging of gray scale image and filtered image is done for enhancing the image quality. Median filter is applied to the enhanced image. High pass filter is used by Rajesh C. Patil, Dr. A. S. Bhalchandra [6] for removing noise and then they applied median filter to enhance the quality of the image.

Noise removal has to be done in such a way that it should not affect the portion of the brain in the image as each portion is the most important part to detect the tumour. Hence noise removal should not blur the image.

III. NOISE AND MEDICAL IMAGE

"Noise" originally means "unwanted signal" i.e. noise represents unwanted information which deteriorates image quality. The process which affects the acquired image and is not part of the scene can be defined as noise. A random variation of brightness or color information in images can also be termed as noise [10].

Noise can be produced by the sensor and circuitry of a scanner or digital camera. The acquisition process for digital images converts optical signals into electrical signals and then into digital signals and is one of the processes by which the noise is introduced in digital images. Each step in the conversion process experiences fluctuations, caused by natural phenomena, and each of these steps adds a random value to the resulting intensity of a given pixel.

MRI scan image of a brain usually contains the patient's information. This image also contains the information about the institute where this test was done and the machine used. All these information are required to identify the patient and institute, but this information are not helpful to detect the

ISBN No. 978-1-4799-3914-5/14/$31.00 ©2014 IEEE

presence of tumour in the brain. So these are unwanted information which can be termed as noise. For further processing of detecting the tumour, this noise needs to be removed.

IV. NOISE REMOVAL USING FILTERING

To modify an image in some way which includes blurring, deblurring, locating certain features within an image etc. filtering is used. A filter is basically an algorithm for modifying a pixel value, over original value of the pixel and the values of the pixels surrounding it. There are literally hundreds of types of filters that are used in image processing. Among all the filtering techniques, common ones are:

- Gaussian Filter or Gaussian smoothing
- Mean Filter
- Median Filter

Blurring an image using Gaussian function can be known as **Gaussian Filter** or **Gaussian Smoothing**. It is a widely used effect to reduce image noise and reduce details.[11].

A **Mean Filter** is a filter that takes the average of the current pixel and its neighbors. The average of intensity values in a m x n region of each pixel (usually m = n) is taken. In mean filter average (mean) of all the pixel values in the window replace the center values in the window.

Median Filters are some nonlinear neighborhood operations that can be performed for the purpose of noise reduction that can do a better job of preserving edges than simple smoothing filters. A median filter is almost similar to an averaging filter. The averaging filter examines the pixel of the required area and its neighbor's pixel values and returns the mean of these pixel values and the median filter looks at this same neighborhood of pixels, but returns the median value. Thus noise can be removed, without blurring the edges much.[5]

V. REGION FILLING METHOD

Sometimes it is required to process a single sub region of an image, leaving other regions unchanged. This is commonly referred to as region-of-interest (ROI) processing. Many operations that support an ROI can execute considerably faster when the ROI is used to define a region that is much smaller than the full image. ROI is completely random i.e. it may be defined by any set of image pixels. In particular, the ROI does not have to be rectangular or connected. It may consist of one or more separate regions.

A process that fills a region of interest (ROI) by interposing the pixel values from the boundaries of the region is known as Region Filling. This process can be used to make objects in an image seem to evaporate as they are replaced with values that blend in with the background area.

Filling of a region is useful for removal of superfluous facts or substances of a binary image. Region filling can be performed using an interpolation method based on Laplace's equation which results in the smoothest possible fill specified the values on the boundary of the region.

VI. PROPOSED METHOD

These are the following steps involve for the region filling process:

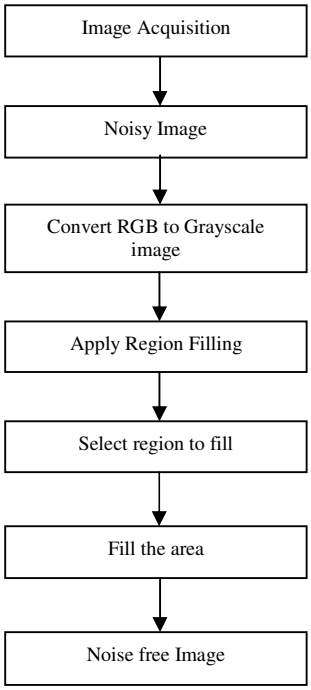

Fig 6.2: Flow of the proposed method

The action of retrieving an image from some source, usually a hardware based source is known as image acquisition [2]. In image acquisition the image can be passed through whatever processes need to modify it or to collect the extract information from it. Here images are obtained from MRI Scan of brain. Different formats like jpg, png etc. are used for storing the digital images obtained from MRI of a brain. These images are stored in matrix form in matlab. MRI Scan images may be in RGB form. In that case, we have to convert this RGB images into grayscale (a grayscale or a grayscale digital image is an image in which the value of each pixel is a single sample, that is, it carries only intensity information) images.After converting RGB image to grayscale image, region filling will be applied on the grayscale image. Here we have to select the area for applying region filling.

After selecting the desired area, the region filling technique is applied for eliminating the noise or for removal of the entire artifact from the image.

Fig 6.1 (a): Grayscale image of MRI of a brain

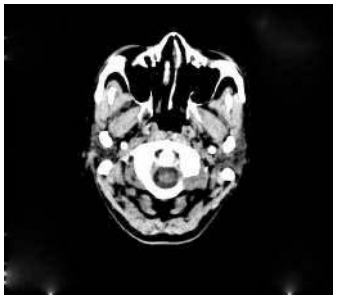

Fig 6.1 (b): Image after applying region filling

This can be passed through any other required process. The output of region filling is shown in fig 7.2. Here with this method noise is removing completely without affecting other portion of image.

VII. RESULT ANALYSIS

Different filtering viz Gaussian filter, Averaging filter, Median filter can be applied to a gray scale image of MRI. Results of different filtering are as follows:

Fig 7.1 (a): Gaussian filter

We can see that Gaussian filter and averaging filter cannot remove the noise from the image whereas median filter removes the noise partially but not completely. Median filter also blurrs the image.

Fig 7.1 (b): Averaging filter

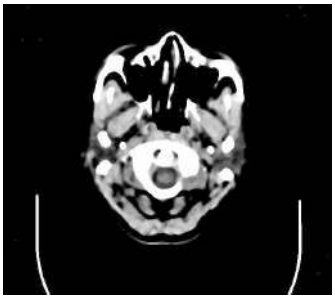

Fig 7.1 (c): Median filter

Median filtering can almost remove noise from the MRI image. With the removing of noise, this technique blurs the main brain image. Due to this, after removing noise, brain image becomes blurs, for which further processing may hamper.

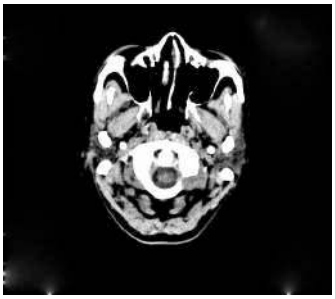

Fig 7.2: Region filling

We need a method which can remove the noise without effecting the main portion of the brain image. Now we will apply region filling method. The above figure 7.2 shown after applying the region filing technique. Histogram of the images can be used to show the improvement between the original image, median filtered image and image after applying region filling. From the above analysis it can be seen that, region filling method is more precise for removing noise from an MRI image of a brain. Modification of the image after applying region filling can be shown by the histogram of the image before and after filling.

Histograms of the different images are given below:

a. Histogram of the original image

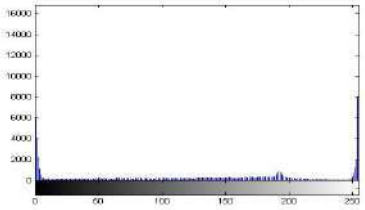

Fig 7.3(a): Histogram of the original image

b. Histogram of the image after applying region filling

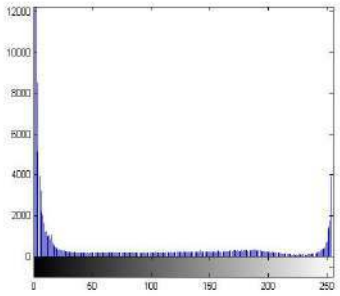

Fig 7.3(b): Histogram of the image after applying region filling

The improvement of the image after applying region filling can be seen in Fig 7.3(a) and Fig 7.3(b). The horizontal axis of both the graphs represents the tonal variation, while the number of pixels in that particular tone is represented by the vertical axis of the graph. The left side of the horizontal axis represents the black and dark areas, the middle represents medium grey and the right hand side represents light and pure white areas. The vertical axis represents the size of the area that is captured in each one of these zones.

VIII. CONCLUSION

Noise removal is one of the very important step for detecting brain tumour. For this reason, noise removal should be precise. Filtering may remove the noise from the image, but it also blurs the portion of the brain in the image. Region filling can do the work pleasantly without affecting the portion of the brain in the image. When the noise is removed from the MRI image, we can proceed further for the detection of the tumor in the brain. For applying this method, the selection of region of interest should be accurate. So selection of region should be done carefully. The only flaw of this method is that, it requires user interaction, which consists of determining the Region of Interest. The time required for applying this method is little more than that required for the filtering. In future, the time constraint should be improved for this method.

REFERENCES

[1] T. Logeswari and M. Karnan, "An improved implementation of brain tumour detection using segmentation based on soft computing", Journal of Cancer Research and Experimental Oncology Vol. 2(1), March, 2010.

[2] Nagalkar V.J., Asole S.S., "Brain tumour detection using digital image processing based on soft computing", Journal of Signal and Image Processing, Volume 3, Issue 3, 2012.

[3] Dr. Samir Kumar Bandyopadhyay,"Detection of Brain Tumour – A Proposed Method", Journal of Global Research in Computer Science, Vol. 2, No. 1, January 2011.

[4] Pratibha Sharma, Manoj Diwakar, Sangam Choudhary, "Application of Edge Detection for Brain Tumour Detection", International Journal of Computer Application, Vol. 58 – No. 16, November 2012.

[5] Sudipta Roy, Samir K. Bandyopadhyay, "Detection and Quantification of Brain Tumour from MRI of Brain and it's Symmetric Analysis", International Journal of Information and Communication Technology Research, Volume 2 No. 6, June 2012.

[6] Rajesh C. Patil, Dr. A. S. Bhalchandra, "Brain Tumour Extraction from MRI Images Using MATLAB", International Journal of Electronics, Communication & Soft Computing Science and Engineering ISSN: 2277-9477, Volume 2, Issue 1.

[7] McAndrew, Alasdair. "An introduction to digital image processing with matlab notes for SCM2511 image processing." School of Computer Science and Mathematics, Victoria University of Technology (2004).

[8] Tarun Kumar and Karun Verma, "A Theory Based on Conversion of RGB image to Gray image", International Journal of Computer Applications (0975 – 8887), Volume 7– No.2, September 2010.

[9] Rafael C. Gonzalez and Richard E. Woods, "Digital Image Processing", Second Edition.

[10] Zakia, Richard Donald, and Leslie D. Stroebel, eds, "The Focal Encyclopedia of Photography", Focal Press, 1995.

[11] Shapiro, L. G., and G. C. Stockman. "Computer Vision. chap. 12." New Jersey*: P* rentice Hall (2001).

[12] Priyanka, Balwinder Singh. "A Review on Brain Tumor Detection using Segmentation." (2013).

[13] Patil, Dinesh D., and Sonal G. Deore. "Medical Image Segmentation: A Review." International Journal Computer Science and Mobile Computing 2, no. 1 (2013): 22-27.

[14] Yasmin, Mussarat, et al. "Brain image enhancement-A survey." World Applied Sciences Journal 17.9 (2012): 1192-1204.

[15] Gerig, Guido, et al. "Nonlinear anisotropic filtering of MRI data." Medical Imaging, IEEE Transactions on 11.2 (1992): 221-232.

[16] Gonzalez, Rafael C., Richard Eugene Woods, and Steven L. Eddins. "Digital image processing using MATLAB". Pearson Education India, 2004.

[17] SELEȚCHI, Emilia Dana. "Medical Image Processing using MATLAB." Journal of Information Systems & Operations Management 2.1 (2008): 194-210.

A New Approach to Overcome the Weakness in DVR Protocol Based on Component Neigbhourin MANET

Mrinal Kanti Deb Barma
Department of Computer Science & Engineering
National Institute of Technology Agartala
Tripura 799055, India
e-mail: mrinal@nita.ac.in

Jhunu Debbarma
Department of Computer Science & Engineering
Tripura Institute of Technology Agartala
Tripura 799055, India
e-mail: jhunudb@gmail.com

S. K. Sen
Department of Computer Science & Engineering,
Guru Nanak Institute of Technology, Kolkata 700114
India
e-mail: santanu.sen@ieee.org

Sudipta Roy
Department of Information Technology
Assam University
Silchar 788011, India
e-mail: sudipta.it@gmail.com

Abstract— By using the distance vector routing (DVR) protocols, each router over internetwork send the neighbouring routers, the information about destination that it knows how to reach and maintains a list of all destinations that only contains the cost of getting to that destination, and the next node to send the messages to. Thus, the source node only knows to which node to hand the packet, which in turn knows the next node (Next hop). This approach has an advantage of massively reduced storage costs compared to link-state algorithms. DVR algorithms are easier to implement and required less amount of required storage space and the actual determination of the route is based on the Bellman-Ford algorithm. Our objective was primarily intended to remove the weaknesses inherent in the widely used DVR algorithm, based on the well-known Bellman-Ford shortest path algorithm. In this paper, we introduce a new technique to solve the weakness in DVR named as component based neighbour routing that uses to create the distance vector routing table that would be truly dynamic, robust and free from the various limitations that have been discussed.

Keywords: Distance Vector Routing, Special Neighbours, Single-Connected Neighbour (SCN) Multi-Connected Neighbour (MCN).

I. INTRODUCTION

A Mobile Ad-hoc network is a collection of mobile devices denoted as nodes, which can communicate between themselves using wireless links without the need or intervention of any infrastructure like base stations, access points etc [1][2][3]. A node in a MANET, which is equipped with a wireless transmitter and receiver (transceiver) and is powered by a battery, plays the dual role of a host and a router as well. Two nodes willing to communicate with each other need to be either in the direct common range of each other or should be assisted by other nodes acting as routers to carry forward the packets from a defined source to a destination in the best possible routing path [3][4].

Internet Engineering Task Force (IETF) activity has standardized several routing protocols for MANET. Routing protocols are the backbone to provide efficient services in MANET, in terms of performance and reliability. Designing routing protocol in MANET is quite difficult and tricky compared to that of any classic or non-ad hoc (formal) network due to some inherent limitations of the MANET like dynamic nature of network topology, limited bandwidth, asymmetric links, scalability, mobility of nodes limited battery power and alike. Moreover, the intrinsic nature of the nodes to move freely and independently in any arbitrary direction by potentially changing ones link to other's on a regular basis, is really an exigent concern while designing the desired routing algorithm. MANET is IP based and the nodes have to be configured with a free IP address not only to send and receive messages, but also to act as router to forward traffic to some destination unrelated to its own use.

The main challenge to setup a MANET is that each node has to maintain the information required to route traffic properly and thus designing a routing protocol for MANET have several difficulties. Firstly, MANET has a dynamically changing topology as the nodes are mobile. However, this behavior favors routing protocols that dynamically discover routes e.g. Dynamic Source Routing [5], TORA [6], Associativity Based Routing (ABR) [7] etc.) over conventional distance vector routing protocols [5][6][8]. Secondly, the fact that MANET lacks any structure and thus makes IP subnetting inefficient. Thirdly, limitation of battery power and power depletion of nodes due to large number of messages passed during cluster formation. Links in mobile networks could be asymmetric at times. If a routing protocol relies only on bi-directional links, the size and connectivity of the network may be severely limited; in other words, a protocol that makes use of unidirectional links can significantly reduce network partitions and improve routing performance.

Distance Vector Routing Protocol (DVRP)[10,13] is one of two major routing protocols for communications approach that use packets which are sent over IP [14]. DVRP required routing how to report the distance of various nodes within a network or IP topology in order to determine the best and most efficient route for packets. DVRP is a dynamic,

978-0-7695-5075-6/14 $26.00 © 2014 IEEE

distributed, asynchronous and iterative routing protocol where the routing tables are continuously updated with the information received from the neighbouring routers [13, 14] and operates by having each node j maintains a routing table, which contains a set of distance or cost $\{D_{ji}(x)\}$, where i is the neighbour of j. Where neighbour j treats the neighbour k as the next hop for data packet destined for node x, if D_{jk}=mid i{(D_{ji})}

The routing table gives the shortest path to each destination and which route to get update and to keep the distance set in the table updated, each router exchanges routing table (RT) with all its neighbours periodically.

There are few drawbacks in distance vector routing as follows:

A. Slow convergence: When there is an increase in the cost of any link or there is a link failure between two neighbouring nodes in a network or internetwork, the algorithm, in the worst case, may require an excessive number of iterations to converge or to terminate. In a network with quickly changing topology, this can lead to situations where the link states have changed before an optimum route has been setup.

B. Count to infinity: The DVR does not work well if there are topological changes in the network. This is primarily due to the fact that the distance vector sent to the neighbours does not contain sufficient information about the topology of the internetwork. As stated earlier, though considerably simple and elegant in concept, the DVR suffers not only from the problem of slow convergence but also from the more serious problem of CTI which sometimes occurs following a link or router failure, due to unending routing loops involving two or more routers. The essence of the problem is that if a node B tells the node A that it has a route to the destination, node A does not know if that route contains node A (which would make it a loop).

There are various proposed methods to overcome this drawback of DVR protocol. However, all of the proposed methods are designed based on the topology of the network. This statistic results is not absolutely solving of the problem for any arbitrary network topology and most of the proposed methods increase the complexity/computation of the routing algorithms.

II. PROPOSED METHOD

In order to find the single connected neighbour (SCN) in a node in the network graph it has to be a degree 1, i.e., a router which is connected only to a single router, is called a Single-Connected Neighbour (SCN) of the sole router to which it is connected. The sole router recognizes its SCN as a Pendant Node (PN) in the network, Multi-Connected Neighbour is a neighbour which is not a SCN, is a Multi-Connected Neighbour (MCN) of each of its neighbouring routers. Multi-connected component Neighbour by Co-neighbour (MCNbCN) is a special kind of MCCN. MCNbCN detection subroutine is used by a router R_j for identifying its neighbour R_k as belonging to out of the following three other special neighbour categories.

(i) For detecting whether the neighbour R_k is SCN of R_j.

(ii) For detecting whether the neighbour R_k is a MCN of R_j

(iii) For detecting whether the neighbour R_k is a MCNbCN for R_j.

The characteristics for a neighbour R_k of R_j to become an SCN, MCN, or a MCNbCN of R_j, The composite subroutine SCN_MCN_MCNbCN detection has been developed in such a way that it is totally by itself, capable of identifying a neighbour R_k as belonging to one of the three SCN_MCN_MCNbCN detection algorithm is given in Figure 1.

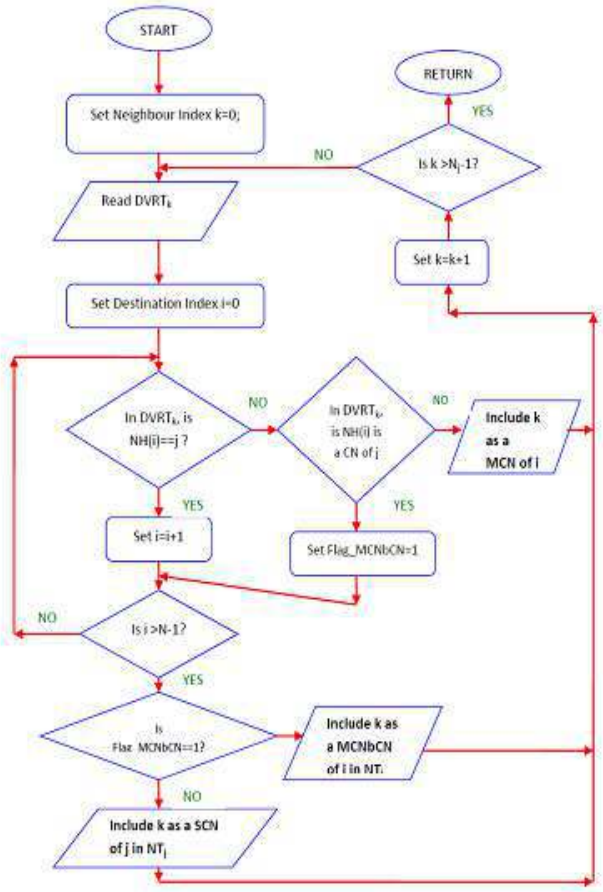

Figure 1: Flowchart of SCN_MCN_MCNbCN_Detection for Router j

III. SCN_MCN_MCNBCN_DETECTION ALGORITHM

In a N-node network, a router R_j having a set of neighbours S_{nj} containing N_j neighbours, may, at view the entire network around itself (excluding itself) as being composed of at most N_j "components", based on its current routing strategy via the N_j neighbours (N_j is total number of neighbour of j). All nodes contained within the particular component C_{jk} are reached by R_j via its all neighbouring router $R_k \in C_{jk}$, $R_k \in S_{nj}$. In other words, the set of nodes contained within the component C_{jk} may be viewed as a subset $S_N(j,k) \in S_N$ of nodes (destinations) that R_j reaches

via its neighbour R_k, ($R_k \in S_{nj}$, $R_k \in S_N(j,k)$), (S_N is set of all nodes in the network and S_{nj} is set of all neighbour of j) including R_k itself. The component C_{jk} must contain at least 2 nodes including R_k itself which will be called a component neighbour of R_j. Obviously; this implies that a component neighbour of R_j must act as the forwarding neighbour (FN) of at least one remote node of R_j. For example, the routers R_k (neighbouring router of j or R_j) and R_n are the component neighbours of the router R_j in Figure 2. The 12-node network shows that, based upon shortest path routing with hop count used as the metric, for simplicity, D creates for its three neighbours, B, G and J, their respective components, namely, C_{DB},C_{DG} and C_{DJ} or that is, the neighbours are given, for each destination, instead of just the estimated distance, the "route" which, besides the distance, provides the next-hop information for reaching that destination.

The next-hop information is vital to the neighbours in selecting alternative routes in case of loss of an existing route, and, especially, to avoid routing loops. The most important among them is the key concept of categorization, by each router, of its neighbouring routers as belonging to one or more categories of special neighbours [16]. With the help of the special neighbours, a router dynamically monitors its neighbours and maintains its current knowledge about neighbourhood. The router utilizes this current knowledge to get advantage in dealing with link or router failures and increases or decreases of link delays, (i) Single-Connected Neighbour or SCN (the router is its sole neighbour), (ii) Multi-Connected Neighbour or MCN (it has other neighbours besides the router), (iii) MCN-by-CN or MCNbCN (a special type of MCN which is connected only to the router and one more of its CNs). (iv) Single Connected Component Neighbour or SCCN (all routers in the component called the Single Connected Component SCC, are connected to the router by a single path that passes via the sole link connecting the SCCN with the router) (v) Multi-Connected Component Neighbour or MCCN (all routers in the entire component, called the MCC, are connected to the router by multiple paths including the one which passes via the link (vi) MCCN-by-CN or MCCNbCN (it is a special type of MCCN) where all routers in the component are connected to the router by multiple paths which all pass via the MCCNbCN of the router but, additionally, the MCCNbCN is directly connected to only the router and to one or more of its CNs, besides the neighbouring routers inside the component.

The concept of the component, namely, Single Connected Component (SCC) and Multi-connected Cop (MCC), along with the concept of the corresponding component neighbours, namely, the SCC Neighbour (SCCN), the MCC Neighbour (MCC) and the MCC Neighbour-by-Co-Neighbour (MCCNbCN) and the method of their detection or identification and utilization by any router were presented. It was shown that a router R_j creates a component against each neighbour R_k that acts as the FN of the router R_j for at least one remote (non-neighbour) destination.

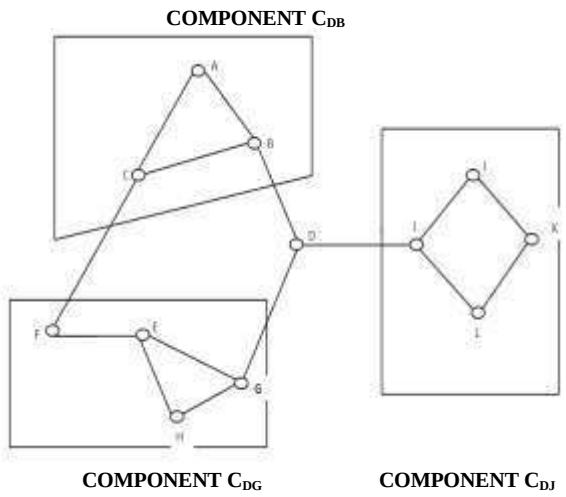

Figure 2 View of the router D of the 12-node network as a set of 3 components, namely, C_{DB}={A, B, C}, C_{DG}={E, F, G, H} and C_{DJ} = { I, J, K, L }, respectively based around its three neighbours B, G and J.

TABLE I. NT_j showing three Component Neighbours based on its three neighbours B, G and J.

Components	Neighbours	SCC	MCC	MCCN
C_{DB}	{A, B, C}	0	D	D
C_{DG}	{E, F, G, H}	0	D	D
C_{DJ}	{ I, J, K, L }	D	0	0

In figure 2, we have three components namely $C_{DB,}$ C_{DG} and C_{DJ} from which C_{DJ} is a SCC of D and, accordingly, J is a SCCN of D. C_{DB} and C_{DG} are MCCs of D so that B and G are MCCNs of D.

TABLE II. DVRTs of router B, G, J and D (a) $DVRT_B$ (b) $DVRT_G$ (c) $DVRT_J$ (d) $DVRT_D$

Dest	NH	Dest	NH	Dest	NH	Dest	NH
A	A	A	D	A	D	A	B
B	-	B	D	B	D	B	B
C	C	C	D	C	D	C	B
D	D	D	D	D	D	D	-
E	C	E	E	E	E	E	G
F	C	F	E	F	E	F	G
G	D	G	-	G	-	G	G
H	D	H	H	H	H	H	G
I	D	I	D	I	D	I	J
J	D	J	D	J	D	J	J
K	D	K	D	K	D	K	J
L	D	L	D	L	D	L	J

Knowledge about SCC and concerned SCCN is utilized by a router R_j in a similar but much more powerful manner than the utilization of the knowledge about an SCN or PN. If R_j ever observes that its (direct) communication with an SCCN has failed (because either the sole connecting link to the SCCN or the SCCN itself has failed), R_j recognizes that

the entire set of routers in the SCC (including the SCCN) has become unreachable and hence has become a Lost Destination Group (LDG). Accordingly, it sets in $DVRT_j$ the distance to all these routers, including the SCCN, as permanent infinity (PMI) and thus advertises the entire set of these routers as LDs, i.e., permanently unreachable. Thereafter, it ignores all subsequent advertisements from all its other neighbours about any possible shorter length (i.e., a finite length) path to reach any of these routers, until it itself discovers that its own direct communication with the SCCN (and hence, hopefully with all the routers in the SCC) has been restored.

In order to find MCCN R_k helps a router R_j in the following three important ways, unless the MCCN R_k is an MCCNbCN.

1) If a link failure occurs between R_j and R_k, R_j is sure that it must have at least one alternative path to reach all the routers in the MCC, unlike as the case of SCC.

2) If the node R_k itself fails, R_j can still reach all the other nodes belonging to the MCC C_{jk} through alternative routes.

3) Even if the MCCN R_k itself fails but R_j has at least one CN for R_k then R_j itself can detect the failure of R_k and use D_{jk}=PMI, so that the network will converge fast.

TABLE III. NTj showing Component Neighbours

Nbr	SCC	MCN	MCNbCN	SCCN	MCCN	C_{DB},C_{DG}, C_{DJ}
B	0	D	0	0	0	
G	0	D	0	0	0	(A, B, C}
J	D	D	D	0	0	{E, F, G, H}
D	J	0	0	J	B,G	{ I, J, K,
L	0	0	0	0	0	L }

In table III, where Nbr represents as neighbour, SCC is single connected component, SCCN is single connected component neighbour, MCN is multi connected component, MCCN is multi connected component neighbour, MCNbCN is Multi-Connected Component Neighbour by co-neighbour.

IV. CONCLUSION

In this paper, we introduced a new method to solve weakness in DVR protocol. This model concludes the existence of link failure thus, it is evident from the above arguments and algorithm that in all of the above possible cases, a router j will always be able to detect whether any of its neighbours is an SCCN or an MCCN or a MCNbCN. Simulation experiment can be done for the above method. Thus our future work is to simulate the proposed methodology and will try to find more efficient, robust, dynamic algorithm as a solution to the scenarios of the component based component neighbours around its neighbours. Our present work is only on DVR based component neighbouring approach in MANET.

REFERENCES

[1] Albeto Leon-Garcia and Indra Widjaja, Communication Networks, Tata McGraw Hill, 2000

[2] M. Abolhasan et al. " A review of routing protocols for mobile ad hoc networks" Elsevier Ad Hoc networks 2 1-22 (2004)

[3] M. Gerla, C.C Chiang, and l. Zhang, "Tree Maulticast Strategies in Mobile, Multihop Wireless Networks," ACM/Baltzer Mobile Networks and Apps. J,. 1988

[4] S. Singh, M. Woo, and C. S. Raghavendra, "Power-Aware Routing in Mobile Ad Hoc Networks," Proc. ACM/IEEE MOBICOM '98, Oct. 1998.

[5] Y. B. Ko and N. H. Vaidya, "Location-Aided Routing (LAR) in Mobile Ad Hoc Networks," Proc. ACM/IEEE MOBICOM '98, Oct. 1998.

[6] S. Das, C. Perkins, E. Royer, "Ad hoc on demand distance vector (AODV) routing, Internet Draft", draft-ietf-manetaodv-11.txt, work in progress, 2002.

[7] G. Finn. "Routing and addressing problems in large metropolitan-scale internetworks", ISI Research Report ISU/RR-87-180, March, 1987.

[8] H. Takagi and L. Kleinrock "Optimal Transmission Ranges for Randomly Distributed Packet Radio Terminals" IEEE Transactions on Communications, Vol.Com-32, No.3, March

[9] M. Abolhasan et al. "A Review of Routing Protocols for Mobile Ad Hoc Networks" Elsevier Ad Hoc Networks 2 (2004) 1-22

[10] A. S. Tanenbaum, "Computer Networks", 3rd Ed., PHI, 2000

[11] M. Golestanian, R. Ghazizzadeh "A New approch to overcome thecount to infinity problem in DVR protocol based on HMM Modelling" Journal of Information System and Telecommunication,Vol 1, No. 4 December 2013.

[12] S. Basagni, I. Chlamtac, V. Syrotiuk, and B. Woodward. "A Distance Routing Effect Algorithm for Mobility (DREAM)" Proceedings of the Fourth Annual ACM/IEEE International Conference on Mobile Computing and Networking (MobiCom'98), Dallas, Texas, USA, August 1998.

[13] M. K. Debbarma, S. K. Sen, Sudipta Roy. "A Review of DVR-based Routing Protocols for Mobile Ad Hoc Networks" International Journal of Computer Applications (0975 – 8887) Volume 58– No.3, November 2012.

[14] S. K. Ray, J. Kumar, S. K. Sen and J. Nath, "Modified Distance Vector Routing Scheme for a MANET", Proc. of the 13th National Conference on Communications (NCC) held at IIT, Kanpur during Jan 26-28, 2007, pp. 197-201.

[15] M. K. Debbarma, S. K. Sen, Sudipta Roy "DVR-based MANET Routing Protocols Taxonomy" International Journal of Computer Science & Engineering Survey (IJCSES) Vol.3, No.5, October 2012.

[16] M. K. Debbarma, Jhunu Debbarma, S. K. Sen, Sudipta Roy "A DVR-based Routing Protocol with Special Neighbours for Mobile Ad-Hoc Networks", IEEE International Symposium on Computational and Business Intelligence (ISCBI 2013), August 24-25, New Delhi, PP-235-238 .

2014 Sixth International Conference on Computational Intelligence and Communication Networks

A New Approach for Gateway Level Load Balancing of WMNs through k-means Clustering

Banani Das[1], Amit Kumar Roy[2], Ajoy Kumar Khan[3] & Sudipta Roy[4]

Department of Information Technology
Assam University, Silchar
India
E-mail: {[1]banani.das.bd, [2]amitkroy12, [3]ajoyiitg, [4]sudipta.it} @gmail.com

Abstract— **Wireless mesh network (WMN) has emerged as a key technology because of their advantages over other wireless networks. Due to the dynamic infrastructure, the traffic volume of the WMN goes in an increasing order, thus balancing the load of the network becomes very crucial. Hence the problem of load balancing is addressed in this paper and for which the cluster based architecture of WMN is considered. In this architecture, a network is subdivided into clusters and each cluster contains a cluster head. Now the problem is also subdivided into the load balancing within each cluster, which is the responsibility of the cluster head. An appropriate selection of a cluster head is very important as it performs a vital role in increasing the network performance. The paper proposes a clustering method based on k-means approach to divide the network into k clusters to manage the load in small scale and hence to reduce the overall load of WMNs. The proposed approach works at the gateway level. The simulation results show that the performance of the WMNs is improved with the proposed clustering method.**

Keywords- Wireless Mesh Networks (WMNs); Load Balancing; Internet Gateways (IGWs); Clustering; k-means.

I. INTRODUCTION

In today's era, Wireless Mesh Networking (WMN) has been found to be the most advantageous one. WMNs are dynamically self-organized and self-configured, maintaining the mesh connectivity throughout the network by automatic configuration of an ad hoc network. WMN [1] is a communication network made up of radio nodes organized in a mesh topology and is a packet-switched network with a static wireless backbone. The topology of wireless backbone is fixed and modifications to infrastructure can only result from addition or removal or failure of access points. WMN consists of wireless access and wireless backbone network, in contrast to any other wireless networks. It is dynamically also self-healing, easily maintainable, highly scalable and reliable. It is also anticipated to resolve the limitations and to significantly improve the performance of other wireless networks.

The architecture of WMN [2] is composed of three different network elements: (i) Network Gateways (NG) (ii) Access Points (AP) or Mesh Routers (MR) and (iii) Mobile Nodes (MN). A typical WMN can have a hierarchical structure of three levels of these network elements. At the top level, there are the internet gateway (IGW) nodes that are directly connected to the wired network. The second level of hierarchy consists of nodes called APs or MRs that forward each other's traffic in multi-hop fashion towards the IGW. These MRs form the backbone of a WMN and are relatively static. The lowest level of hierarchy is the Mobile Clients or Nodes or the end users connected to the MRs for accessing the wired network services.

Usually, most of the traffic in WMNs is oriented towards the Internet [3], which increases the traffic load on certain paths leading towards the IGW. As the IGWs are responsible for forwarding all the network traffic, they are likely to become potential bottlenecks in WMNs. The high concentration of traffic at a gateway leads to saturation which in turn can result in packet drops due to potential buffer overflows. The packet dropping at the IGWs is not desirable and it makes WMN inefficient because already it had consumed a lot of network resources en route from source to the IGW. Thus, to overcome congestion, the traffic load has to be balanced over different IGWs [4].

The term load balancing refers to optimization of usage of network resources by transferring traffic from congested links to less loaded parts of the network based on knowledge of network state. In a WMN, load balancing is the best approach to increase network throughput and to reduce congestion [5].

Though the load balancing in WMN is critical issue but it is an important concern to utilize the network capacity efficiently [6]. The effects of unbalanced load include gateway loading, center loading, and the formation of bottleneck node. As the gateway nodes connect the WMN to the external Internet, the traffic aggregation at the gateway nodes creates load imbalance at certain gateways which in turn results in congestion and packet loss. Also the backhaul connection to the external network may

978-1-4799-6929-6/14 $31.00 © 2014 IEEE
DOI 10.1109/CICN.2014.118

become bandwidth constrained. Hence, load balancing across gateways in a WMN is important to improve the bandwidth utilization and network scalability.

The remaining sections of the paper are organized as follows: in section II, a brief description about gateway level load balancing for WMN is discussed along with its requirement. The clustering technique for load balancing of WMNs is discussed thoroughly in section III. Section IV shows the proposed work based on k-means clustering for load balancing in WMN, Section V shows the results of the proposed work and section VI concludes the discussion.

II. Gateway Level Load Balancing In WMNs

Gateway nodes are the heart of the WMN as they connect the WMNs to wired networks [3]. Therefore, all the traffics are aggregated at gateway nodes. Due to bandwidth constraint of the gateway, the capacity of the WMNs is limited. In addition to this, the gateway node consumes high energy as it forwards large number of packets which leads to quicker failure of the gateway. Therefore, gateway load balancing assumes significance in order to achieve the following goals [3]:

- *Efficient traffic allocation*
- *Efficient use of backhaul links*
- *Maximal use of network capacity*
- *Minimizing the resource consumption at the gateway nodes*
- *To counter the effects of traffic imbalance due to node mobility*

In a WMN, wireless backbone is formed by IGWs which allows the mesh clients to access the Internet. As all the traffic is forwarded towards this gateway, traffic congestion may easily occur at the gateway which leads to performance degradation of WMN. Load balancing helps to reduce the traffic congestion between IGWs and improve the network performance and provide a better quality of service *(QoS)*. Gateways route internal traffic to external networks. Gateways have some limited capacity as a result when number of requests to gateway increases then it can't service all requests punctually. Thus, load balancing is needed to decrease workload of gateways. Balancing of load between gateways is important to avoid over-utilized and under-utilized regions. There are many factors that can easily cause load imbalance, such as heterogeneous traffic demands, time-varying traffic and uneven number of nodes served by gateways. This can lead to inefficient use of network capacity, throughput degradation and unfairness between flows in different domains. On the other hand, arbitrary load-balancing can hurt performance.

III. Clustering

In cluster based system, [7], [8] WMNs are partitioned into number of clusters by grouping the nodes in the network. After clustering, the cluster head is selected based on *G_value* known as gateway value within each cluster which acts as the Gateway connected to the wired networks while the rest of the nodes become ordinary node. Clustering reduces the workload of the gateway nodes by reducing the number of nodes connected to cluster head or gateway. The cluster head coordinates the transmissions of packets or traffic within the cluster and may also exchange data to the neighboring nodes. Till now several techniques have been employed for clustering the WMNs like Greedy algorithm [9], position-based approaches, Load-balanced approaches and Interference-based approaches [10], [11].

IV. Load Balancing Based On K-Means Algorithm

The k-means approach divides the mesh network into k clusters, where k is the number of clusters decided by the user and thus performs the load balancing at IGWs to gain better network performance and providing a better quality of service *(QoS)* by reducing the traffic congestion at the gateways [12]. After clustering, the cluster head is chosen on the basis of *G_value, which* is calculated by the Eqn. (1). The *G_value* has been chosen to select the most appropriate gateway as the cluster head based on some important parameters, which reflects the status of the network with respect to that gateway.

The parameters have been discussed in detail in the following section. This research work considers the limit of gateway head as queue length of the gateway.

Proposed K-Means Clustering Algorithm:

Step 1: Consider a WMN consisting of few gateways, which are labeled as G1, G2, etc. and the rest are simple routers or nodes as in Figure 1.

Step 2: Arbitrarily choose k (the mean) gateways from the network as the initial cluster centers or mean. Initially the value of k is selected based on the average queue length of the gateways.

Say if k=2, then partition the network into two clusters based on the mean.

Step 3: Assign or reassign each nodes to the newly formed clusters based on the mean value of the nodes in the cluster as shown in Figure 2.

Step 4: Calculate the *G-value* of all the available gateways within each cluster. And then select the cluster head based on the highest *G-value*.

$$G - value = \frac{Power_{Supply} * Power_{CPU} * D_{From\_Centre} * C * T\_QL}{V + |QueueLength_{Avg} - QueueLength_{value}|} \quad \ldots (1)$$

- $Power_{supply}$: It refers to the energy that is accommodated to the nodes. Therefore, node with highest energy is suitable to be chosen as GW as it consumes more energy during traffic consumption and have longer lifetime as compared to other nodes.
- *Velocity(V):* Nodes with lower velocity has less mobility. Hence, it will have lesser chance to move away from the cluster and being suitable to be chosen as a GW.
- *Constancy (C):* Node constancy includes the time that a node exists in the cluster. Therefore, node that has longer lifetime is of more constancy and more suitable for being GW.
- $Distance_{From\_centre}$ *(D):* To select the shortest path for optimal routing, mostly all the nodes forward the traffic through the central of the node which results in early congestion and packet drops. Therefore, it is suitable to select the GW that is suited at the boundary of the cluster.
- $Power_{CPU}$*:* A node with high processing power has the capability to do quick computation. Therefore, it is more suitable to choose a node as a GW with high processing power.
- *T_QL (Total_QueueLength)*: Total queue capacity of the gateway.
- $QueueLength_{Avg}$: Average queue length of the gateway.
- $QueueLength_{value:}$ Preset service requests that are available in the gateway's queue.

Step 5: When the cluster heads G4 and G5 exceed their limit for accepting the further service requests, then update the cluster mean and continue the process from step 1. And this process will continue till the gateway heads of clusters are not exceeding their limits.

Step 6: Continue the process whenever the gateway, cluster head exceeds its limit.

Advantages of the proposed k-Means Clustering Algorithm:

- High intra-cluster similarity.
- All nodes are aware of each other within the cluster.
- Make the resulting *k* clusters as compact and separate as possible.
- All the nodes are close to each other within a cluster leads to power efficiency and simple routing.
- Minimize the path cost.
- Saves a time against selecting a new cluster head for new cluster.
- Minimize the number of nodes connected to a cluster head within a cluster.
- Minimize the traffic forwarded towards the cluster head (a gateway).

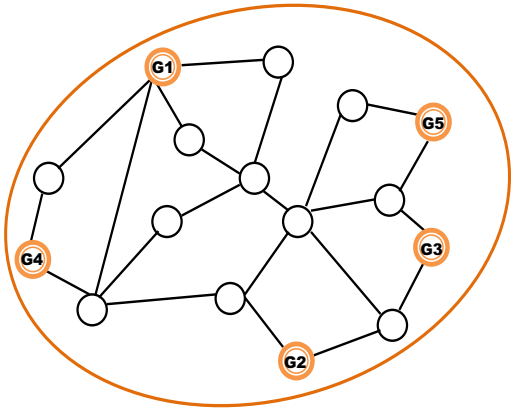

Figure 1. A Simple WMN before clustering

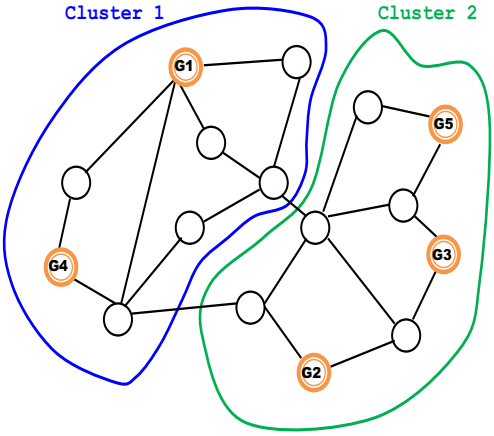

Figure 2. WMN after k-means clustering

V. Experimental Results

A. Experimental Model Setup

This section describes the implementation of the proposed k-means clustering algorithm and also analyzes the results of the experiments. The proposed algorithm is simulated with NS2 with the parameters listed in Table 1. The simulation results have been analyzed with four different performance metrics. The experiment has been designed by varying the total number of nodes and holding all other parameters constant to compare with respect to the different performance metrics. The results of the proposed method, i.e. WMN with k-means clustering approach, have been compared with the simple WMN scenario, i.e. WMN without cluster.

TABLE I: EXPERIMENTAL MODEL SETUP

Parameter	Values
Simulator	NS 2.34
Traffic Type	CBR/TCP
Simulation Area	1000X1000m
MAC Layer Protocol	802.11
# No. of Nodes	12,18, 24
Simulation Time	150 sec
Routing Protocol	AODV
Node Placement	Randomly

B. Performance Metrics

To evaluate the performance of the proposed algorithm some standard performance metrics are chosen so that with the help of these results the proposed algorithm could be compared with the existing algorithms. The four most important and common performance metrics have been chosen for performance evaluation of the algorithm and these are as follows:

Average End-to-End Delay: It refers to the time taken for a packet to be transmitted across a network from source to destination.

Throughput: This performance metric measure the rate of information transfer. They are all measured in bytes/ bits per second. It is the rate of successful message delivery over a communication channel.

Packet Drop: Packet loss occur when a router receive the packet and specifically decides not to pass it onto. This deliberates loss of a packet is called as packet dropping.

Packet delivery rate: The ratio of the number of data packets delivered and total data packets sent to the destination. This illustrates the level of delivered data to the destination in the next hop.

C. Result & Discussion

The results generated from the different performance metrics after implementing k-means clustering method in the WMN scenario are compared with the simple WMN scenario. The results are represented in the Figures 3 to 6. The comparison has been made with respect to the above mentioned four performance metrics and it is clearly visible that while k-means clustering method is applied to WMN, it gives better result in comparison to that of a simple WMN scenario.

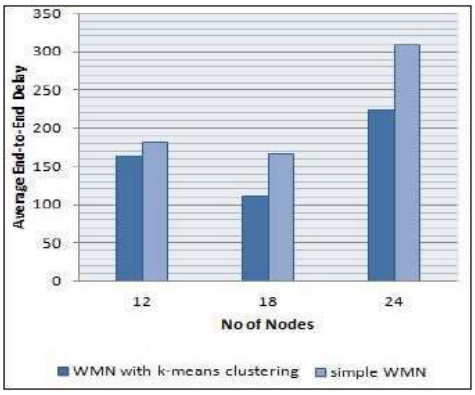

Figure 3. Average End-to-End Delay

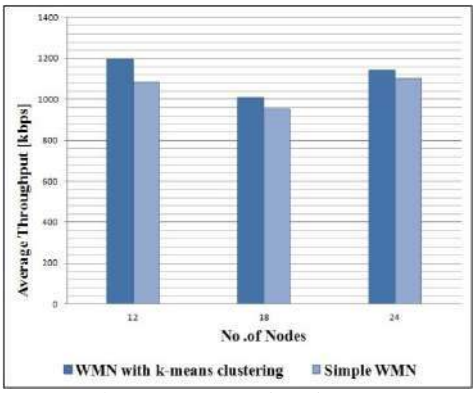

Figure 4. Average Throughput

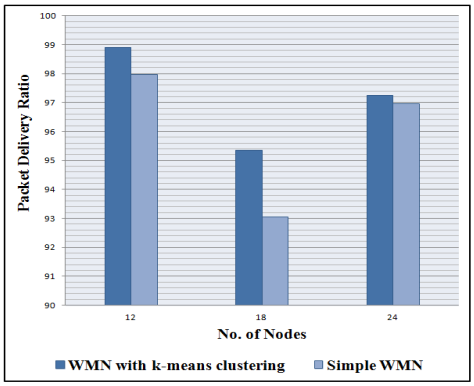

Figure 5. Packet Delivery Ratio

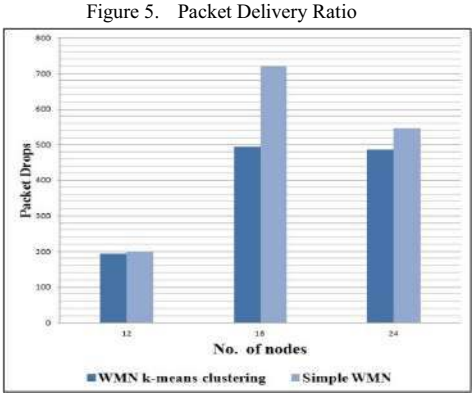

Figure 6. Packet Drop

VI. CONCLUSION

The internet gateways play an important role in WMNs. And the limited capacity of the gateway forbids it from handling a large amount of traffic and making load balancing a crucial factor to improve the network performance. A new approach to reduce the overall workload of the gateways by distributing the overall workload into a number of clusters throughout the whole network is proposed based on the k-means clustering approach to do the job of load balancing. The simulation results confirm that by introducing the k-means clustering approach the performance of WMNs has increased in different aspects.

REFERENCES

[1] I. F. Akyildiz, X. Wang, "A survey on wireless mesh networks," IEEE Radio Communications, pp. S23-S30, September 2005.

[2] I. F. Akyildiz, X. Wang, W. Wang, "Wireless mesh networks: a survey," Computer Networks, Science Direct, Elsevier, pp. 445-487, June 2005.

[3] Abhishek Majumder, Sudipta Roy, Kishore Kumar Dhar, "Design and Analysis of an Adaptive Mobility Management Scheme for Handling Internet Traffic in Wireless Mesh Network", International Conference on Microelectronics, Communication and Renewable Energy (ICMiCR 2013), pp. 1-6, June, 2013.

[4] Yan Zhang, Jijun Luo, Honglin Hu, "Wireless mesh network. architecture, protocols and standards," Auerbach Publications, 2007.

[5] Banani Das, Sudipta Roy, "Load balancing techniques for wireless mesh networks: a survey," IEEE International Symposium on Computational and Business Intelligence (ISCBI 2013), pp. 247-253, August 24-26, 2013, New Delhi, India.

[6] Sudip Misra, Subhas Chandra Misra, Isaac Woungang, "Guide to wireless mesh networks," Springer-Verlag London Limited, 2009.

[7] Yan Zhang, Jijun Luo, Honglin Hu, "Wireless Mesh Network. Architecture, Protocols and Standards", Auerbach Publications, 2007.

[8] Tomas Johansson and Lenka Carr-Motyˇckov´, "On Clustering in Ad Hoc Networks," Division of Computer Science and Networking Lulea University of Technology, August 17, 2003.

[9] Feng Zeng and Zhigang Chen, "Load Balancing placements of gateways in Wireless mesh networks with QoS constraints", Young Computer Scientists. 2002. ICYCS 2008. The 9th International Conference for IEEE, 2008.

[10] Waharte, Sonia, Raouf Boutaba, and Pascal Anelli, "Impact of Gateways Placement on Clustering Algorithms in Wireless Mesh Networks", ICC.2001.

[11] Mohammad Shahverdy, Misagh Behnami, Mohmood Fathy, "A new paradigm for load balancing in WMNs," in International Journal of Computer Networks (IJCN), 3(4), pp.239-224, 2011.

[12] D. Chakraborty, M. K. Debbarma and Sudipta Roy, "QoS Provisioning in WMNs: Challenges and a Comparative Study of Efficient Methodologies", International Journal of Computer Application (IJCA), 65(3), pp.24-27, March 2013.

A Tree Based Mobility Management Scheme for Wireless Mesh Network

Abhishek Majumder[1], Sudipta Roy[2]
[1]Department of Computer Science & Engineering
Tripura University, Suryamaninagar
[2]Department of Information Technology
Assam University, Silchar

***Abstract*- The importance of wireless mesh network is increasing day by day with the popularity of hand held devices. But like other wireless networks, one major problem of wireless mesh network is maintenance of network connectivity to the mobile nodes in-spite-of their random movement. For solving this problem, several mobility management schemes such as Infrastructure-mode Wireless Mesh Network (iMesh), MEsh networks with MObility management (MEMO), Wireless mesh Mobility Management (WMM) and Mesh Mobility Management (M^3) have been proposed. But the difficulty with these existing schemes is their high communication cost. In this paper a tree based proactive mobility management scheme has been proposed for handling both internet and intranet traffic. A numerical analysis of the proposed scheme has been carried out. Finally, the scheme has been compared with iMesh, MEMO and WMM.**

Keywords: **Wireless Mesh Network, Mobility Management, Handoff, Mesh Client, Mesh Router.**

I. INTRODUCTION

Wireless Mesh Network (WMN) [1], [2] has a huge potential to be the future technology for providing internet connections to hand held devices. WMN has three types of nodes: mesh router (MR), mesh client (MC) and gateway (GW). MCs are the users of the WMN. Routing of packets from source MC to destination MC is performed by the MR. The GW receives and transmits the internet packets to and from the WMN.

WMN offer the advantages of self organizing and self healing but it has the problem of providing seamless mobility. Many mobility management schemes have been proposed. These schemes are categorized into two types: tunnel based approach and non-tunnel based approach. In tunnel based approach, packets from the GW to MC will be sent through a tunnel but in case of non-tunnel based approach no tunnel is used for sending of packets. Mesh mobility management (M^3) [3] is an example of tunnel based approach. On the other hand, MEsh networks with MObility management (MEMO) [4], infrastructure-mode Wireless Mesh Network (iMesh) [5] and Wireless mesh Mobility Management (WMM) [6] are the examples of non-tunnel based approach. The advantage of non-tunnel based scheme over tunnel based scheme is that it does not have any tunnelling cost. But, it has the problem of heavy routing overhead. In this paper, a non-tunnel based mobility management scheme FPBR [7] has been enhanced to handle both internet and intranet traffic.

The rest of the paper is organised as follows. Section II presents a discussion on some of the mobility management schemes. The proposed scheme has been discussed in section III. System model and assumptions are presented in section IV. The proposed scheme has been analyzed and compared in section V and section VI respectively. Finally, the paper has been concluded in section VII.

II. RELATED WORK

For solving the problem of mobility management, many non tunnel based mobility management schemes have been proposed. In this section some of those such as iMesh, MEMO and WMM has been discussed.

In iMesh [4], when the MC moves out of the vicinity of a MC and enters into the other, it broadcasts route update message in the entire network using OLSR routing protocol.

In MEMO [5], as the MC move from old MR to new MR, the old MR broadcasts a route error message in the entire network. On receiving the route error message, all the MRs delete the entry of the MC from its routing table. The MC then sends a route reply message to the GW preemptively. If any corresponding MC wants further communication with the MC, it broadcasts route request message in the entire network. In response, the corresponding MC sends back route reply message. The same operation will be performed if the MC needs to communicate with other MCs.

In WMM [6], each MR maintains a proxy table along with the routing table. The proxy table will be used to store the mesh router information of the MC. No separate route update message is used in this scheme. Instead of that each data packet carries the information of host MR of source MC. Intermediate MR uses this information to update the host MR of the source MC in the proxy table.

The problem of using MEMO and iMesh is that they have high routing overhead. On the other hand, though WMM does not have high routing overhead but it suffers from high packet delivery cost due to the use of forward chain.

978-1-4799-6986-9/14/$31.00©2014 IEEE

III. PROPOSED SCHEME

In this section, the enhanced FPBR scheme has been presented. The scheme uses a tree based approach and gateway (GW) initiates the process to form the tree. This tree structure of the MCs is used for mobility management of MCs. The scheme has three parts:

A. Tree formation

The GW periodically broadcasts GW advertisement in the entire network. The advertisement contains the level information. Initially, the level is set to 0 by the GW. On receiving the GW advertisement, each MR increments the value of the level by 1, stores the level information and rebroadcasts this message to its neighbour only once. This rebroadcasting process continues till minimum distanced path is formed from every MR to the GW. Thus, the GW acts as root of the tree and each MR has three types of relationship with its neighbours: child, parent and sibling. This information is maintained in neighbour table of the MRs. There are mainly two objectives to form the tree: minimization of hop count between GW and MRs of the network and setting up of relationship between the MRs. The relationships between the MRs are set up to categorize the handoff of the MCs. Since, most of the traffic to and from the MC belongs to the internet; the tree is formed to reduce the packet delivery cost of internet packets thus reducing the communication cost of the MCs.

B. Mobility Management

After the completion of link layer handoff, network layer handoff will start. When the MC moves from one MR to another, the MC sends route update message to the new MR. On receiving the route update message, the new MR checks its relationship with old MR. Based on the relationship, it performs one of the following actions:

- If the new MR is the child of old MR, the new MR forwards the route update message to the old MR. The old MR sets the new MR as the next hop corresponding to the MC in its routing table. The old MR will not forward the route update message.
- If the new MR is the sibling of old MR, the new MR broadcasts the route update message in the entire network using OLSR [8] routing protocol. The GW and all the MRs of WMN will update the routing table entry corresponding to the MCs. Thus the forward pointer towards the MC is reset.
- If the new MR is the parent of old MR, the new MR first forwards route update message to its siblings. If the sibling has entry of the MC in its routing table it will send back an ACK message to the new MC and a forward pointer is added from old MR to new MR. Otherwise, a NACK message will be sent to the new MR. On receiving the NACK message from all its siblings the MR broadcasts the route update message to all the MRs of WMN using OLSR and the forward pointer towards the MC gets reset.

C. Routing

There are mainly two types of traffic: internet and intranet. Unlike FPBR [7] which is capable of handling only internet traffic, the enhanced FPBR scheme can handle both internet and intranet traffic.

Since the enhanced FPBR scheme uses a proactive routing scheme, the GW and all the MRs of the WMN maintain a route to every MC. When the GW receives an internet packet destined to the MC it forwards the packet to the next hop towards the destination. The intermediate MRs will also follow the process. On receiving the packet the serving MR of the MC checks the entry corresponding to the destination MC in its routing table. If the MC is present in its vicinity the packet will be forwarded to the MC. Otherwise, the packet will be forwarded to the current MR of the MC through the forward chain.

Because of periodic gateway advertisement, each MC has a route to the GW. Therefore, the uplink internet packets of the MC will be directly sent from the current MC to the GW.

The MC sends upstream intranet packets to its current MR. MR then routes the packets to the serving MR of the destination MC. In case downlink intranet traffic, packets are received by the serving MR of the MC. The serving MR forwards those packets directly to the destination MC if the MC is within the vicinity of the MR. Otherwise, the packets are forwarded to the current MR of the MC and subsequently the current MR forwards those packets to the MC.

IV. SYSTEM MODEL AND ASSUMPTIONS

In this section, the system model assumptions have been presented. Without loss of generality, it can be assumed that MC residence time in a MR follows exponential distribution with rate λ_s [9] and session arrival rate and session departure rate follows poission distribution with rate λ_a and λ_d respectively [10]. Therefore, mobility of the MC follows poission distribution with rate λ_s [11]. Let, average number of neighbours, parents and children of a MR in the topology tree be n, p and c respectively. The parameters used for analysis of the proposed scheme and comparison with other existing schemes are shown in table I.

TABLE I
PARAMETERS AND THEIR INTERPRETATIONS

Parameter	Interpretation
M	Number of MRs in the WMN
α	Average hop count between an arbitrary MR and the GW
β	Average hop count between two arbitrary MRs
γ	Per hop communication latency
h	Number of levels in the WMN
M_l	Average number of MRs in each level
p_r	Average probability that the MR rebroadcasts the route request message in its neighbourhood
λ_p	Average number of packets in a session per time unit
I_a	Probability that the arriving session to MC be an internet session
I_d	Probability that the departing session from MC be an internet session
p_{NACK}	Probability that MR receives only NACK from its

	siblings
N_{active}	Average number of corresponding MCs in the WMN per MC
r_{inter}	Percentage of downstream packets per internet session
r_{intra}	Percentage of downstream packets per intranet session
p_g	In WMM probability that current MR of MC does not know the location information of destination MC
P_q	Probability that location query procedure is executed in WMM scheme
c_{move}	Average displacement of the MC per MR association with respect to serving MR[12]

V. NUMERICAL ANALYSIS AND COMPARISON

In this section, the proposed scheme has been analysed and compared with iMesh, MEMO and WMM. The comparison has been carried out considering handoff cost/time unit, packet delivery cost/time unit, query cost/time unit and total communication cost/time unit.

A. Handoff Cost

As described in the previous section, handoff of a MC is classified into three categories: sibling to sibling, parent to child and child to parent. When the new MR is the sibling of the old MR, the new MR broadcasts the route update message in the entire network using OLSR protocol. Therefore, in this case the handoff cost is

$$C_{hstosFPBR} = p_r \times M \quad (1)$$

When the new MR is the child of the old MR route update message will be forwarded to the old MR only. So, in this case handoff cost is

$$C_{hstosFPBR} = \gamma \quad (2)$$

When the new MR is the parent of old MR, new MR sends route update message to sibling MRs. In response, if the new MR receives only negative acknowledge (NACK) from all neighbouring MRs, the new MR will send a location update message in the entire network. Here handoff cost is the summation of the cost incurred by message transfer between old and new MR and broadcasting of route update message. Therefore, the cost is, $(2\times\gamma + p_r\times M)$. On the other hand, if the new MR receives an acknowledge (ACK) from any neighbour MR the cost for handoff will be $2\times\gamma$.Therefore, in case of parent to child movement the handoff cost is,

$$C_{hctopFPBR} = 2\times\gamma + p_{NACK}\times p_r\times M \quad (3)$$

Since the handoff takes place when MC moves into the vicinity of new MR, handoff cost per time unit of the proposed scheme is,

$$C_{hFPBR} = \{C_{hstosFPBR} \times (n\text{-}c\text{-}p)/n + C_{hctopFPBR} \times c/n + C_{hctopFPBR} \times p/n\}\times\lambda_s\times c_{move} \quad (4)$$

In [11] the handoff cost of WMM has been calculated as,

$$C_{hWMM} = 2\times \gamma \times\lambda_s \quad (5)$$

As presented in [11] the handoff cost per time unit of MEMO is,

$$C_{hMEMO} = \{M+\alpha\times\gamma+N_{active}\times(M+\beta\times\gamma)\}\times\lambda_s \quad (6)$$

In case of iMesh, every handoff triggers broadcast of route update messages in the entire network using OLSR. Therefore, handoff cost per time unit is,

$$C_{himesh} = \lambda_s\times p_r \times m \quad (7)$$

B. Packet Delivery Cost

In the proposed scheme, the forward chain length will be incremented by 1 if the MC performs two consecutive movements between parent to child and child to parent and the new MR does not receive ACK from any of its neighbouring MR. In figure 1, green lines indicate node movement and red lines forward chain to forward the packets. When the node moves from MR1 to MR2 and then MR2 to MR3, a forward pointer is added from MR1 to MR3. The forward pointer is extended to next level if there are two consecutive parents to child movements followed by one child to parent movement. In the example shown in figure 1when the MC moves from MR9 to MR10, then MR10 to MR11 and MR11 to MR8 the forward pointer is added from MR9 to MR8 via MR10.

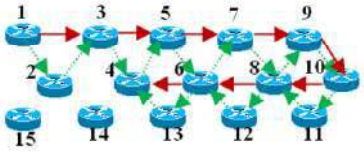

Figure 1. Movement scenario of MC

The MC can move in any direction. In the proposed scheme the forward chain length of the MC depends upon the mobility pattern of the MC. Out of all these movement patterns, the pattern creating longest forward chain as a result of least MR change is considered for calculating average forward chain length. This is because the probability of occurring such scenario is the highest among all the other mobility patterns creating the same length forward chain. Therefore, the other scenarios have been ignored. The maximum forward chain length in the same level is M_l. Since, the number of levels in the network is h, maximum forward chain length is $M_l \times h$. The average forward chain length is,

$$S = S_1+S_2+S_3+\ldots\ldots+S_i+\ldots\ldots+S_h \quad (8)$$

Where S_i is the average forward chain length in level i. Average forward chain length in level 1 is,

$S_1 = 1\times((p-1)/n) \times(c/n) \times(1-p_{NACK})+2\times((p-1)/n)^2 \times(c/n) \times((c-1)/n) \times (1-p_{NACK})^2+3\times((p-1)/n)^3 \times(c/n) \times((c-1)/n)^2 \times (1-p_{NACK})^3+\ldots\ldots+ M_l\times((p-1)/n)^{Ml} \times(c/n)\times((c-1)/n)^{(Ml-1)}\times(1-p_{NACK})^{Ml}$

$$=\left(\frac{p-1}{n}\right)\left(\frac{c}{n}\right)\left(1-p_{NACK}\right)\left[\begin{array}{l}\frac{1-\left(\frac{c-1}{n}\right)^{M_l}\left(\frac{p-1}{n}\right)^{M_l}\left(1-p_{NACK}\right)^{M_l}}{1-\left(\frac{c-1}{n}\right)\left(\frac{p-1}{n}\right)\left(1-p_{NACK}\right)^2} \\ \frac{M_l\left(\frac{c-1}{n}\right)^{M_l}\left(\frac{p-1}{n}\right)^{M_l}\left(1-p_{NACK}\right)^{M_l}}{1-\left(\frac{c-1}{n}\right)\left(\frac{p-1}{n}\right)\left(1-p_{NACK}\right)}\end{array}\right] \quad (9)$$

If the forward chain is extended to level 2, the forward chain length in level 2 is,

$S_2 = (M_l+1)\times((p-1)/n)^{(Ml+1)} \times(c/n)^2\times((c-1)/n)^{Ml} \times(1-p_{NACK})^{Ml+1}+(M_l+2)\times((p-1)/n)^{(Ml+2)} \times(c/n)^2\times((c-1)/n)^{Ml+1}\times(1-p_{NACK})^{Ml+1}+\ldots..+2\times M_l\times((p-1)/n)^{2Ml}\times((c-1)/n)^{2Ml-1}\times(c/n)^2\times(1-p_{NACK})^{2Ml}$

$$= \left(\frac{p-1}{n}\right)^{Ml+1} \times \left(\frac{c}{n}\right)^2 \times \left(\frac{c-1}{n}\right)^{Ml} \times \left(1-p_{NACK}\right)^{Ml+1}$$

$$\times \frac{1}{1-\left(\frac{p-1}{n}\right)\left(\frac{c-1}{n}\right)\left(1-p_{NACK}\right)} \times \quad (10)$$

$$\left[\begin{array}{l} M_l\times\left\{1-\left(\frac{p-1}{n}\right)^{M_l}\left(\frac{c-1}{n}\right)^{M_l}\left(1-p_{NACK}\right)^{M_l}\right\} \\ -M_l\times\left(\frac{p-1}{n}\right)^{M_l}\left(\frac{c-1}{n}\right)^{M_l}\left(1-p_{NACK}\right)^{M_l} \\ +\frac{1-\left(\frac{p-1}{n}\right)^{M_l}\left(\frac{c-1}{n}\right)^{M_l}\left(1-p_{NACK}\right)^{M_l}}{1-\left(\frac{p-1}{n}\right)\left(\frac{c-1}{n}\right)\left(1-p_{NACK}\right)}\end{array}\right]$$

For $2 \le i \le h$ if the forward chain is extended to level i, the forward chain length in level i is,

$$S_i = \left(\frac{p-1}{n}\right)^{(i-1)M_l+i-1} \times \left(\frac{c}{n}\right)^i \times \left(\frac{c-1}{n}\right)^{(i-1)M_l+i-2}$$

$$\times \left(1-p_{NACK}\right)^{(i-1)M_l+1} \times \frac{1}{1-\left(\frac{p-1}{n}\right)\left(\frac{c-1}{n}\right)\left(1-p_{NACK}\right)} \quad (11)$$

$$\times\left[\begin{array}{l}(i-1)\times M_l\times\left\{1-\left(\frac{p-1}{n}\right)^{M_l}\left(\frac{c-1}{n}\right)^{M_l}\left(1-p_{NACK}\right)^{M_l}\right\} \\ -M_l\times\left(\frac{c-1}{n}\right)^{M_l}\left(\frac{p-1}{n}\right)^{M_l}\left(1-p_{NACK}\right)^{M_l} \\ +\frac{1-\left(\frac{p-1}{n}\right)^{M_l}\left(\frac{c-1}{n}\right)^{M_l}\left(1-p_{NACK}\right)^{M_l}}{1-\left(\frac{p-1}{n}\right)\left(\frac{c-1}{n}\right)\left(1-p_{NACK}\right)}\end{array}\right]$$

The serving MR of the MC receives the downstream internet packets from the GW and forwards those to the current MR. Per packet delivery cost of downstream internet packet is,

$$C_{pinterdFPBR} = \gamma\times(\alpha+S) \quad (12)$$

The upstream internet packets are directly sent by the current MR of the GW. Therefore, per packet delivery cost of upstream internet packet is,

$$C_{pinteruFPBR} = \gamma\times\alpha \quad (13)$$

The upstream intranet packets are directly sent from the current MR to the serving MR of corresponding MC. The serving MR then forwards those packets to the current MR of the MC. Therefore, per packet delivery cost of upstream intranet packet is,

$$C_{pintrauFPBR} = \gamma\times(\beta+S) \quad (14)$$

Like upstream intranet packets the downstream intranet packets will also incur the same packet delivery cost because the routing process of both of them is similar. So,

$$C_{pintradFPBR} = \gamma\times(\beta+S) \quad (15)$$

For calculating packet delivery cost per time unit both internet and intranet packets are considered. In case of intranet packets, upstream intranet packets from a MC are also downstream intranet packets for other MCs. Therefore, to calculate intranet packet delivery cost per time unit only downstream intranet packets have been considered. Packet delivery cost per time unit is,

$$C_{pFPBR} = \{C_{pinterdFPBR}\times\frac{r_{interer}}{100} + C_{pinteruFPBR}\times\left(1-\frac{r_{interer}}{100}\right)\} \times(\lambda_a\times I_a+\lambda_d\times I_d)\times\lambda_p+ C_{pintradFPBR}\times\{\lambda_a\times(1-I_a)\times\frac{r_{intra}}{100}+\lambda_d\times(1-I_d)\times\frac{r_{intra}}{100}\}\times\lambda_p \quad (16)$$

In case of WMM average forward chain length for downstream internet packets is [11],

$$FC_{gmWMM} = \lambda_s\times c_{move}\times\left[\begin{array}{l}\lambda_a\times\lambda_p\left\{I_a\times\left(1-\frac{r_{interer}}{100}\right)+\left(1-I_a\right)\times p_g\times\left(1-\frac{r_{intra}}{100}\right)\right\} \\ +\lambda_d\times\lambda_p\left\{I_d\times\left(1-\frac{r_{interer}}{100}\right)+\left(1-I_d\right)\times p_g\times\left(1-\frac{r_{intra}}{100}\right)\right\}\end{array}\right]^{-1} \quad (17)$$

Per packet delivery cost of downstream internet packet is [11],

$$C_{pinterdWMM} = (\alpha+ FC_{gmWMM})\times\gamma \quad (18)$$

Per upstream internet packet delivery cost is [11],

$$C_{pinteruWMM} = \alpha\times\gamma \quad (19)$$

Delivery cost of a downstream intranet packet routed through the GW to the MC is [11],

$$C_{pintragdWMM} = (2\times\alpha+ FC_{gmWMM})\times\gamma \quad (20)$$

Average forward chain length for the downstream intranet packets that are directly routed from the corresponding MC to the receiving MC is [11],

$$FC_{intraWMM} = \lambda_s \times c_{move} \times N_{active} \left\{ \begin{matrix} \lambda_a \times \lambda_p \times (1-I_a) \times \left(1-\frac{r_{interra}}{100}\right) \\ +\lambda_d \times \lambda_p \times (1-I_d) \times \left(1-\frac{r_{interra}}{100}\right) \end{matrix} \right\}^{-1} \quad (21)$$

Per packet delivery cost of downstream intranet packets from corresponding MC is [11],

$$C_{pintradWMM} = (\beta + FC_{intraWMM}) \times \gamma \quad (22)$$

Considering only downstream intranet packets, packet delivery cost per time unit is,

$$C_{pWMM} = \{C_{pinterdWMM} \times r_{inter} + C_{pinteruWMM} \times (1-r_{inter})\} \times \lambda_p \times \{\lambda_d \times I_d + \lambda_a \times I_a\} + \{(C_{pintragdWMM} \times p_g + C_{pintradWMM} \times (1-p_g)\} \times \lambda_p \times r_{intra} \times \{\lambda_a \times (1-I_a) + \lambda_d \times (1-I_d)\} \quad (23)$$

In case of MEMO per packet delivery cost of downstream and upstream internet packets is [11],

$$C_{pinterdMEMO} = C_{pinteruMEMO} = \alpha \times \gamma \quad (24)$$

The intranet packet delivery cost is calculated as,

$$C_{pintraMEMO} = \beta \times \gamma \quad (25)$$

Therefore, considering only the downstream packets in case of intranet traffic, packet delivery cost per time unit can be calculated as,

$$C_{pMEMO} = C_{pinterdMEMO} \times \lambda_p \times \lambda_a \times I_a \times \frac{r_{interer}}{100} + C_{pinteruMEMO} \times \lambda_p \times \lambda_a \times I_a \times \left(1 - \frac{r_{interer}}{100}\right) + C_{pinterdMEMO} \times \lambda_p \times \lambda_d \times I_d \times \frac{r_{interer}}{100} + C_{pinteruMEMO} \times \lambda_p \times \lambda_d \times I_d \times \left(1 - \frac{r_{interer}}{100}\right) + C_{pintraMEMO} \times \lambda_p \times \frac{r_{interra}}{100} \times \{\lambda_a \times (1-I_a) + \lambda_d \times (1-I_d)\} \quad (26)$$

In iMesh downstream internet packets are directly sent from the GW to the host MR. The host MR then forwards the packets to the MC. So, downstream intranet packet delivery cost is,

$$C_{pinterdimesh} = \alpha \times \gamma \quad (27)$$

The upstream internet packets will also be directly sent from the host MR to the GW. Therefore upstream internet packet delivery cost is,

$$C_{pinteruimesh} = \alpha \times \gamma \quad (28)$$

The host MR of the MC directly sends the upstream intranet packets to the MR of corresponding MC. The same process will be followed when the corresponding MC sends intranet packets to the MC. Therefore, packet delivery cost of upstream and downstream intranet packet is,

$$C_{pintradimesh} = C_{pintrauimesh} = \beta \times \gamma \quad (29)$$

Internet as well as intranet packets are considered for calculating packet delivery cost per time unit. In case of intranet packets only downstream packets have been taken under consideration. Therefore, packet delivery cost per time unit is,

$$C_{piMesh} = C_{pinterdimesh} \times \lambda_p \times \lambda_a \times I_a \times \frac{r_{interer}}{100} + C_{pinteruimesh} \times \lambda_p \times \lambda_a \times I_a \times \left(1 - \frac{r_{interer}}{100}\right) + C_{pinterdimesh} \times \lambda_p \times \lambda_d \times I_d \times \frac{r_{interer}}{100} + C_{pinteruimesh} \times \lambda_p \times \lambda_d \times I_d \times \left(1 - \frac{r_{interer}}{100}\right) + C_{pintradimesh} \times \lambda_p \times \frac{r_{interra}}{100} \times \{\lambda_a \times (1-I_a) + \lambda_d \times (1-I_d)\} \quad (30)$$

C. *Query Cost*

The enhanced FPBR scheme uses proactive strategy for routing of packets. Each MR maintains a route to the serving MR of the MC. Therefore, no query message will be sent in this scheme.

In WMM the GW broadcasts route request message in the entire network only when the MC wakes up from sleep mode or the GW initiates the first internet session to the MC. Therefore, query cost per time unit is [11],

$$C_{qWMM} = (p_r \times M + \beta \times \gamma) \times P_q \times \left(\frac{\omega_w \times \omega_s}{\omega_w + \omega_s}\right) \quad (31)$$

Where ω_w and ω_s are switching rates from sleep mode to active and from active mode to sleep mode respectively.

In MEMO before initializing an intranet session if the host MR of the source MC does not have route to destination MC, it broadcasts a route request message in the entire network. Cost for broadcasting the message is, M. The host MR of destination MC sends back route reply message and cost for that is $\beta \times \gamma$. Therefore, query cost per time unit,

$$C_{qMEMO} = (M + \beta \times \gamma) \times (1-I_d) \times \lambda_d \times p_g \quad (32)$$

In iMesh each MR maintains a route to all the MCs of the network. So, this scheme will not have any query cost.

D. *Total Communication Cost*

Total communication cost per time of the enhanced FPBR scheme, WMM, MEMO and iMesh is,

$$TC_{FPBR} = C_{hFPBR} + C_{pFPBR} \quad (33)$$

$$TC_{WMM} = C_{hWMM} + C_{pWMM} + C_{qWMM} \quad (34)$$

$$TC_{MEMO} = C_{hMEMO} + C_{pMEMO} + C_{qMEMO} \quad (35)$$

$$TC_{iMesh} = C_{himesh} + C_{piMesh} \quad (36)$$

VI. PERFORMANCE ANALYSIS

This section presents a performance comparison of the enhanced FPBR scheme with WMM, MEMO and iMesh. The parameters used for comparison are: handoff, packet delivery cost and total communication cost per time unit. For comparison with respect to any parameter the following metric is used [11],

$$F\% = \left(\frac{|C_{other} - C_{FPBR}|}{C_{FPBR}} \right) \times 100 \quad (37)$$

If $C_{FPBR} > C_{other}$, the cost of FPBR is F% higher than that of the other scheme. Otherwise, the cost of FPBR is F% less than other scheme. Typical values of parameters are shown in table II.

TABLE II
TYPICAL VALUES OF PARAMETERS

Parameter	Value
M	1000
A	50
B	30
Γ	0.1
N	6
P	2
M_l	20
h	50
p_r	0.4
λ_p	1000
r_{inter}	0.8
r_{intra}	0.5
I_a	0.8
I_d	0.7
p_{NACK}	0.1
N_{active}	30

Fig. 2 shows a comparison of handoff cost/sec of FPBR, WMM, iMesh and MEMO. In this case, the value of λ_s and λ_d is set to 0.5. The handoff cost of MEMO is the highest because in this scheme after every handoff the old MR broadcasts route error message, the new MC sends a proactive route reply message to the GW and the corresponding MCs initiates a route discovery process to the MC. Handoff cost of iMesh is higher than that of FPBR and WMM. This is because after every handoff the host MC broadcasts a route update message using OLSR routing protocol. On the other hand, in FPBR route update message is broadcasted using OLSR only when the conditions discussed in section III are satisfied. Therefore, FPBR incurs handoff cost less than that of MEMO and iMesh. WMM has the lowest handoff cost since no separate route update message is used in this scheme and only forward pointer is added from old MR to the new MR.

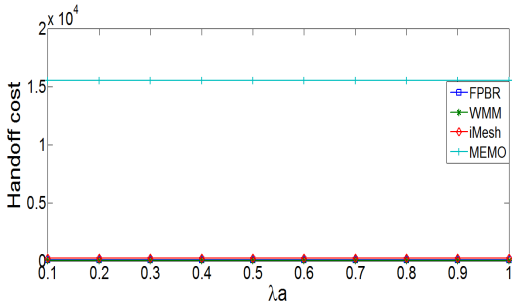

Figure 2. Effect of λ_a on Handoff cost

Fig. 3 shows the variation of packet delivery cost/sec with the increase in λ_a. WMM has the highest packet delivery cost because the scheme uses forward pointer to forward packets from old MR to new MR till the sender MR or GW has updated route information. Packet delivery cost of FPBR is much less than that of WMM because forward pointer is added only when the conditions discussed in subsection B of section V are satisfied. MEMO and M^3 has the lowest packet delivery cost because the schemes do not use any forward pointer. With the increase in λ_a number of downstream packets increases. Therefore, packet delivery cost of all the schemes also increases.

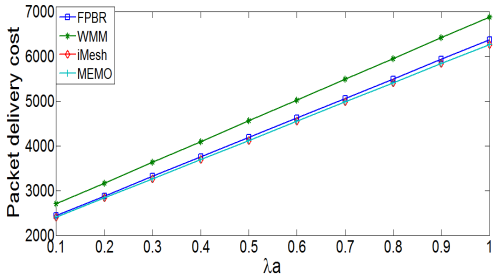

Figure 3. Effect of λ_a on Packet delivery cost

Figure 4 shows the change in total communication cost/sec of MEMO, WMM, iMesh and FPBR. MEMO has the highest total communication cost because of its high handoff cost and query cost. The total communication cost of WMM is higher than that of iMesh and FPBR. This is because of its high packet delivery cost and query cost. iMesh has higher total communication cost than FPBR because of its high handoff cost. FPBR incurs low handoff cost and packet delivery cost. Therefore, it has the lowest packet delivery cost. FPBR incurs 379.71%, 2.07% and 7.59% less total communication cost/sec compared to MEMO, iMesh and WMM respectively.

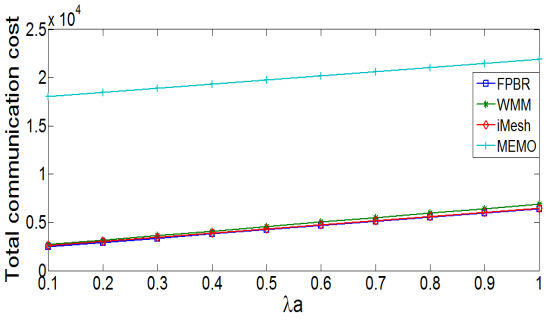

Figure 4. Effect of λ_a on Total communication cost

Handoff cost/sec, packet delivery cost/sec and total communication cost/sec of MEMO, iMesh, FPBR and WMM are shown in figure 5, figure 6 and figure 7 respectively. The value of both λ_a and λ_s is set to 0.5. As λ_d increases handoff cost/sec, packet delivery cost/sec and total communication cost/sec of all the four schemes also follow the same behaviour as shown in figure 2, figure 3 and figure 4 respectively. The reasons for this are also similar. The total communication cost of FPBR is 373.94%, 2.58% and 8.01% less than that of MEMO, iMesh and WMM respectively.

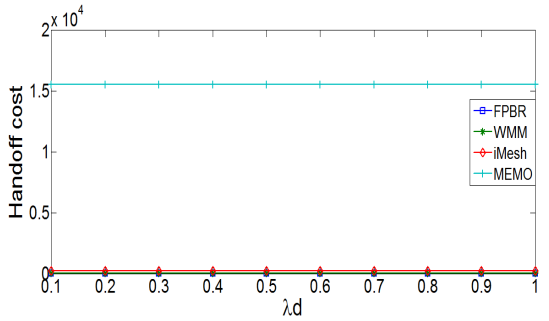

Figure 5. Effect of λ_d on Handoff cost

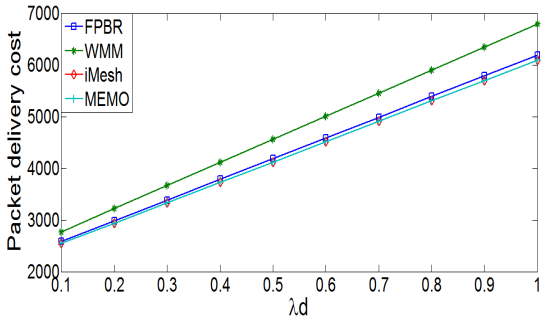

Figure 6. Effect of λ_d on Packet delivery cost

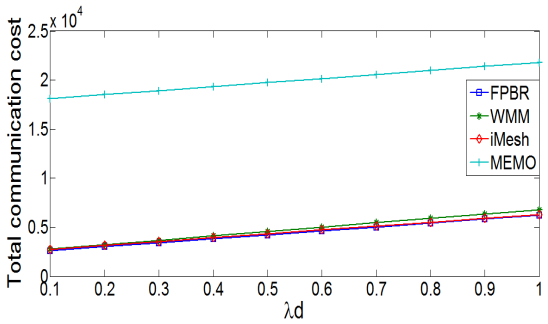

Figure 7. Effect of λ_d on Total communication cost

Figure 8 shows the variation of handoff cost/sec as λ_s increases. Here λ_a = 0.5 and λ_d = 0.5. With the increase in λ_s handoff cost of MEMO increases at a higher rate compared to the rest three schemes. This is because increase in λ_s increases number of handoff/sec of a MC. Moreover, per handoff cost in case of MEMO is also high. The handoff cost of iMesh increases at a much lower rate compared to MEMO. But the rate is higher than that of FPBR and WMM. This is because after every handoff the MC broadcasts a route update message using OLSR. The increase rate of handoff cost of FPBR is less than that of iMesh since in this scheme the MC broadcasts route update message only in limited occasion. WMM does not use any route update message. Therefore, its handoff cost does not change with increase in λ_s.

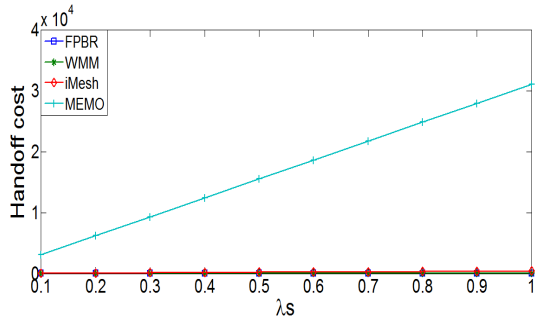

Figure 8. Effect of λ_s on Handoff cost

Figure 9 shows effect of λ_s on packet delivery cost/sec. As λ_s increases the packet delivery cost of MEMO and iMesh remains unchanged because the packets are directly sent from the source MR to the host MC. In case of WMM forward chain length increases as the value of λ_s increases. Therefore, packet delivery cost of WMM also increases. The packet delivery cost FPBR remains unaffected with increase in λ_s because the forward chain length is only dependent upon mobility pattern. It does not depend on mobility rate of the MC.

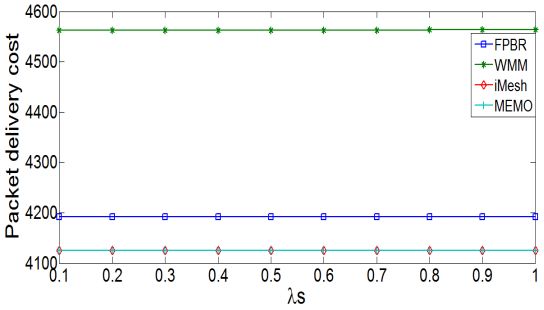

Figure 9. Effect of λ_s on Packet delivery cost

Variation in total communication cost/sec of MEMO, iMesh, WMM and FPBR are shown in figure 10. The total communication cost of MEMO increases at the highest rate compared to rest of the schemes. The reason behind this is its high handoff cost. WMM has higher total communication cost compared to iMesh and FPBR because of its high packet delivery cost and query cost. But the increase rate is less than that of iMesh. The handoff cost of iMesh is high and it increases at a higher rate compared to WMM. Therefore, the total communication cost of iMesh is higher than that of FPBR but it increases at a rate higher than both FPBR and iMesh. FPBR has the lowest total communication cost compared to all the three schemes. This is because of its low handoff cost and packet delivery cost. Total communication cost of FPBR is 403.5%, 2.86% and 8.03% less than that of MEMO, iMesh and WMM respectively.

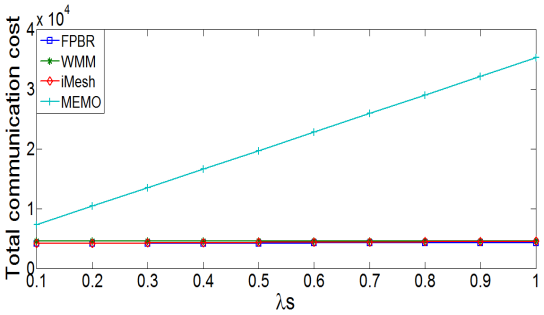

Figure 10. Effect of λ_s on Total communication cost

VII. CONCLUSION

This paper proposes a mobility management protocol named FPBR for handling both intranet and internet traffic. The scheme has been analysed and compared with MEMO, iMesh and WMM. Numerical analysis shows that FPBR performs better than MEMO, iMesh and WMM with respect to handoff cost, packet delivery cost and total communication cost.

REFERENCES

[1] I.F.Akyildiz and X. Wang, "A Survey on Wireless Mesh Networks", IEEE Communications Magazine, vol. 43, no. 9, pp.S23 - S30.

[2] I. F. Akyildiz, X. Wang, and W. Wang, "Wireless mesh networks: a survey," Computer Networks, vol. 47, no. 4, pp. 445–487, 2005.

[3] R. Huang, C. Zhang and Y. Fang, "A Mobility Management Scheme for Wireless Mesh Networks", IEEE GLOBECOM, pp. 5092-5096, 2007.

[4] Ren M. et al., "MEMO: An Applied Wireless Mesh Network with Client Support and Mobility Management", IEEE GLOBECOM, pp. 164-170, 2007.

[5] V.Navda, A.Kashyap and R.S.Das, "Design and Evaluation of iMesh: an Infrastructure-mode Wireless Mesh Network", Sixth IEEE International Symposium on a World of Wireless Mobile and Multimedia Networks, pp. 164-170, 2005.

[6] D. Hwang, P. Lin and C. Gan, "Design and performance study for a mobility management mechanism (WMM) using location cache for wireless mesh networks," IEEE Transaction on Mobile Computing, vol. 7, no. 5, pp. 546-556, 2008.

[7] A. Majumder, S. Roy, "A Forward Pointer Based Mobility Management Scheme for Multi-Hop Multi-Path Wireless Mesh Network", ICDSE, pp. 194-197, 2012.

[8] T. Clausen and P. Jacquet. Optimized link state routing protocol (OLSR). RFC 3626, October 2003.

[9] S. Pack, H. Jung, T. Kwon and Y. Choia, "SNC: a selective neighbor catching scheme for fast handoff in 802.11 wireless networks," ACM SIGMOBILE Mobile Computing and Communication Reviews, vol. 9, no. 4, pp. 39-49, 2005.

[10] S. Kwon, S. Y. Nam, H. Y. Hwang, and D. K. Sung, "Analysis of a mobility management scheme considering battery power Conservation in IP-based mobile networks, " IEEE Transactions on Vehicular Technology, vol. 53, no. 6, pp. 1882-1890, 2004.

[11] A. Majumder and S. Roy, "Design and Analysis of a Dynamic Mobility Management Scheme for Wireless Mesh Network," The Scientific World Journal, vol. 2013, Article ID 656259, 16 pages, 2013. doi:10.1155/2013/656259.

[12] A. Majumder, S. Roy, and K. K. Dhar, "Design and analysis of an adaptive mobility management scheme for handling traffic in wireless mesh network," International Conference on Microelectronics, Communications and Renewable Energy, pp. 1–6, 2013.

Automatic Brain Tumor Segmentation in MRI: Hybridized Multilevel Thresholding and Level Set

Malsawm Dawngliana
Department of IT,
Assam University,
Silchar, India
mschhangte@gmail.com

Daizy Deb
Department of IT,
Assam University,
Silchar, India
daizydebkar@gmail.com

Mousum Handique
Department of IT,
Assam University,
Silchar, India
mousum78@yahoo.co.in

Sudipta Roy
Department of IT,
Assam University,
Silchar, India
sudipta.it@gmail.com

***Abstract*— Segmentation of tumor from magnetic resonance image (MRI) brain images is an emergent research area in the field of medical image segmentation. As segmentation of brain tumor plays an important role for necessary treatment and planning of tumor surgery. However, segmentation of the brain tumor is still a great challenge in clinics, specially automatic segmentation. In this paper we proposed hybridized multilevel thresholding and level set method for automatic segmentation of brain tumor. The innovation for this paper is to interface the initial segmentation from multilevel thresholding and extract a fine portrait using level set method with morphological operations. The results are compared with the existing method and also with radiologist manual segmentation which confirm the effectiveness of this hybridized paradigm for brain tumor segmentation.**

Keywords*— *Magnetic Resonance Imaging(MRI), Brain tumor, multilevel thresholding, level set method, medical image processing.

I. INTRODUCTION

Brain is built up of numerous types of cells. These cells typically grow and divide in a self-restrained and formal manner to produce new cells. Worthlessly, new cells continue to produce which lead to a mass of extra tissue called brain tumor. Brain tumor can be benign (not cancerous) or malignant (cancerous), the cells of malignant tumors are abnormal and divide numerously, nearby cells will be attack and damage the healthy adjacent tissues.

Modern technology does not provide information about tumor observation and pattern, judgment of lesion is still carried out manually. The main disadvantages of manual segmentation are: it is time consuming and fully rely on human decision. According to the population and the number of patients, manual judgment is bulky in everyday clinic and led to human errors. Therefore development of tools for automatic judgment of lesion is a demand in today's senario.

To overcome these problems, automatic brain tumor segmentation was proposed by Singh,P [1] for initial segmentation, FCM algorithm is employed which cluster the MRI brain image, from these clusters the desired cluster must be selected manually for automatic initialization. Hence one can say that it is not fully automatic as human intervention is involved. The selected cluster is taken as input for levelset method, which segment the tumor part without the need of re-initialization. If the initial segmentation is automated, it will give fully automatic segmentation method.

In medical image segmentation, classical thresholding plays an important role as it separate the object from the background using simple intensity value variation, it separate the image into two groups according to threshold value [2]. Natarajan,P [3] employs classical thresholding operation with morphological operation for automatic brain tumor detection, in this approach, the threshold value must be adjusted manually depending upon the input image intensity. Classical thresholding is not effective for initial medical image segmentation due to the presence of uneven intensity variation in an image.

Multilevel thresholding using type-II fuzzy sets was proposed by Ritambhar Burman [4]. This multilevel thresholding can segment an image into number of groups, which will make thresholding more robust for initial segmentation in medical images. Hence, a hybridized technique for fully automatic brain tumor segmentation is proposed in this paper which make use of multilevel thresholding based on image intensity for initial segmentation and level set method for refinement of tumor based on image boundary variation.

This paper is organized as follows. The background work is discussed in section II. The proposed method is discussed in section III which starts with a flowchart of the proposed technique. Experimental results and performance evaluation of our proposed method and existing method is illustrated in section IV, followed by the conclusions in section V.

II. BACKGROUND WORK

By using just a powerful magnetic field and radio frequency pulses MRI operates, which gives input to a computer which produce detailed image of organs, soft tissues and bones. Detailed MR images allow physicians to evaluate

978-1-4673-6708-0/15/$31.00 ©2015 IEEE

various treatment and surgery can be plan by the use of brain MRI. Initially MRI images are stored in DICOM format, which can be further pre-processed for higher image analysis.

The sample images are acquired from BraTS database which is in DICOM format [5]. As the dataset contain skull, which is included in the image volume, it is prefer to remove this skull before the system process. Skull stripping is performed using Brain Extraction Tool (BET) [6] using this tool, the skull part is removed and only the brain is extracted. The output MRI slice is fed to the system which give advantages in speed and accuracy for higher image analysis.

III. Proposed Method

The flowchart shown in Fig. 1 fully illustrates the overall procedure of the system. Firstly, the system starts with an MRI brain image as an input. Here, pre-processing of the input image with the help of median filter algorithm and histogram equalization. The produced image undergo Multilevel Thresholding method which partition the image into meaningful parts and morphological operation is to filter out noises but preserve the important information. Finally, enhanced level set method for fine delineation of brain tumor takes place. The segmented tumor image is produced as an output.

A. Pre-processing

In this phase, the input image is treated with initial processing before it passes through any special purpose processing. Here the image improves the quality and noises are removed. As the brain tumor is going to be segmented from the MRI brain image, it must have minimum noise with high image quality. It consists of two sub-steps:

1) Median Filtering:

Median filter is often choose to perform noise reduction in an image. Window slide entry by entry which is the main idea of median filter, it slide over the whole image, the pixel at the centre is the central pixel. The neighboring pixels are ranked according to intensity and the median value replace the central pixel value Advantage of median filters algorithm is that it can perform an excellent operation of rejecting certain types of noise, in particular impulse noise in which some individual pixels have extreme values[7]. Since the output pixel value is one of the neighboring values, new alien values are not created. Edges are preserves while removing noise; it is possible to apply repeatedly if necessary. This filtering algorithm enhances the quality of the MRI brain images.

2) Histogram Equalization:

Histogram equalization makes use of image histogram for contrast adjustment, so that the intensities can be distributed better. The input image may be composed of uneven distribution of intensity, which makes the image having weak contrast and low quality. The solution is to perform histogram equalization. It is applied for enhancing the appearance of an image.

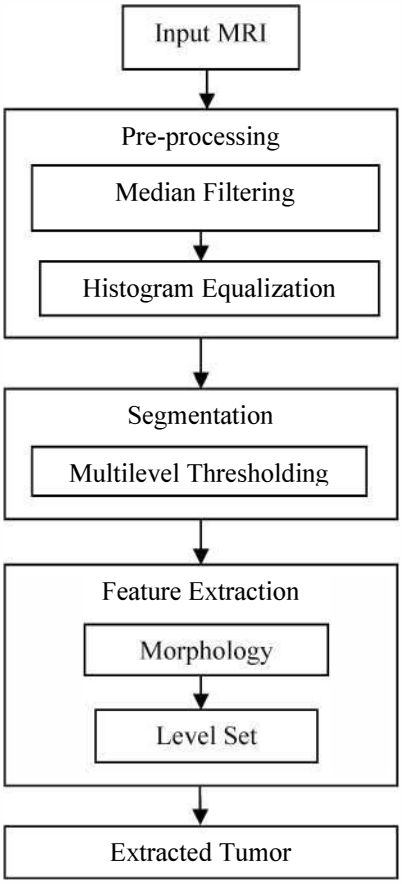

Fig. 1 Block diagram of proposed method

B. Multilevel Thresholding

After the MRI brain images undergo pre-processing stage, images are fed to Multilevel Thresholding stage. This Multilevel Thresholding method threshold an image by using fuzzy membership values which partition the histogram of an image. Using Type-II fuzzy sets, it obtain optimal image threshold by employing ultra fuziness [4]. The obtained results are hereby more justifiable for medical images.

A Type-II fuzzy set A in a fuzzy finite set $X=\{x_1 + x_2 +\ldots\ldots+ x_n\}$ may be represented as [8]:

$$A = \{x, \mu_U(x), \mu_L(x), |x\epsilon X, 0 \leq \mu_U(x), \mu_L(x) \leq 1\} \quad (1)$$

Where, $\mu_U(x)$ and $\mu_L(x)$ are the upper and lower membership function respectively which range from 0 to 1.

Let the input image D be of size M*N, with f(m,n) as the grey value. L is the number of grey values in which image I can be represented, the set of all grey levels {0,1,2…L-1} is represented as G.

$$f(m,n)\epsilon G \forall (m,n)\epsilon I$$
$$D_k = \{(m,n): f(m,n) = k, k\epsilon\{0,1,2 \ldots, L-1\}\} \quad (2)$$

Let $H=\{h_0,h_1,\ldots h_{L-1}\}$ be the normalized histogram of the image where $h_k=n_k/(M*N)$, n_k is the number of pixels in D_k.

The ultra-fuzziness for an image for the k^{th} level is given by:

$$P_k = \sum_{i=0}^{L-1} h_i * ((\mu_U)_k(i) - (\mu_L)_k(i)) \quad (3)$$

Where $0<k<=N+1$, N is the number of threshold level. Here we consider N=3. I represent the grey levels.

Here we have used $(\mu_U)_k = ((\mu_U)_k)^{\frac{1}{\alpha}}$ and $(\mu_L)_k = ((\mu_L)_k)^{\alpha}$, considering α=1.5.

The thresholds for the image is that point, where the membership value of a level of segmentation falls to 0.5, DE is used to reduce the search time to find the optimal thresholds.

Algorithm for Multilevel image thresholding based on type II fuzzy sets:

i. Calculate the image histogram.
ii. Give the number of threshold level N.
iii. Apply Differential Evolution to optimize the search space.
iv. Calculate the upper and lower membership functions.
v. Calculate the ultra fuziness for each position.
vi. Obtain the membership values.
vii. Get the optimal threshold image.

C. Feature Extraction:

After multilevel thresholding, the segmented image undergo feature extraction stage where removal of noise is done without destroying the original properties and extract the feature. In this stage two methods are used: Morphological operation and Level Set method.

1) Morphological Operation:

The term morphology discuss about image processing technique which takes into consideration of the structure and shape of an objects. Binary images may contain numerous noise, hence it is used here as object refinement. It refines the noise present but still preserve the original properties of the object. It works on the principle of pre-defined rules in short time. It simply means to identify the shape and structure of object within the image. It operates on the basis of pixel comparision with the neighbouring pixels. Morphological operation usually performed on binary images, the binary image have a pixel value of 0 or 1.

The advantage of morphological operations here is to filter the object in multilevel thresholding due to noise but preserve the original image components. We observe that the noises are discrete and diverse. So at first morphological operations should shrink and eliminate small pieces of objects in Multilevel Thresholding segmentation, and then expand to recover the meaningful objects.

2) Levelset method:

In this paper, we have used a level set evolution method without re-initialization introduced by Li Chunming et al., [9], which is based on energy penalty term to extract the brain tumor. Level set segment an image on the basis of pixels intensity and variational boundaries.

In the level set method, the evolution equation of the level set function Ø is given by:

$$\frac{d\emptyset}{dt} + F|\nabla\emptyset| = 0$$
$$\emptyset(0,x,y) = \emptyset_0(x,y) \quad (4)$$

Where F is the external force which dependents on image information like image gradient and image intensity, this force F attracts the curves toward the edges. $|\nabla\emptyset|$ is the normal direction, $\emptyset_0(x,y)$ is the initial contour.

The moving force F has to be stopped at the edge by an edge indication function g

$$g = \frac{1}{1+|\nabla(G_\sigma * I)|^2} \quad (5)$$

Where G_σ is a Gaussian function with the standard deviation σ, $*$ represents convolution, I is a given 2D image, ∇ is the gradient operator, $|.|$ is the modulus of smoothed image gradients.

External energy function $\emptyset_0(x,y)$ is defined as

$$\mathcal{E}_{g,\lambda,v}(\emptyset) = \lambda\mathcal{L}_g(\emptyset) + v\mathcal{A}_g(\emptyset) \quad (6)$$

Where v are constants and $\lambda > 0$.

The terms $\mathcal{L}_g(\emptyset)$ and $\mathcal{A}_g(\emptyset)$ can be defined as

$$\mathcal{L}_g(\emptyset) = \int_\Omega g\delta(\emptyset)|\nabla\emptyset|dxdy \quad (7)$$
$$\mathcal{A}_g(\emptyset) = \int_\Omega gH(-\emptyset)dxdy \quad (8)$$

Where δ is the univariate Dirac function, and H is the Heaviside function.

The total energy function is defined as

$$\mathcal{E}(\emptyset) = \lambda\mathcal{L}_g\mathcal{P}(\emptyset) + \mathcal{E}_{g,\lambda,v}(\emptyset) \quad (9)$$

Here the total energy consist of internal energy term and external energy term. The internal energy term $\mathcal{P}(\emptyset)$penalizes the deviation of the level set function from signed distance function and the external energy term $\mathcal{E}_{g,\lambda,v}(\emptyset)$ drives to

motion of the zero level set to the required image features like object boundaries.

The evolution equation of the level set function is defined as:

$$\frac{d\emptyset}{dt} = \mu\left[\Delta\emptyset - \operatorname{div}\left(\frac{\nabla\emptyset}{|\nabla\emptyset|}\right)\right] + \lambda\delta(\emptyset)\operatorname{div}\left(g\frac{\nabla\emptyset}{|\nabla\emptyset|}\right) + vg\delta(\emptyset) \quad (10)$$

The modification of level set algorithm lead to fast image segmentation without the need of re-initialization.

IV. Result And Evaluation

We evaluate the performance of our proposed method and existing method by taking MRI brain dataset from BraTS database [5] which was segmented by experts having different location, shape, size and contrast of tumor. The dataset is provided with ground truth, from which we can evaluate the segmentation accuracy. The same images are segmented with FCM-Levelset method [1] and proposed MLT-Levelset method performance have been recorded and performance assessment table is shown in Table 1 and Figure 2.

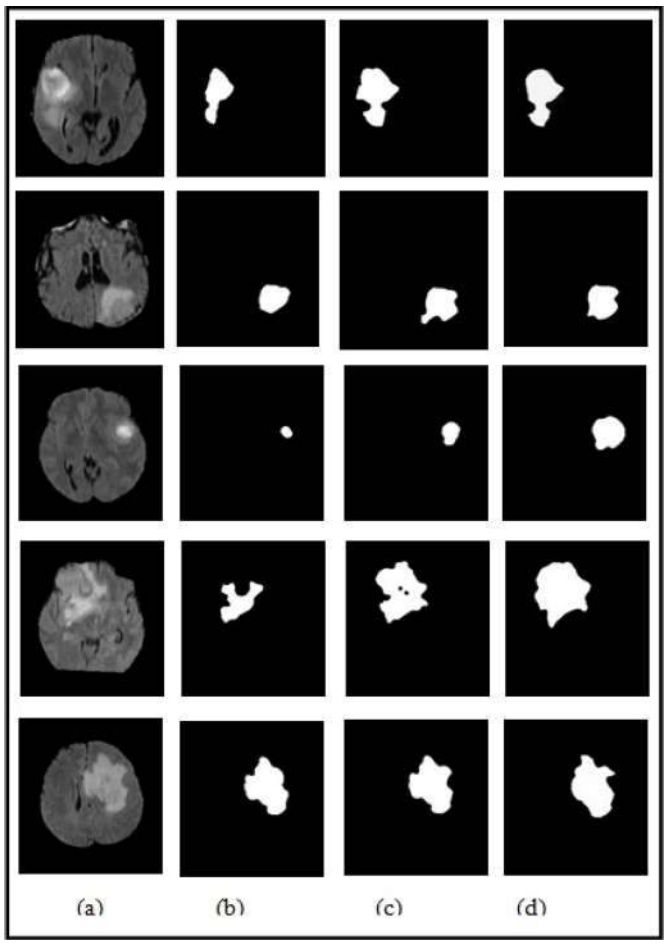

Fig. 2 (a) Input MRI brain image. (b) Segmented tumor with FCM-Levelset algorithm. (c) Segmented tumor with MLT-Levelset algorithm. (d) Ground truth segmented manually by the radiologist.

Table 1: Evaluation of the segmentation results for FCM-Levelset method and MLT-Levelset method.

	Volume metric functions for FCM-Levelset		Volume metric functions for MLT-Levelset	
	S	Ji	S	Ji
1	1.29	0.65	1.76	0.88
2	1.42	0.71	1.70	0.85
3	0.24	0.12	0.75	0.37
4	0.72	0.36	1.55	0.77
5	1.60	0.80	1.65	0.83
Average	1.05	0.53	1.48	0.74

The performance of these segmentation are validated by Dice similarity coefficient(S) [10] and Jaccard index [11]. Let a given image have pixels Ax and Bx belonging to class x in manual and in automatic segmentation respectively. |Ax| imply the number of pixels in Ax. |Bx| imply the number of pixels in Bx.

Dice similarity coefficient S is defined as:

$$S = \frac{(|2|Ax \cap Bx||)}{|Ax \cup Bx|} \quad (11)$$

Dice value ranges from [0,1], 0 for no similarity and 1 for full similarity.

Jaccard index between two volumes is defined as,

$$Ji = \frac{|Ax \cap Bx|}{|Ax \cup Bx|} X100 \quad (12)$$

Higher the value of S and Ji, and lower the value of FPVF, FNVF gives better segmentation result.

The performance assessment of our proposed method with the existing method [1] is shown in table 1 and figure 2. It shows that, the existing method gives 1.05 out of 2 and 53% in similarity coefficient and Jaccard index while our proposed method gives 1.48 out of 2 and 74% respectively, which implies that our proposed method gives higher accuracy. This also implies that our proposed method have lower segmentation error and loss of expected tumor pixels are also greatly reduced.

V. Conclusion

Our proposed method deals with the hybridization of Multilevel Thresholding method and Levelset method. The Thresholding method segment the tumor region from the brain image in a multiple level and Levelset without re-initialization technique is use to extract a fine portrait of the tumor area.

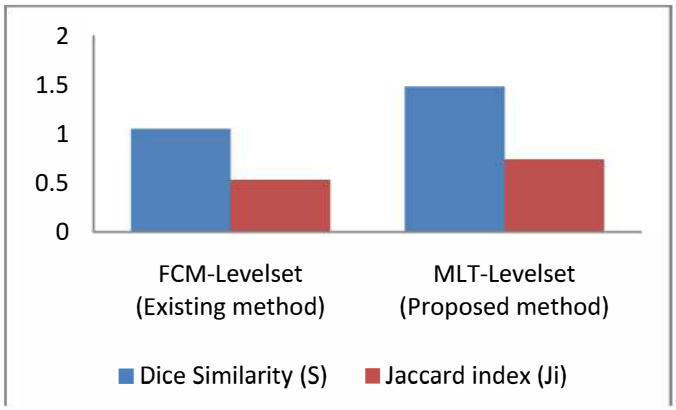

Fig. 3 Graphical representation of Dice similarity and Jaccard index for FCM-Level Set and proposed MLT-Level Set. (Higher the value of S and Ji, gives better segmentation result.)

To summarize, we proposed a new hybridized technique for the segmentation of tumor from MRI brain images. By comparing with the existing method and the ground truth provided, our proposed method demonstrate an impressive performance. However, in the future work the shape deformation feature must be improve so as to get higher segmentation accuracy.

REFERENCES

[1] Singh, P.; Bhadauria, H.S.; Singh, A., "Automatic brain MRI image segmentation using FCM and LSM" Reliability, Infocom Technologies and Optimization (ICRITO) (Trends and Future Directions), 2014 3rd International Conference, pp.1,6, 8-10 Oct. 2014.

[2] Gonzalez and R.C. Richard, Digital Image Processing, 2nd ed. India: Pearson Education, 2004.

[3] Natarajan, P.; Krishnan, N.; Kenkre, N.S.; Nancy, S.; Singh, B.P., "Tumor detection using threshold operation in MRI brain images," Computational Intelligence & Computing Research (ICCIC), 2012 IEEE International Conference, pp.1,4, 18-20 Dec. 2012.

[4] Burman,Ritambhar; Paul,Sujoy; Das,Swagatam,"A Differential Evolution Approach to Multi-level Image Thresholding Using Type II Fuzzy Sets," Swarm, Evolutionary, and Memetic Computing, 2013, 8297, 274-285, Springer International Publishing.

[5] www2.imm.dtu.dk/projects/BRATS2012/

[6] S.M. Smith. Fast robust automated brain extraction. Human Brain Mapping, 17(3):143-155, November 2002.

[7] Jasdeep Kaur and Preetinder Kaur, "Fuzzy Logic based Adaptive Noise Filter for Real Time Image Processing Applications", International Journal of Computer Applications 58(9):1-5, November 2012.

[8] Jianhua Wu; Zhaoyu Pian; Li Guo; Kun Wang; Liqun Gao, "Medical Image Thresholding Algorithm Based on Fuzzy sets Theory," Industrial Electronics and Applications, 2007. ICIEA 2007. 2nd IEEE Conference, pp.919,924, 23-25 May 2007.

[9] Chunming Li; Chenyang Xu; Changfeng Gui; Fox, M.D., "Level set evolution without re-initialization: a new variational formulation," Computer Vision and Pattern Recognition, 2005. CVPR 2005. IEEE Computer Society Conference, vol.1, pp.430,436 vol. 1, 20-25 June 2005.

[10] D Shattuck, R Leahy, BrainSuite: an automated cortical surface identification tool. Med. Imag. Anal. 6(2), 129–142 (2002).

[11] Jaccard, P., 1912. The distribution of flora in the alpine zone. New Phytologist 11, 37–50.

Identification of WBC based on Dynamic Clustering using Modified FCM Algorithm with an Approach to Optimal Result

Nur Alom Talukdar
Department of Computer Science and Engineering
Assam University
Silchar, India
+91 3842 270988
nuralom1988@gmail.com

Sudipta Roy
Department of Computer Science and Engineering
Assam University
Silchar, India
+91 3842 270990
sudipta.it@gmail.com

ABSTRACT
In medical diagnosis, analysis of the blood components is the most vital process. Among all the blood components, analysis of the White Blood Cell (WBC) is very crucial and important. Almost all types of deadly diseases including cancer are due to the abnormal presence of WBC. Proper identification of WBC is the only way for proper treatment. For the identification of WBC, in this paper, modified Fuzzy C-Means (FCM) clustering is used. In FCM, selection of the cluster is predefined and fixed based on assumption that degrades the quality of the result. It is unable to give the optimal result if the chosen cluster is wrong. In this paper, a dynamic clustering algorithm with a novel approach to produce the optimal result is proposed which can overcome these problems of classical FCM.

Keywords
White Blood Cell; Dynamic Clustering; Optimal Result; Modified FCM; Cancer.

1. INTRODUCTION
WBC has a great importance in medical diagnosis for proper treatment. WBC can be categorized into five different classes; namely neutrophils, basophils, eosinophils, lymphocytes and monocytes shown in Figure 1. Classes with "Phil" called granulocytes and indicate presence of granules. Classes with "cyte" called agranulocytes, indicates absence of granules [1].

From the study of related work and literature, it is observed that different researchers used different approach to implement FCM like, modified FCM [2], efficient FCM [3], penalized FCM [4] etc.

A method to segment image is proposed in [4] using a penalty term in FCM. The penalty term employed as a regulizer to penalize the object function of FCM. To implement this, the authors used neighborhood exception maximization approach and tried to reduce the sensitivity of FCM to noise.

ICCCT '15, September 25-27, 2015, Allahabad, India
© 2015 ACM. ISBN 978-1-4503-3552-2/15/09 $15.00
DOI: http://dx.doi.org/10.1145/2818567.2824992

Hung and Yang in [3] proposed a clustering approach to implement the FCM efficiently to reduce the computation time. For that they first recognized the centroid of the cluster from the original simplified set that accelerates the convergence time by refines the initial value of FCM.

Chinwarabhatet. al. address in [2] a work to segment WBC using modified FCM where they tried to minimize the iteration for clustering process. They used neighboring color pixel of its scattering as a reference. They considered the scattering size greater than a threshold value and then applied a thickening morphology.

In this paper, dynamic clustering approach is proposed for modified FCM algorithm for the optimal result.

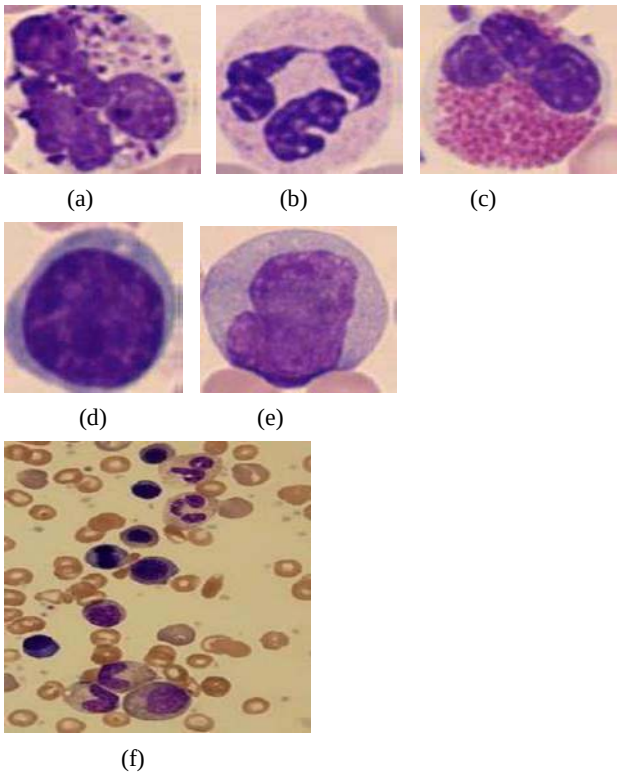

Figure 1. (a) Basophil; (b) neutrophil; (c) eosinophil (d) lymphocyte; (e) monocyte; (f) original blood image;

The rest of the paper is organized as below:

Section 2 discusses about Clustering; Fuzzy C-Means is discussed in section 3; section 4 discusses the proposed Modified

FCM. Section 5 discusses the proposed Dynamic Clustering approach using the Modified FCM. Experimental result is presented in section 6 and the work is concluded in section 7.

2. CLUSTERING

Clustering is the process of sub-dividing a data set into many parts with the homogeneity of the characteristics of data. It's a state of art approach for segmentation. Clustering of data can be done by one of the two approaches namely Hard partition (crisp) and soft partition (fuzzy). In hard partition one point of data can belong to only one cluster i.e. membership of belongingness of the data is either 0 or 1 [5][6]. Whereas in fuzzy partition one data point can belong to more than one cluster i.e. membership of belongingness of the data is between 0 and 1.

3. FUZZY C-MEANS (FCM)

FCM clustering is an approach of clustering data where each datum may belong to more than one cluster. FCM works by assigning membership to each data point corresponding to each cluster center on the basis of distance between the cluster and the data point [7][8]. It is an iteration process, the partition matrix U is updated by Equation (1).

$$\cup_{ij} = \frac{1}{\sum_{k=1}^{C}\left(\frac{\|D_{ij}\|}{\|D_{ik}\|}\right)^{\frac{2}{m-1}}} \quad (1)$$

Which is followed by the update of the cluster centers Vjby Equation (2).

$$V_j = \frac{\sum_{i=1}^{N} U_{ij}^{m} \cdot x_i}{\sum_{i=1}^{N} U_{ij}^{m}} \quad (2)$$

The algorithm is processed by minimizing Equation (3).

$$J_m\ (U,V) = \sum_{i=1}^{N}\cdot\sum_{j=1}^{C} U_{ij}^{m}\ D_{ij}^{2} \quad (3)$$

Where,

$X = \{x_1, x_2, x_3 \ldots x_n\}$ = the data,

C= cluster numbers in X,

m = fuzziness index, $1 \le m < \infty$,

U = fuzzy c-partition of X,

$V = (v_1, v_2, v_3 \ldots v_c)$ = vectors of centers,

U_{ij}= the membership value of the i^{th} datum for the j^{th} cluster, V_j= $(v_{j1}, v_{j2}, v_{j3} \ldots v_{jn})$= center of cluster j,

D_{ij}= Euclidean distance betweeni^{th} data andj^{th} cluster center using proposed metrics [9].

The FCM algorithm is stated as below:

A. Algorithm FCM

1. Set cluster number (C), Fuzziness index (m), Maximum iteration (I_{max}).
2. Initialize matrix $U^{(0)}$ as U= $[u_{ij}]$
3. For $I = 1,2,\ldots, I_{max}$, do:

   a. Update the cluster centers v_i^I using Equation (2)
   b. Update the membership matrices $U^{(I)}$ using Equation(1)
   c. Check $U^{(I)}$ with $U^{(I+1)}$,
   if $\|U^{(I+1)} - U^{(I)}\|$ < termination criteria, then stop;

   Else

   Update $U^{(I)} = U^{(I+1)}$.

4. MODIFIED FCM

The FCM algorithm works by assigning membership to each data point corresponding to each cluster center on the basis of distance between the cluster and the data point. It is an iterative process and in each iteration the cluster centers change their positions based on the distance between the data point and cluster center; distance calculation plays an important role in FCM. In modification of FCM, a new distance metric is proposed which outperforms the Euclidean metric. Experimental results are shown in the Figs. 4(a) and 4(b).

Considering the proposed metric; Equations (1), (2) and (3) can be rewritten as:

$$\cup_{ij} = \frac{1}{\sum_{k=1}^{C}\left(\frac{\|PD_{ij}\|}{\|PD_{ik}\|}\right)^{\frac{2}{m-1}}} \quad (4)$$

$$V_j = \frac{\sum_{i=1}^{N} U_{ij}^{m} \cdot x_i}{\sum_{i=1}^{N} U_{ij}^{m}} \quad (5)$$

$$J_m\ (U,V) = \sum_{i=1}^{N}\cdot\sum_{j=1}^{C} U_{ij}^{m}\ ||PD_{ij}||^2 \quad (6)$$

Where, PD is the proposed metrics and can be expressed as:

PD(x,v)= PD(v,x)=$\sqrt{\sum_{i=1}^{n}|v_i - x_i|^2}$, v and x are two points in the feature space.

5. DYNAMIC CLUSTERING APPROACH WITH MODIFIED FCM

In FCM, the selection of the cluster number is predefined, fixed and is based on assumption. It is very crucial to select the best cluster by only assumption. If the chosen cluster is wrong it degrades the quality of final result. This is a time consuming process also to select a cluster based on assumption and test the result and repeat the process for better result. In this paper a dynamic clustering approach is proposed. Instead of selecting the fixed cluster number a priory, here it is needed to select the minimum cluster to execute the clustering process. For the result optimization process, image quality measurement metric are used. The DCAMFCM algorithm is as below:

A. DCAMFCM Algorithm

1. Set minimum and maximum cluster number (C_{min} and C_{max}), Fuzziness index (m), Maximum iteration (I_{max}).
2. Initialize matrix $U^{(0)}$ as U= $[u_{ij}]$
3. For $C = 2,3,\ldots,C_{max}$, do;
4. For $I = 1,2,\ldots, I_{max}$, do:
   a. Update the cluster centers v_i^I using Equation (5)
   b. Update the membership matrices $U^{(I)}$ using Equation(4)
   c. Check $U^{(I)}$with $U^{(I+1)}$,
   if $\|U^{(I+1)} - U^{(I)}\|$ < termination criteria, then stop;

   Else

   Update $U^{(I)} = U^{(I+1)}$.
5. Check for optimal result; if optimal, then stop;

   Else

   Increment C.

6. EXPERIMENTAL RESULT

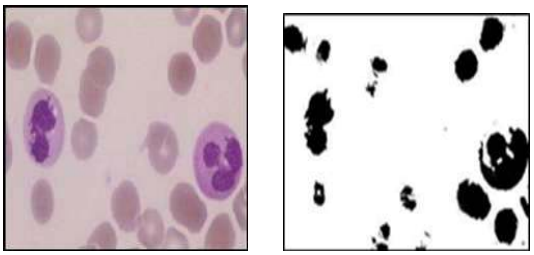

(a) (b)

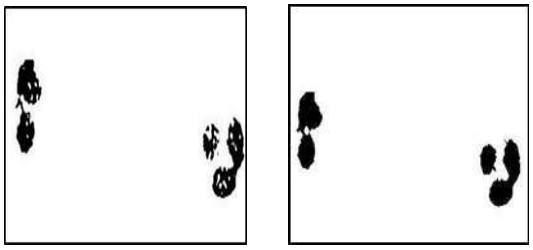

(c) (d)

Figure 2. (a) Original blood image; (b) segmented result using FCM with cluster number 3; (c) segmented result using FCM with cluster number 5; (d) segmented result with the proposed method.

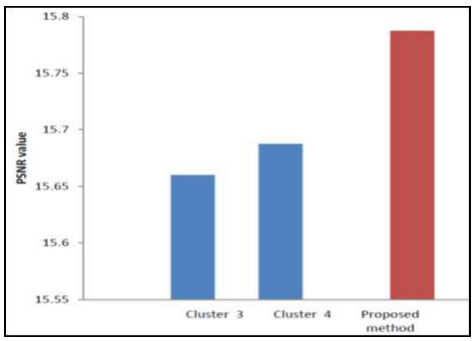

Figure 3. Graphical representation of PSNR values of regular FCM with pre-defined cluster vs. proposed method.

Figures 2(b) and (c) are segmented results of Figure 2(a) using FCM with predefined cluster number as 3 and 5 respectively. From the observation, it can be concluded that the cluster numbers did not produce the best result. Then the segmentation is done with the proposed method and depicted in Figure 2(d). It is observed that this method gives the optimal result where the cluster number is not selected a priory, overcoming the drawback.

Table 1. COMPUTING TIME OF FCM VS. MODIFIED FCM

Image	Cluster number	FCM	Modified FCM
Image (a)	2	2.52	2.03
	3	1.89	1.82
	4	7.65	5.86
	5	9.36	8.69
	6	16.51	14.35
	7	19.58	16.86
	8	22.46	19.24

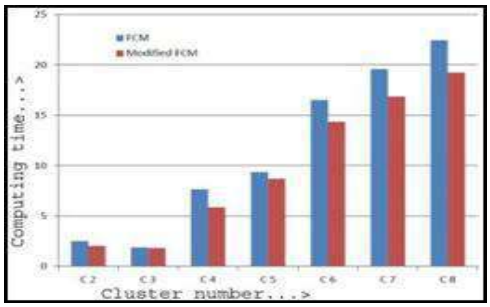

(a)

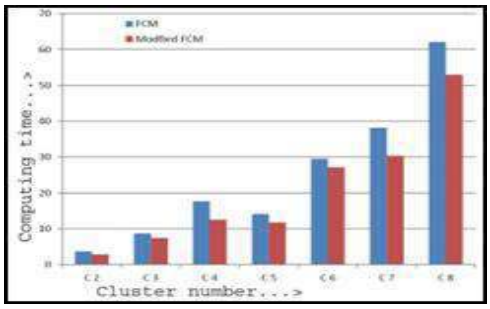

(b)

Figure 4. (a) Computing time of FCM; (b) computing time of Modified FCM.

A. Insight of the clustering process

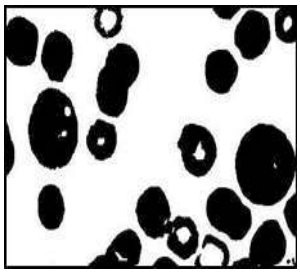

(a) cluster 2

(b) cluster 3

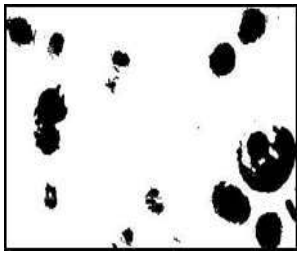

(c) cluster 4

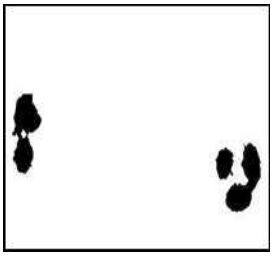

(d) cluster 5

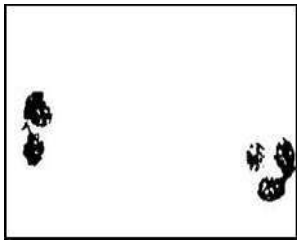

(e) cluster 6

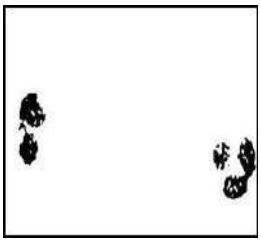

(f) cluster 7

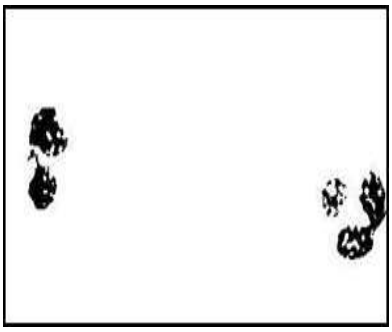

(g) cluster 8

Figure 5. Insight view of dynamic clustering with different cluster number.

7. CONCLUSION

In this research work, a novel approach of dynamic clustering has been implemented with modified FCM. The main drawback of FCM, which is unknowingly selects the cluster numbers can be overcome with the proposed method. Through the experimental result, it has been demonstrated that wrong selection of cluster may lead to the degradation of the final results. The proposed method is applied on different blood images and the method works efficiently almost with all types of blood image. Also the computation time of FCM can be reduced with the modified FCM and it does not affect the quality of the segmented result.

8. REFERENCES

[1] J.B. Nemane, V.A. Chakkarwar, P. B. Lahoti, 2013. White Blood Cell Segmentation and Counting Using Global Threshold, International Journal of Emerging Technology and Advanced Engineering, 3, 6(June 2013), 639-643.

[2] S. Chinwaraphat, A. Sanpanich, C. Pintavirooj, M. Sangworasil and P. Tosranon, A Modified Fuzzy Clustering for White Blood Cell Segmentation, 3rd International Symposium on Biomedical Engineering (ISBME 2008). 356-359.

[3] M.C. Hung, D.L.Yang, 2001. An efficiect Fuzzy C-Means Clustering Algorithm, IEEE International conference on Data mining, ICDM 2001, 225-232.

[4] Y.Yang and S.Huang, 2007. Image segmentation by Fuzzy C-Means Clustering Algorithm with a Novel Penalty Term, Computing and Informatics,26,2007,17-31.

[5] R.L. Cannon, J.V. Dave, J.C. Bezdek, 1986. Efficient Implementation of the Fuzzy c-Means ClustengAlgornthms, IEEE Transactions on Pattern Analysis and Machine Intelligence, PAMI-8, 2 (March 1986), 248-255.

[6] J.C. Bezdek, R. Ehrlich, W. Full, 1984. FCM: the Fuzzy c-Means Clustering Algorithm, Computers & Geosciences, 10, 2-3(1984), 191-203.

[7] N.B. Karayiannis, J. C. Bezdek, An Integrated Approach to Fuzzy Learning Vector Quantization and Fuzzy C-Means Clustering, IEEE Transaction On Fuzzy Systems, 5, 4 (Nov 1997), 622-628.

[8] K.L. Wu, 2012. Analysis of Parameter Selections for Fuzzy C-Means, Pattern Rcognition,45 (2012), 407-415.

[9] L. Putzu, C.D. Ruberto, White Blood Cells Identification and Counting from Microscopic Blood Image, International Journal of Medical, Health, Pharmaceutical and Biomedical Engineering, 7, 1 (2013), 15-22.

Video Shot Boundary Detection: A Review

Ananya SenGupta
Department of Computer Science & Engineering
National Institute of Technology Silchar
Assam, India
ananyasengupta1991@gmail.com

Dalton Meitei Thounaojam
Department of Computer Science & Engineering
National Institute of Technology Silchar
Assam, India
dalton.meitei@gmail.com

Kh. Manglem Singh
Department of Computer Science and Engineering
National Institute of Technology Manipur
Manipur, India
manglem@gmail.com

Sudipta Roy
Department of Information Technology
Assam University Silchar
Assam India
sudipta.it@gmail.com

Abstract— **Due to huge growth in multimedia and technology, it is very important to go through the point of interest rather than accessing the entire video. For efficient indexing and retrieving the interest points, content based video retrieval is used. The first step toward CBVR is shot boundary detection. It is necessary to partition the video into shots for easy indexing and retrieval of video. Therefore, segmentation plays an important role in digital media processing, pattern recognition, and computer vision. In this paper, we present different approaches to shot boundary detection problem.**

Keywords: Shot boundary detection, cut, dissolve, fades, wipes.

I. INTRODUCTION

Now a days, in many areas of digital libraries, hospitals, distance learning, video-on-demand, digital video broadcast, interactive TV, multimedia information large collections of digital videos are being created. Searching of videos can be text based or content based. In text based video retrieval, videos are annotated with text and a textual keyword is used for searching. Text based approach is more time consuming as well as it populates the database with a lot of data. Therefore efficient retrieval process is content based retrieval which gives more appropriate result than traditional text based approach.

Indexing, searching and retrieval of videos from large databases like YouTube, daily-motion etc. can be more efficient if we divide the entire video sequence into segments (shots). A shot is unbroken sequence of frames taken from a camera [1]. To segment the video into shots we need to locate the shot boundaries in a video. Transition of shots within a video can be of two types: abrupt and gradual transitions. Abrupt transition also known as hard cuts or cuts occur within a single frame when stopping and restarting of camera. Gradual transitions are also known as edit effects or cinematic effects, often used effects are fades, dissolve, wipes. A fade-in is a gradual increase in intensity starting from a black frame to a bright frame where as a fade-out is a gradual decrease in intensity starting from a bright frame and results to a black frame. When one frame gets superimposed on other frame i.e. frames of previous shot gets dimmer while those of second shot gets brighter, are called dissolve. A wipe is a type of transition where one shot replaces another by travelling from one side of the frame to another or with a special shape like clock, rectangle, oval etc [2]. Early work focused on cut detection, while more recent techniques deal with gradual transition detection. Abrupt transitions are easier to detect than gradual transition. Despite countless proposed approaches and techniques so far, robust algorithms for detecting various types of shot boundaries i.e. constant quality of detection for abrupt as well as gradual, have not been found yet. [3]

II. SHOT BOUNDARY DETECTION

The different approaches for shot boundary detection are:

A. Pixel comparison:

Pair wise pixel comparison between two consecutive frames evaluates the difference in intensity value of the corresponding pixel.

$$D(f, f+1) = \frac{\sum_{x=1}^{X}\sum_{y=1}^{Y}(I_f(x,y) - I_{f+1}(x,y))}{XY} \quad (1)$$

Where f and $f+1$ are two adjacent frames of size X×Y, I_f is the intensity value of pixel at coordinate (x, y) of frame f. Pixel wise comparison is limited to object and camera motion. Due to a small change in camera or object motion can result in large pixel difference [4].

B. Block based comparison:

Each frame is divided into n blocks and each block is compared with corresponding block of next frame. A transition is declared if the number of changed blocks between two consecutive frames is greater than a given threshold.

Each frame is divided into blocks mean of each block is taken which results in statistical image (reduced image). [5][6]

978-1-4799-6085-9/15/$31.00©2015

Mean Square Error of corresponding pixels is calculated for adjacent statistical frames to find the exact wipe transition region. They used Hough transform to determine the thickness of the strips in statistical image (single line or two lines). Value of average gradient and number of lines determines the wiping pattern [5]. In [7] technique based on pixel wise difference between consecutive frame is calculated for wipe transition detection and some methodologies based on horizontal, vertical and box- shaped wiping pattern is considered. The X and Y trajectory estimation of boundary line (horizontal, vertical, diagonal, clock) between two adjacent frame is calculated in [8].

Sugano M. et al [9] used techniques to locate abrupt, dissolve and wipes in compressed domain. A frame is considered as abrupt shot boundary if sum of forward prediction macro blocks and intra macro blocks is greater than a predefined threshold T_1 and number of backward macro blocks are smaller than T_2 where $T_1 > T_2$.(P and I frames). In case of B frames, number of forward macro blocks is less than T_3 , and sum of backward prediction and intra macro blocks is greater than T_4 where $T_4 > T_3$.

C. Histogram comparison:

For digital images, a color histogram represents the number of pixels that have fixed colors in color range. A color histogram can be build for color space like RGB, HSV, CMYK, YC_bC_r [10] etc. [4]

i. *Global histogram comparison*:

Histogram of two successive frames is computed and compared. If the histogram difference is greater than some predefined threshold then a transition happens.

$$D(f, f+1) = \sum_{i=1}^{n} \left| H_f(i) - H_{f+1}(i) \right| \qquad (2)$$

Where $H_f(i)$ is the histogram value for gray level i of frame f and n is the total number of gray levels.

ii. Local histogram comparison:

Each frame is divided into n blocks and histogram of each block is compared with histogram of corresponding block of next frame.

$$D(f, f+1) = \sum_{k=1}^{x} \sum_{i=1}^{n} (H_f(i,k) - H_{f+1}(i,k)) \qquad (3)$$

Where $H_f(i,k)$ is the histogram value for gray level i for block k of frame f and x is the total number of blocks.

Xue L. et al [11] proposed an algorithm that improves performance by eliminating smooth intervals from video. Features such as pixel wise difference, HSV color histogram and edge histogram are of the new video sequence are extracted and given as input vectors to support vector machine. The outputs of SVM are classified into three categories as abrupt, gradual and etc.

Using HSV color histogram difference and adaptive threshold hard cuts are detected in [12] [9]. They also calculated the local histogram difference and local adaptive threshold for gradual shot transition detection.

Histogram is extracted from each video frames and a matrix is created from the histogram values as the column of the matrix and Singular Value Decomposition is applied to the matrix thereby reducing the feature vector and provides fast computation [13][14][15]. Similarity measures like Euclidian [13] and cos distance [14] [15] distance are used to find the abrupt and gradual transitions. In [15], an inverted triangle pattern matching is used to find the gradual transitions.

[16] Deals with the false shot boundary detection due to flash light. If the histogram difference is greater that a predefined threshold then flash light detector is invoked. In flashlight model two models are introduced namely cut model (for cut detection) and flash model (flash light detection). The model for flash light is average intensity changes from one level to another on occurrence of flashlight and comes back to the original level after one frame.

A modification to simple histogram comparison technique is presented in [17]. Initially I frames are extracted from the MPEG video stream. Intensity, row/horizontal, column/vertical histograms are computed for all the I frames and compared by chi-square test [18]. Both algorithms operate in the compressed domain, requiring only partial decoding of the compressed video stream.

The first step towards video scene segmentation and indexing is shot detection as described in [19] [20]. They used twin threshold approach which means a high threshold *Th* and a low threshold *Tl* is selected and if gray level histogram difference, *D* of two adjacent frames is larger than *Th*, a cut is declared. If *D* is larger than *Tl* and less than *Th*, they are accumulated. Now if accumulated difference is greater than *Th*, a gradual transition exists.

Joyce and Liu [21] presented two algorithms for detecting dissolve and wipes. The first is a dissolve detection algorithm which is implemented both as a simple threshold-based detector and as a parametric detector by modelling the error properties of the extracted statistics. The second is an algorithm to detect wipes based on image histogram characteristics during transitions.

Pardo A. [22] proposed an algorithm for hard cut detection that gives better results than feature based, pixel based or simple histogram based approaches. Initially inter frame histogram difference between frames are calculated for a set of bins. Probability for inter frame difference to be greater than a predefined threshold is set and tested. If a shot change occurs, histogram difference is expected to be more whereas for no shot change, histogram difference is expected to be less and in agreement with previous histogram difference.

D. Feature based video segmentation:

a. Local features based segmentation:

SIFT [23], SURF [24] and MSER [25] [26] are local feature descriptor. Local features of successive frames are computed

and compared. If the numbers of matched features are less than some predefined threshold, a transition is declared.

To reduce computational cost and improve performance, non shot boundary frames are removed from the original video. SIFT features [23] are extracted from the frames belonging to only shot boundaries to identify the abrupt and gradual transition [27].

Deepak, C. R., et al [28] proposed an algorithm for shot boundary detection using color correlogram and Gauge Speeded-up robust features [29]. Initially linear frame comparison of color correlogram and G-SURF features are extracted for transition detection. To improve performance same method is applied by extracting key frames of the video sequence.

In [30], feature vector of each frame is computed by applying local feature transform (LFT) on each frame. After applying LFT on each frame of the video sequence, features are extracted and first and second moments are computed for channels of colour space to compute the feature vector.

A frame is considered as abrupt boundary if it has less/ no matched SURF features [24] with its successive frame. For fade detection, entropy of all the frames are computed and compared with adjacent frames. [31] Uses both local features (SURF) and global features (entropy) for video segmentation.

b. Global feature based segmentation:

Colour, texture, shape, edge, text, audio [32] and motion features of a frame are computed and compared with the next frame.

Counting the entering and exiting edge pixels between two consecutive frames shot boundary can be detected. A part from counting the number of entering and exiting edge pixels, cuts, fades, wipes and dissolve is located in presence of camera and image motion by computing global motion between frames [33] using image registration technique described in [34].

Hauptman et al [35] used text features to segment video which was implemented in Informedia Digital Video Library Project at Carnegie Mellon University.

Shot boundary detection in the presence of illumination change, fast object motion, and fast camera motion Mishra, R., Singhai, S. K., & Sharma M. [36] proposed an algorithm that extracts structure feature of each frame and similarity is computed between adjacent frames. Structure feature is extracted by using dual tree complex wavelet transform (CWT) [37].

In [38] mutual information and joint entropy is calculated between all pairs of frames. Object motion and shot transition is detected with canny edge detector.

Uncompressed sports video consists of huge camera movement, similar background and motion of dissimilar objects. [39] Describes an algorithm based on feature correlation, histogram difference and running average difference for hard cut detection in this type of videos. Also a motion based algorithm to identify shots cut is proposed in [40]. By calculating the normalized correlation between blocks of frames and locating the maximum correlation coefficient, an inter frame difference metric is generated.

An object based shot boundary detection is described in [41] and [42] for abrupt and gradual transition detection. A time stamp is attached with each object to locate the number of frames in which that particular object appears. Change is object appearance is considered as shot transition. Object tracking using some modification to Canny's egde detection algorithm is shown in [41]. The limitations of object based detection [41] [42] are large object movements, if objects suddenly disappear in the frames, flashlight light scenes [41].

Mutual information and joint entropy are calculated for all the frames of video. The amount of information transported to the next frame is mutual information which is sufficient for detecting cuts where intensity changes abruptly. For fade in/out, joint entropy between two consecutive frames are calculated for each components of RGB. [43] [44]

Cuts and wipes are detected using Markov energy model based on color and texture discontinuities in shot boundaries. Texture and color features and are computed by Gabor decomposition [45] and RGB histogram respectively. All computations are performed on spatio-temporal slices (collection of 1D image in sequence). For dissolve detection, within a specific time interval, mean intensity and variance of a slice is calculated. The periods having constant mean values and concave upward parabola curves are considered as dissolve. [46]

X. Gao, J. Li, and Y. Shi [47] proposed an algorithm that extracts a set of corner-points (features) from the first frame of a shot. Using Kalman Filtering [48] these features are matched with the features of the subsequent frames, accordingly with the changing pattern of pixel intensity shot boundary is detected.

An algorithm for video segmentation in uncompressed domain is proposed in [28]. For abrupt transition detection only I frames are uncompressed to DC images and characters of these DC images are extracted and compared with the adjacent DC image. For gradual transition, the range of shot boundary is detected by CDDC algorithm and located by the change in amount of intra coding macro blocks in P frames.

DC images are extracted from MPEG video and features are extracted and selected through Ada Boost [49] for cut detection [50]. A fade out followed by fade in is detected by considering the change in luminance, where the intensity values shows a V-shaped graph, detection of dissolve is identification of downward parabola / U- shaped pattern [50].

E. Clustering based approach:

In this approach, n frames are selected at random as initial cluster centres. The distance between each frame and cluster centres are calculated and the frames with small distance are clustered together. The common clustering algorithms are fuzzy clustering [51], mean sift clustering [52], K means clustering [53] etc.

B.Han, X.Gao, and H.Ji [54] used techniques Fuzzy c-means clustering (abrupt detection), Gaussian Weighted

Housdorff Distance and edge count ratio (fade transition), method based on similarity of color distribution (dissolve transition) and motion vector based on the three-dimension wavelet transformation (wipe transition).

A pre-processing technique [15][55] or frame skipping technique [56] is used to reduce the computing time thereby finding cluster/group of frames where a possible abrupt or gradual transitions may present by using thresholding technique.

Table 1: List of survey

Year	Reference	Author
2001	[57]	Koprinska I. et al.
2001	[58]	Lienhart, R
2002	[3]	Hanjalic A.
2006	[59]	Cotsaces, C
2007	[60]	Jinhui Yuan et al
2008	[61]	Geetha P. et al.
2014	[62]	Sao Nikita et al.
2014	[32]	Thounaojam D. M et al

Table 2: Results of some existing algorithm

Year	Reference	Abrupt	Fade	Dissolve	Wipes
1995	Zahib R. et al[33]	✓	✓	✓	✓
1997	Patel N.V. et al [17]	✓	×	×	×
1998	Sugano M. et al [9]	✓	✓	×	✓
1999	C. W. Ngo et al [34]	✓	×	✓	✓
2000	Gong Y. et al [13]	✓	✓	✓	✓
2001	D. Zhang et al [16]	✓	×	×	×
2001	W.J. Heng et al [41]	✓	✓	✓	✓
2003	Porter et al [40]	✓	×	×	×
2006	Joyce et al [21]	×	×	✓	✓
2006	Zuzana C. et al[43]	✓	✓	×	×
2006	Pardo A. [22]	✓	×	×	×
2008	Huan et al [38]	✓	✓	✓	×
2009	A.Hameed [39]	✓	×	×	×
2009	Ren J. eta al [45]	✓	✓	✓	×
2010	Chen H. et al [20]	✓	✓	✓	✓
2011	Hua Z. et al [12]	✓	✓	✓	×
2011	B.H. Shekar et al[30]	✓	×	×	×
2013	Baber J. et al [31]	✓	✓	×	×

III. COMPARISON OF SOME EXISTING TECHNIQUES

Table 3 shows some of the simple video shot boundary detection techniques. In this, a threshold is selected experimentally and no specific thresholding technique is applied. Only abrupt transitions are considered for the comparison.

Table 3: Results for abrupt transition

Video	anni003.mpg	hcil2001_01.mpg	indi002.mpg
Frame no.	4297	4202	845
No. of Cut	24	20	6
Color Histogram Difference [12]	21	20	6
Pixel Difference [4]	18	18	4
Mean and Standard Deviation	22	19	5
MSER [26]	22	20	6

The videos are downloaded from OPEN VIDEO PROJECT. The threshold is selected through experiments and the result can be met more efficient if we apply some verification system [31].

IV. CONCLUSION

Video shot segmentation is the first step towards automatic annotation and indexing of digital video for efficient browsing and retrieval. In this paper we presented different approaches for shot boundary detection and comparison of results among some algorithm. The system can be improved, if the output is verified further whether it is actual abrupt or gradual transitions. In almost all the algorithms, abrupt transitions are effectively detected than gradual transitions. Lighting effect (flash), large object motion in front of camera, fast camera motion, etc., are some of the challenges in detecting gradual transitions as it produces false detection.

ACKNOWLEDGEMENT

We are thankful to the OPEN VIDEO PROJECT for providing the video data free and for the use of it in the research purpose.

REFERENCES

[1] Chung-Lin Huang; Bing-Yao Liao, "A robust scene-change detection method for video segmentation," *Circuits and Systems for Video Technology, IEEE Transactions on* , vol.11, no.12, pp.1281,1288, Dec 2001

[2] Koprinska, I., &Carrato, S. (2001). Temporal video segmentation: A survey. Signal processing: Image communication, 16(5), 477-500

[3] Hanjalic, A., "Shot-boundary detection: unraveled and resolved?," *Circuits and Systems for Video Technology, IEEE Transactions on* , vol.12, no.2, pp.90,105, Feb 2002

[4] Jadon, R. S., Santanu Chaudhury, and K. K. Biswas. "A fuzzy theoretic approach for video segmentation using syntactic features." Pattern Recognition Letters 22.13 (2001): 1359-1369.

[5] Fernando, W.A.C.; Canagarajah, C.N.; Bull, D.R., "Wipe scene change detection in video sequences," *Image Processing, 1999. ICIP 99. Proceedings. 1999 International Conference on* , vol.3, no., pp.294,298 vol.3, 1999

[6] Chavan, S., Fanan, S., &Akojwar, S. (2014). An Efficient Method for Detection of Wipes in Presence of Object and Camera Motion

[7] Min Wu; Wolf, W.; Liu, B., "An algorithm for wipe detection," *Image Processing, 1998. ICIP 98. Proceedings. 1998 International Conference on* , vol.1, no., pp.893,897 vol.1, 4-7 Oct 1998

[8] Campisi, P.; Neri, A.; Sorgi, L., "Wipe effect detection for video sequences," *Multimedia Signal Processing, 2002 IEEE Workshop on* , vol., no., pp.161,164, 9-11 Dec. 2002

[9] Sugano, M.; Nakajima, Y.; Yanagihara, H.; Yoneyama, A., "A fast scene change detection on MPEG coding parameter domain," *Image Processing, 1998. ICIP 98. Proceedings. 1998 International Conference on* , vol.1, no., pp.888,892 vol.1, 4-7 Oct 1998.

[10] Tkalcic, M., & Tasic, J. F. (2003, September). Colour spaces: perceptual, historical and applicational background. In *Eurocon.*

[11] Xue Ling; Li Chao; Li Huan; Xiong Zhang, "A General Method for Shot Boundary Detection," *Multimedia and Ubiquitous Engineering, 2008. MUE 2008. International Conference on* , vol., no., pp.394,397, 24-26 April 2008

[12] Hua Zhang; Ruimin Hu; Lin Song, "A shot boundary detection method based on color feature," *Computer Science and Network Technology (ICCSNT), 2011 International Conference on* , vol.4, no., pp.2541,2544, 24-26 Dec. 2011

[13] Gong, Yihong, and Xin Liu. "Video shot segmentation and classification." In*Pattern Recognition, 2000. Proceedings. 15th International Conference on*, vol. 1, pp. 860-863. IEEE, 2000.

[14] Cernekova, Zuzana, Constantine Kotropoulos, and Ioannis Pitas. "Video shot segmentation using singular value decomposition." In *Acoustics, Speech, and Signal Processing, 2003. Proceedings.(ICASSP'03). 2003 IEEE International Conference on*, vol. 3, pp. III-181. IEEE, 2003.

[15] Zhe-Ming Lu; Yong Shi, "Fast Video Shot Boundary Detection Based on SVD and Pattern Matching," *Image Processing, IEEE Transactions on* , vol.22, no.12, pp.5136,5145, Dec. 2013.

[16] Zhang, Dong, Wei Qi, and Hong Jiang Zhang. "A new shot boundary detection algorithm." In *Advances in Multimedia Information Processing—PCM 2001*, pp. 63-70. Springer Berlin Heidelberg, 2001.

[17] Patel, N. V., &Sethi, I. K. (1997). Video shot detection and characterization for video databases. *Pattern Recognition*, *30*(4), 583-592.

[18] Chi-square tests. Defense Technical Information Center, 1976

[19] Zhang, Hong Jiang, Atreyi Kankanhalli, and Stephen W. Smoliar. "Automatic partitioning of full-motion video." *Multimedia systems* 1.1 (1993): 10-28

[20] Hui Chen; Cuihua Li, "A practical method for video scene segmentation," *Computer Science and Information Technology (ICCSIT), 2010 3rd IEEE International Conference on* , vol.9, no., pp.153,156, 9-11 July 2010

[21] Joyce, R.A.; Liu, B., "Temporal segmentation of video using frame and histogram space," *Multimedia, IEEE Transactions on* , vol.8, no.1, pp.130,140, Feb. 2006

[22] Pardo, Alvaro. "Probabilistic shot boundary detection using interframe histogram differences." *Progress in Pattern Recognition, Image Analysis and Applications.* Springer Berlin Heidelberg, 2006. 726-732

[23] Lindeberg, T. (2012). Scale invariant feature transform. Scholarpedia, 7(5), 10491.

[24] Bay, Herbert, TinneTuytelaars, and Luc Van Gool. "Surf: Speeded up robust features." *Computer Vision–ECCV 2006*. Springer Berlin Heidelberg, 2006. 404-417.

[25] Donoser, M.; Bischof, H., "Efficient Maximally Stable Extremal Region (MSER) Tracking," *Computer Vision and Pattern Recognition, 2006 IEEE Computer Society Conference on* , vol.1, no., pp.553,560, 17-22 June 2006.

[26] Anjulan, A.; Canagarajah, N., "Video Scene Retrieval Based on Local Region Features," *Image Processing, 2006 IEEE International Conference on* , vol., no., pp.3177,3180, 8-11 Oct. 2006.

[27] Jun Li; Youdong Ding; Yunyu Shi; Wei Li, "Efficient Shot Boundary Detection Based on Scale Invariant Features," *Image and Graphics, 2009. ICIG '09. Fifth International Conference on* , vol., no., pp.952,957, 20-23 Sept. 2009

[28] Deepak, C.R.; Babu, R.U.; Kumar, K.B.; Krishnan, C.M.R., "Shot boundary detection using color correlogram and Gauge-SURF descriptors," *Computing, Communications and Networking Technologies (ICCCNT),2013 Fourth International Conference on* , vol., no., pp.1,5, 4-6 July 2013

[29] Alcantarilla, Pablo F., Luis M. Bergasa, and Andrew J. Davison. "Gauge-SURF descriptors." *Image and Vision Computing* 31.1 (2013): 103-116.

[30] B. H. Shekar, M. SharmilaKumari, and RaghuramHolla. "Shot boundary detection algorithm based on color texture moments." *Computer Networks and Information Technologies.* Springer Berlin Heidelberg, 2011. 591-594.

[31] Baber, J., Afzulpurkar, N., & Satoh, S. I. (2013). A framework for video segmentation using global and local features. *International Journal of Pattern Recognition and Artificial Intelligence*, *27*(05).

[32] Thounaojam, D. M., Trivedi, A., Singh, K. M., & Roy, S. (2014). A Survey on Video Segmentation. In *Intelligent Computing, Networking, and Informatics* (pp. 903-912). Springer India.

[33] Zabih, R., Miller, J., & Mai, K. (1999). A feature-based algorithm for detecting and classifying production effects. *Multimedia systems*, *7*(2), 119-128.

[34] Ngo, C.W.; Pong, T.C.; Chin, R.T., "Detection of gradual transitions through temporal slice analysis," *Computer Vision and Pattern Recognition, 1999. IEEE Computer Society Conference on.* , vol.1, no., pp.,41 Vol. 1, 1999

[35] Hauptmann, A., and M. Smith. "Text, Speech, and Vision for Video Segmentation: The Informedia TM Project." *AAAI fall symposium, computational models for integrating language and vision.* 1995.

[36] Mishra, R., Singhai, S. K., & Sharma, M. (2013, February). Video shot boundary detection using dual-tree complex wavelet transform. In *Advance Computing Conference (IACC), 2013 IEEE 3rd International* (pp. 1201-1206). IEEE.

[37] Selesnick, I.W.; Baraniuk, R.G.; Kingsbury, N.C., "The dual-tree complex wavelet transform," *Signal Processing Magazine, IEEE* , vol.22, no.6, pp.123,151, Nov. 2005.

[38] Zhao Huan; Li Xiuhuan; Yu Lilei, "Shot Boundary Detection Based on Mutual Information and Canny Edge Detector," *Computer Science and Software Engineering, 2008 International Conference on* , vol.2, no., pp.1124,1128, 12-14 Dec. 2008

[39] Hameed, A., "A novel framework of shot boundary detection for uncompressed videos," *Emerging Technologies, 2009. ICET 2009. International Conference on* , vol., no., pp.274,279, 19-20 Oct. 2009

[40] Porter, S., Mirmehdi, M., Thosmas, B.: Temporal video segmentation and classification ofedit effects. Image Vis. Comput. 21(13), 1097–1106 (2003).

[41] Heng, W. J., &Ngan, K. N. (2001). An object-based shot boundary detection using edge tracing and tracking. *Journal of Visual Communication and Image Representation*, *12*(3), 217-239.

[42] Wei Jyh Heng; Ngan, K.N., "Integrated shot boundary detection using object-based technique," *Image Processing, 1999. ICIP 99. Proceedings. 1999 International Conference on* , vol.3, no., pp.289,293 vol.3, 1999

[43] Cernekova, Z.; Pitas, I.; Nikou, C., "Information theory-based shot cut/fade detection and video summarization," *Circuits and Systems for Video Technology, IEEE Transactions on* , vol.16, no.1, pp.82,91, Jan. 2006

[44] Cernekova, Z., Nikou, C., & Pitas, I. (2002, June). Shot detection in video sequences using entropy based metrics. In *Image Processing. 2002. Proceedings. 2002 International Conference on* (Vol. 3, pp. III-421). IEEE.

[45] Jain, A.K.; Farrokhnia, F., "Unsupervised texture segmentation using Gabor filters," *Systems, Man and Cybernetics, 1990. Conference Proceedings., IEEE International Conference on* , vol., no., pp.14,19, 4-7 Nov 1990

[46] Ngo, C.W.; Pong, T.C.; Chin, R.T., "Detection of gradual transitions through temporal slice analysis," *Computer Vision and Pattern Recognition, 1999. IEEE Computer Society Conference on.* , vol.1, no., pp.,41 Vol. 1, 1999

[47] Gao, Xinbo, Jie Li, and Yang Shi. "A video shot boundary detection algorithm based on feature tracking." *Rough Sets and Knowledge Technology*. Springer Berlin Heidelberg, 2006. 651-658.

[48] Haykin, S. S. (Ed.). (2001). *Kalman filtering and neural networks* (pp. 123-174). New York: Wiley.

[49] Freund, Yoav, and Robert E. Schapire. "A desicion-theoretic generalization of on-line learning and an application to boosting." *Computational learning theory*. Springer Berlin Heidelberg, 1995

[50] Jinchang Ren; Jianmin Jiang; Juan Chen, "Shot Boundary Detection in MPEG Videos Using Local and Global Indicators," *Circuits and Systems for Video Technology, IEEE Transactions on* , vol.19, no.8, pp.1234,1238, Aug. 2009

[51] Chi-Chun Lo; Shuenn-Jyi Wang, "Video segmentation using a histogram-based fuzzy c-means clustering algorithm," *Fuzzy Systems, 2001. The 10th IEEE International Conference on* , vol.2, no., pp.920,923 vol.3, 2-5 Dec. 2001

[52] Lu Bei, Li Qiuhong. Video key-frame-extraction based on block localfeatures and mean shift clustering. Wireless Communications Networking and Mobile Computing,2010, 1-4

[53] B Gunsel, AFerman,A M Tekalp. Temporal video segmentation usingunsupervised clustering and semantic object tracking[J].Journal of Electronic Imaging, 1998;7(3):592-604.

[54] Han, Bing, XinboGao, and HongbingJi. "A unified framework for shot boundary detection." *Computational Intelligence and Security*. Springer Berlin Heidelberg, 2005. 997-1002.

[55] Y. N. Li, Z. M. Lu, and X. M. Niu, "Fast video shot boundary detection framework employing pre-processing techniques," *IET Image Process.*, vol. 3, no. 3, pp. 121–134, Jun. 2009.

[56] Gao, Yue, Jun-Hai Yong, and Fuhua Frank Cheng. "Video shot boundary detection using frame-skipping technique." *2011-02-18. http://www. cs. uky. edu/-cheng/PUBL/Paper BD 1. pdf*.

[57] Koprinska, I., &Carrato, S. (2001). Temporal video segmentation: A survey. Signal processing: Image communication, 16(5), 477-500

[58] Lienhart, R. (2001). Reliable transition detection in videos: A survey and practitioner's guide. International Journal of Image and Graphics, 1(03), 469-486.

[59] Cotsaces, C.; Nikolaidis, N.; Pitas, I., "Video shot detection and condensed representation. a review," *Signal Processing Magazine, IEEE* , vol.23, no.2, pp.28,37, March 2006

[60] Jinhui Yuan; Huiyi Wang; Lan Xiao; Wujie Zheng; Jianmin Li; Fuzong Lin; Bo Zhang, "A Formal Study of Shot Boundary Detection," Circuits and Systems for Video Technology, IEEE Transactions on , vol.17, no.2, pp.168,186, Feb. 2007.

[61] Geetha, P., and Vasumathi Narayanan. "A survey of content-based video retrieval." Journal of Computer Science 4.6 (2008): 474.

[62] Sao, Nikita, and Ravi Mishra. "A survey based on Video Shot Boundary Detection techniques."

An Impressive Approach for Incorporating Parallelism in Designing DMFB with Cross Contamination Avoidance

Debasis Dhal[1], Piyali Datta[2], Arpan Chakrabarty[2], Sudipta Roy[1], and Rajat Kumar Pal[2]

[1] ***Department of Information Technology, Triguna Sen School of Technology***
Assam University, Silchar, Cachar – 788 011, Assam, India
Debasisdhal06@gmail.com, sudipta.it@gmail.com

[2] ***Department of Computer Science and Engineering, University of Calcutta***
92, A. P. C. Road, Kolkata – 700 009, West Bengal, India
piyalidatta150888@gmail.com, arpan250506@gmail.com, pal.rajatk@gmail.com

Abstract— **These days, in emergency, multiple assay operations are required to be performed at parallel. Area of a given chip as a constraint, how efficiently we can use the chip and how much parallelism can be built-in are the objectives of this paper. A typical application of an assay may characterize a sample where, say only one type of reagent and multiple samples have been considered, or vice versa, and identify some factor(s) of the sample(s) under requirement in parallel. A generalized application may also consider more samples and more reagents for respective findings at parallel. In our experimentation, we effectively do this task in parallel for five such sets of sub regions of a given restricted sized chip in Digital microfluidics using an array based partitioning pin assignment technique, where cross contamination problem has also been considered, and efficiency of proper taxonomy of a given sample has also been improved.**

I. INTRODUCTION

In recent years, biochips have been evolved as an enormous rebellion in terms of performance and efficiency to discover the status of samples. At the present time, it is the most advanced device in the micro-level for diagnosing, more specifically for analyzing, testing, and detecting some specimen like blood, stool, urine, cough, saliva, DNA, and many others that we like to examine in our everyday life for many reasons. Now even if the biochips have already been deployed, there are some challenging scopes for making its performance better. This device is usually known as DMFB (Digital Microfluidic Biochip) [1,2,5,6,9] (or DMFS (Digital Microfluidic System)). The tasks that a biochip can perform are droplet creation (or dispense of droplet), transportation (or routing of droplet), mixing (or amalgamation of sample and reagent droplets), and sensing (or detection of ingredients present in a sample); such tests are much more cost-intensive and time-consuming if the same is performed in a pathological laboratory than that we do (or suggest) using a microarray biochip.

This technology of digital microfluidics has the capability to handle fluids and their movement on a chip. As the tasks could be programmed, the movement of droplets follows a laboratory procedure which is entirely automated, and that is why such a chip based laboratory experimentation is also called 'Lab-on-a-Chip' (LOC). The application of such a microfluidic biochip is mostly observed in Biochemistry and in Biomedical sciences; it is realized at the level of microelectronic arrays of electrodes (or cells) that can be viewed as an advancement of technology over VLSI. These devices operate on microlitre or nanolitre volume of biological samples and chemical reagents, which are routed right through the chip using electrowetting in a 'digital' manner under clock control on a 2D array of electrodes [23]. These electrodes in a DMFB combine Electronics with Biology (and/or Chemistry) and integrate various bioassay operations from sample preparation to detection. The primary objective of such experimentation is to minimize the time required to get the result(s) of the assay using micro- and nano-level samples and reagents, where the perfectness of results is the key requirement to be augmented.

A. The Digital Microfluidic Biochip (DMFB)

The name of the device DMFB is commonly known as Electro-Wetting-on-Dielectric (EWOD) toolkit [9]. This EWOD is usually made with the help of a sufficient number of unit cells. It makes a two-dimensional (2D) array. Fig. 1(a) shows a typical $m \times n$ 2D array of microfluidic biochip showing two droplets and one detection site. Fig. 1(b) shows a cross sectional side view of the biochip. Also it represents a typical detection site, where a mixed droplet can be detected optically and generate some desired results. This site (or the electrode) should be transparent such that light of a preferred strength can go through it. One LED is placed, say at the bottom side and a photoelectric diode is placed on the other side of the electrode (as shown in Fig. 1(b)).

Note that a droplet, either single or mixed, is sandwiched by the two plates placed in a cell of an array that are known as top plate and bottom plate. Each top plate contains ground electrode and each bottom plate contains control electrode. In the past, many small devices were invented that are capable to perform a particular job, such as detector which can detect particular signals, flow sensors which can determine the intensity of flow of mixed droplets only, etc. But EWOD is a combination of many such devices that can execute many tasks like transportation of liquid, division of one droplet into two droplets, merging of two droplets into one droplet, detecting and discarding, and so on. Some of the characteristics of such a device are higher throughput, minimal human intervention, higher sensitivity, smaller sample / reagent consumption, and increased productivity [6,9,14].

The concept of DMFB took place only in two decades back. The key sense of DMFB is that a unit volume of some fluid under

test is constant. It depends on the geometry of the system, an array that consisting of cells of electrodes of a matching size (to the droplet). This system is based on volume flow rate and again the volume flow rate is based on the number of droplets transported for performing some assay. This is how a droplet constitutes the fluid volume. The volume of these droplets may be several microlitres. This very small amount of liquid acts on the principle of modulating the interfacial tension between a liquid and an electrode coated with a dielectric layer of insulation [9].

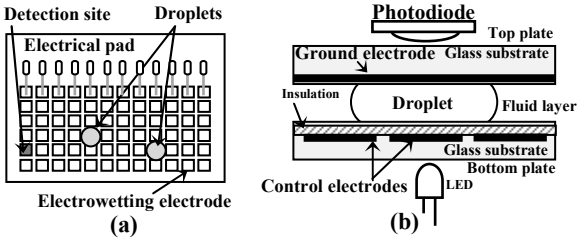

Fig. 1. (a) Top view of a microfluidic array with two droplets and a detection site. (b) A cross sectional side view of digital microfluidic platform (of a cell) with a conductive glass plate present in a detection site referring to Fig. 1(a).

An electric field established in the dielectric layer creates an inequality of interfacial tension if the electric field is applied to only one end of the droplet on an array that forces the droplet to move. Typically, 20–80 V is applied to each electrode [6,9].

B. Problem under Consideration and Its Importance

To achieve high throughput, numerous bioassay operations are supposed to be executed at the same time. Besides, we have to stay away from droplet interference as well as contamination problems at the cost of minimum number of pins, i.e., the stipulation for availability of a minimum number of distinctive input voltages. In biomedical fields we may have to perform the operations as mentioned in the following cases:

Case I: Same diagnosis may have to be performed on multiple samples. So, there can be one reagent which is to be mixed with different samples separately and then individual optical detection is made.

Case II: Different diagnosis may have to be performed on a particular sample with the help of several reagents that are to be mixed with one sample in isolation and then it is sent for detection optically.

Case III: In order to achieve good approximation, sometimes it is required to perform the same diagnosis on a given sample several times, and then the average of the results is considered for further processing.

The abovementioned cases are very much time consuming even using an LOC. To reduce the total time and to get accurate results in a reasonable amount of time, often the task(s) is (are) required to be performed in parallel. Hence, multiple operations often can be performed at the same time, if all the constraints and requirements are maintained up to a desired level of satisfaction. Mixing between proper reagent and sample is the main operation, which takes maximum time [9] with respect to transportation and detection of droplets. So, we need to adopt parallel distribution of reagent and/or sample to proper region on a chip such that mixing can be performed in parallel. In our design procedure we like to formulate a technique that ensures performance as well as efficiency of the detection process in a reasonable amount of time in parallel. Here we focus to take a kind of design procedure which can be used in the above three cases that needs massive parallelism. Böhringer [4] talked about parallel tasks, but it is not in the true sense of mixing in parallel or detection in parallel; this parallelism is true for simultaneous movement of droplets only.

II. Some Fundamental Tasks and Inherent Constraints

A. Fundamental Tasks

In this section, we define some terms coupled to the problem of DMFB in a few words. We know that in such a chip droplets are dispensed from the outside of an array. So, there are several sources of droplets; these are either sample droplet that we like to test or reagent droplet that is mixed with sample for detection, or wash droplet for washing the cells used for droplet movement.

Droplet creation is a process of making a desired sized droplet from a source of the material we like to dispense into the array perpendicularly by activation and deactivation of adjacent electrodes. It is an additional task of creating a droplet that happens outside the array for a minimum of three clock pulses. A *routing path* is the passageway that a droplet uses for its movement following adjacent cells of an array through a synchronized activation and deactivation of the electrodes. Length of such a path is usually measured by the number of cells belonging to the path from one module to another module.

Mixing is the most important operation that is occurred in a module called *mixer*. Here different sample(s) and reagent(s) come from their respective sources and mix for detection. The *mixing* operation takes a maximum amount of time needed for an assay. There are varieties of mixing procedures. During mixing of two droplets, a mixed droplet may be routed in a different pattern of movement like circular or zigzag way of rotation, etc. Accordingly, mixer size also vary like 1×2, 1×3, 2×2, 2×3, 2×4 [12,13,15], etc. A mixer can also be used for splitting of a droplet or dilute a sample droplet. A typical mixer takes 1000–2000 clock cycles. Mixing completion time depends on the size of a mixer and the number of droplets to be mixed along with their viscosity.

The *detection site* is a small module usually formed by a single cell in the array that helps to detect the parameters present in a sample from its mixed droplet. As optical detection is done in such a site, the electrodes used in that cell are transparent and light of an LED can pass through it, and a photodiode placed on the top (see Fig. 1(b)) can measure the intensity of light [17] that can detect anomalies, if any in the sample. Usually, as it is a costly module, the number of detection sites is not many and their locations are also tentatively fixed.

An *assay* is a whole operation that includes creation of droplets, their routing and mixing, and detection of a sample's status. We usually deploy an array of electrodes that are activated and deactivated in a preferred synchronized fashion, and all subsequent steps of an assay are tracked to meet the objective(s) affirmed by the assay.

B. Constraints involving Bioassay Operations

As there are several tasks like routing, mixing, detection, and many others involving a bioassay operation, of course, some inherent constraints are there that we are supposed to abide by in designing any algorithm for the successful execution of an assay. Some of these constraints are briefly discussed as follows.

1. Fluidic constraint: During droplet routing, in static condition, at least one cell is supposed to be kept in between two electrodes

containing two droplets to prevent accidental mixing; in case of scheduled mixing, two droplets may come closer to adjacent electrodes and mixed. During movement of droplets following a particular direction, we may observe that at least a gap to two electrodes is required to avoid unwanted mixing. These are known as static and dynamic fluidic constraints [3,16,19].

2. Electrode constraint: In case of pin constrained design [5], more than one electrodes are controlled by a single pin. This may introduce unnecessary effect of voltage on some electrode, and as a result this electrode may activate a droplet staying in an adjacent electrode unintentionally. Hence the droplets may fail to follow a given schedule defined by an assay. This is known as electrode constraint [19].

3. Timing constraint: Timing constraint in droplet routing is given by an upper bound on droplet transportation time [6,19]. It is defined to have the proper synchronization among all the bioassay operations held in different modules. All the operations are pre-scheduled and the result should be out within some specified time limit. The droplet routing time is very short [9]. But to start a mixing or detection, the droplets must reach the module in time to ensure that the result acquired is valid. So, there is an upper bound on time for each individual operation, which is referred to as the timing constraint.

4. Area constraint: We want to perform all the bioassays in a minimum chip area allowing for all the aforesaid constraints. All kinds of assignments include droplet transportation from the source of droplet to the mixing region and also to the detection region. A mixer is supposed to be located in a correct position for utilization of total array area. So, a design must support how efficiently a chip of some fixed area can be used.

In any DMFB related design, in isolation, we are supposed to satisfy all the aforesaid constraints, but often a bioassay may come across the cross contamination problem. This problem tells that an overlapping region may occur for two routing paths of two different droplets that are not supposed to be mixed. The problem of contamination may also occur when a common path is shared by two distinct droplets while maintaining their time constraint.

It is apparent that cross contamination between different bio-molecules may lead to generate erroneous results. The avoidance of contamination is a challenge in designing and scheduling a biochip. In this paper too, we desire to assign pins to electrodes and to design an algorithm for performing multiple parallel assay operations with the most effective utilization of a given restricted sized biochip by satisfying all the abovementioned constraints along with cross contamination avoidance.

III. A Very Brief Review on DMFB

At the beginning of this century, the digital microfluidics is being tried to have parallelism in the form of pipelining in bioassay analysis [4,18]. This parallelism consequently requires concurrent bioassay operations, i.e., concurrent movement of multiple droplets throughout a path and/or mixing of two or more reagents and samples in different regions of a bioassay in parallel. Droplets are moved by proper sequence of activation and deactivation of electrodes which are controlled by some external control pins. So the pins must be so chosen that we can achieve pipelining in droplet routing [7]. Simultaneous movement of droplets can easily be done by using different pins for different droplets, which has been used in *direct addressing pin configuration* [5,6]. However, this kind of pin configuration requires a large number of control pins for a large chip, as the number of pins required for an $n \times n$ array is n^2, and hence the circuit is more complex even from its operation point of view.

In *array based partitioning*, only a restricted number of distinct voltages are provided as input [5,6,18,21,22]. The whole chip is divided into some partitions depending on the activities performed and an optimum number of pins is used to assign the electrodes of a partition. These partitions can be repeated anywhere on a chip to reduce the total number of control pins in the chip. Though only a few pins are sufficient to assign all the electrodes on an array of any size, only a single droplet can safely be allowed to move in such a huge area. This problem is resolved by adopting cross reference based method.

Another pin constrained design technique is *cross referencing* [5,6,18,19], where only $m+n$ number of control pins are required to assign to all the electrodes in an $m \times n$ array. In this case, the electrode to be actuated is defined by the row and column number whose intersection contains a next-active (droplet holding) electrode. A next-active electrode is certainly such an adjacent electrode of an electrode that currently holds a droplet. A method named after 'cross referencing' [6,18] has been introduced to directly decide the voltage to be applied ('1' or '0') at the row and column combination for proper movement of a droplet. When we activate a row and a column for moving a droplet using '1-0' or '0-1' combination, then some unwanted cells might also be activated that may allow unwanted movement of droplet. To authorize only wanted movements, electrode constraints have been introduced accordingly.

In *broadcasting*, control pins are assigned to electrodes considering the movement of the droplets which is predefined in terms of scheduling of a complete assay, i.e., the activation-deactivation sequence of electrodes [11,20]. It is stored in a microcontroller in digital term and the electrodes used to route a droplet are assigned to control pins maintaining a said activation-deactivation sequence. Thus for a given bioassay it reduces the number of pins significantly and hence no electrode interference occurs. In case of pin constrained design, more than one electrodes are controlled by a single pin. It is voltage efficient, but there is a deficiency that if more than one droplets are to move we have to maintain electrode constraints as well.

By the way, in the broadcasting method, activation as well as deactivation is very important for the movement of droplets through the electrodes of an array. Here the problem of a bioassay is converted to the problem of pin distribution to control the desired activation of electrodes for movement of droplets. By the way, this problem is analogous to clique partitioning problem in graph theory, which is known to be NP-hard [10].

IV. A 15×15 Array for Sequential Processing

A. The Existing Assay Operation

A DMFB is shown in Fig. 2(a) that contains a restricted sized array of capacity 15×15 cells for performing a multiplexed biochemical assay consisting of a glucose assay and a lactate assay based on colorimetric enzymatic reaction [6,18]. In other words, in such an array two operations can be performed on two samples and two reagents one after another [5,6,15]. Here, only one shared mixer is used, where a first sample (say S_1) and a first reagent (say R_1) are routed from their respective sources to the mixer and after a desired level of mixing, the mixed droplet is

then routed to detection site 1 (D_1) for necessary finding(s). After completion of this phase, a second sample (say S_2) and a second reagent (say R_2), in a similar manner from their respective origins, route to the mixer for their mixing and then the mixed droplet goes to detection site 2 (D_2) for necessary outcome(s).

So, there must be a delay between the said two operations as the array contains a common mixer, some path below the mixer is common to different reagents, and some path above the mixer is common to different mixed droplets to respective detection sites. Hence washing is necessary in between every alternative assay; otherwise, unwanted contamination of residual samples, reagents, and mixed droplets might cause for erroneous results.

The aforementioned operations may be achieved by applying the *Connect-5* structure [5,6] of pin assignment as shown in Fig. 2(b). Thus, for a pair of samples and for a pair of reagents, six different combinations of mixing are S_1-R_1, S_1-R_2, S_2-R_1, S_2-R_2, S_1-R_1-R_2, and S_2-R_1-R_2 for their subsequent detections in different instances of time [8], where washing is necessary in between two assay operations to avoid cross contamination [15].

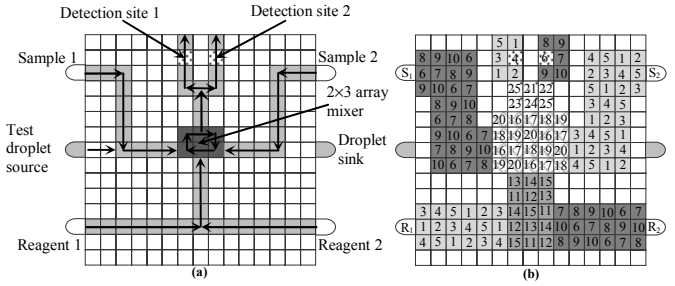

Fig. 2. (a) A 15×15 array layout of droplet routing containing two sources of samples and two sources of reagents with one 2×3 mixer and two detection sites. Direction of arrows shows the movement of droplet(s) (either sample, or reagent, or mixed droplet) along the paths. (b) Pin assignment of the array using *Connect-5* algorithm that covers all the distinct cells and uses not more than 25 pins. Here for the movement of a droplet, the adjacent cells are used as guard band; hence for a mixer of size 2×3, an array of size 4×5 is deployed for its realization.

B. Formulation of a Framework for Minimum Area Arrangement

There are several assumptions and concerns to achieve the goals in performing bioassay operations; some of which are as follows: (1) A *sequencing graph* that tells about the flow of execution of an assay; accordingly we are supposed to frame a minimum array area required. (2) The *assay response time* that includes routing of droplets, mixing, detecting, and washing for making the array ready for a next assay operation, is the next important factor that we like to minimize. (3) The *voltage distribution* in terms of the number of distinct control pins assigned to electrodes for a set of assays is also to be minimized. The use of less number of pins makes a design less complex for synchronized activation and deactivation of electrodes.

In our design, we introduce a mixer of size 1×3 for splitting and merging of two droplets. So, a minimum array size is 3×3 wherein detection is performed at cell (3,3), as shown in Fig. 3(a).

Besides, the guard band is a row of cells that usually does not help to route droplets but used for secured movement of droplets [5,6,9] irrespective of whether the paths for movement of droplets are predefined. Hence, we cover the array size 3×3 using guard bands by making it an array size 5×5 as shown in Fig. 3(b), which is also necessary as we like to perform several assay operations simultaneously on a given restricted sized biochip of array capacity 15×15, where tasks are to be executed in parallel. We call such a minimum area arrangement a *unit array*.

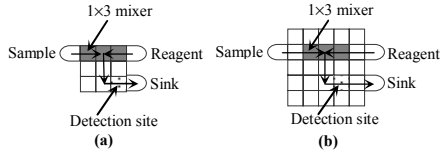

Fig. 3. (a) A probable minimum array of size 3×3 for mixing of two droplets in a mixer of size 1×3, and then subsequent detection of the mixed droplet. (b) A *unit array* of size 5×5 for performing the preceding assay operation by introducing necessary guard band over the earlier 3×3 array structure.

V. The 15×15 Array for Multiple Parallel Processing

In this section, our objective is to generalize a framework that can execute all the tasks that are usual in performing an assay operation using a minimum area arrangement of rectangular array structure satisfying all the constraints that are supposed to obey. Needless to mention that, accordingly a different pin assignment might require satisfying our objectives. Besides, our target is to make more parallelism, if attainable, so that several such tasks can be performed in parallel using a 15×15 array. This is how a maximum throughput of some assay operation(s) can be accomplished using a minimum feasible array area retaining all necessary constraints along with cross contamination avoidance in a minimum probable time to detect sample(s).

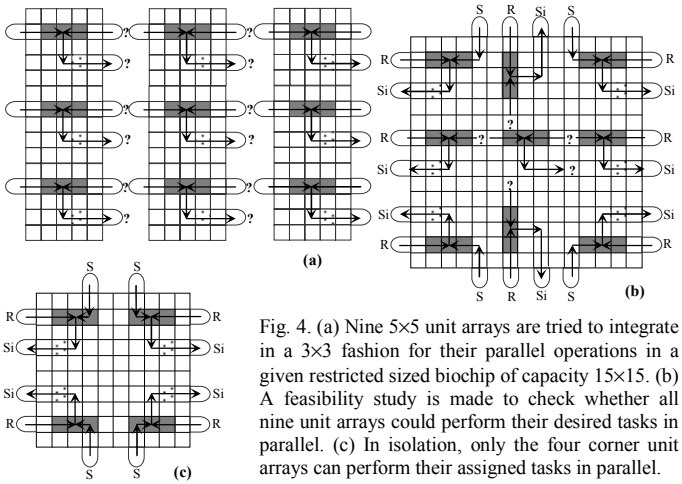

Fig. 4. (a) Nine 5×5 unit arrays are tried to integrate in a 3×3 fashion for their parallel operations in a given restricted sized biochip of capacity 15×15. (b) A feasibility study is made to check whether all nine unit arrays could perform their desired tasks in parallel. (c) In isolation, only the four corner unit arrays can perform their assigned tasks in parallel.

A. Feasibility of Achieving Multiple Assay Operations

Now we may observe that there are nine 5×5 arrays in a given chip of size 15×15 as shown in Fig. 4(a). Then the question arises, whether we can assure all nine assay operations in parallel by introducing nine unit arrays as have been achieved in Fig. 3(b)? Certainly the answer is 'no', as sample and reagent droplets are provided from two other sides of the array. Hence from such a generalization, we may observe that at most four corner unit arrays can someway be used for four distinct assay operations only, whereas the remaining five 5×5 arrays (comprising 125 cells) stay behind unutilized (see Fig. 4(b)). Then, why should we employ those arrays of cells that are not consumed in any assay operation? Rather, we may exclude all those cells in unused arrays and obtain a much smaller 10×10 array in Fig. 4(c), for the same output of only four separate assay operations in parallel.

B. Multiple Assay Operations Attained in the 15×15 Array

So, up to this point in time, the brilliancy of parallelism is not realized for a given restricted sized chip of capacity 15×15. Rather, we may observe that if the top-left unit array is used for

dispensing droplets of a sample (reagent) and the three central unit arrays are used for its routing, then eventually the remaining five unit arrays could be used (with an essential shift of the mixer) for their relevant tasks in parallel, where reagent (sample) droplets are dispensed from their own sources to the unit arrays and also mixed droplets are disposed after compulsory detections, all in parallel, as shown in Fig. 5(a). Due to space restraint, we depart almost all allied aspects; a configured pin assignment in such a chip is directly shown in Fig. 5(b). Here the five mixers of size 1×3 each belong to the unit arrays 1, 2, and 4 (Ua_1, Ua_2, and Ua_4) on the right part and the unit arrays 3 and 5 (Ua_3 and Ua_5) on the left part of the given array, as shown in the figure.

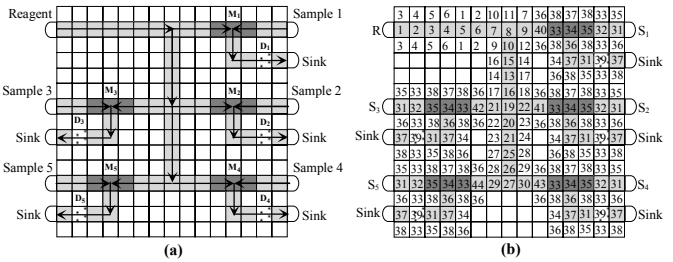

Fig. 5. (a) Layout of a modified droplet routing that uses five 1×3 mixers in a 15×15 array. (b) Pin configuration in the 15×15 array that assigns same set of pins 33, 34, and 35 for each 1×3 mixing region and pin 39 for each detection site.

In very brief, according to Fig. 5(b), exactly eight pins (1 through 8; though only six pins are required in Ua_1) help to route the reagent R up to the middlemost column of the given array, then it follows rectilinear routes for distributing successive droplets of R to the five mixing regions belonging to five unit arrays. Particularly, one after the other two droplets of R move up to pin 27 (in the middlemost column) for their own routes in Ua_4 and Ua_5, and in a similar way, in succession two more droplets of R move up to pin 19 (in the same column) for their own routes in Ua_2 and Ua_3, and a last droplet of R goes straight for mixing in Ua_1. In addition, for synchronous multiple operations, the pin configuration in a unit array on the left is obtained by making a mirror image of that in a unit array on the right (using exactly nine pins 31 through 39). The pins in the central unit arrays are configured for propagation of R as we desire them to move (using 24 pins, 7 through 30). Five distinct pins are used for holding reagents ready to enter into the mixers (pins 40 through 44).

Accordingly, a total of 44 pins are used to do all desired tasks of multiple bioassay operations in synchronism, and a very few unused spare cells are obtained that are not assigned any pin; anyway, the blank rows of spare cells in Ua_1 may be used as an alternative path for routing of R, if utmost necessary for any reason. This completes the pin arrangement that we design for a set of five multiple bioassay operations to be executed in parallel.

C. An Example Run for Multiple Bioassay Operations

An assay that performs two or more assignments for their execution in parallel may enhance the efficiency of an array of size 15×15, where the same array in Fig. 2 is truly underutilized. Let us consider Case I in Section I.B, where a reagent R is mixed in isolation with five different samples S_1 through S_5; the related sequencing graph is shown in Fig. 6(a).

Now till we do not know whether there is any overlapping of routing paths or risk of cross contamination among the droplets used herein. The routes of different droplets along with associated tasks are overtly shown in Fig. 6(b), which we call the placement graph. In this design our objective is to realize an isomorphic representation of the placement graph that contains no crossing of edges or less crossing as much as we can. Here such a crossing indicates that the related droplets share at least a common cell (in different time instance) that is to be washed in between to avoid cross contamination; otherwise, intra-assay washing is redundant.

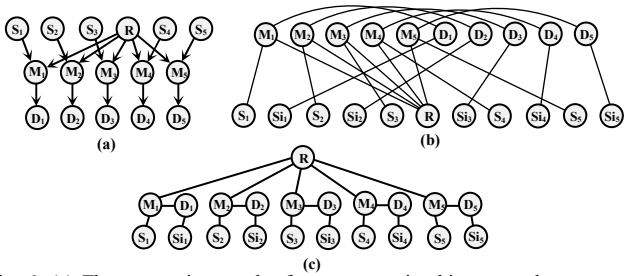

Fig. 6. (a) The sequencing graph of a representative bioassay, where reagent R mixes disjointedly with each of the samples S_1 through S_5 in respective mixers M, and then the mixed droplets are sent for individual detection (D), all in parallel. (b) The placement graph of the assay, where the top row of circles indicates the operations (M and D) performed inside the array, and the bottom row of circles shows the sources (S and R) and sinks (Si) available outside the array. (c) The resultant placement graph after assigning the modules of the assay, which is crossing-free.

Here R represents the reagent, S_i is the ith sample, M_i is the ith mixer, D_i is the ith detection site, and Si_i is the ith sink, $1 \le i \le 5$. Naturally, there are one source of reagent and five sources of sample(s), either same or different. So, there are six ports as sources of regular droplets and five sinks to dispose the mixed droplets after detection. Now to avoid cross contamination, i.e., to avoid crossing between the paths the devices can first be ordered in the following way. As there is only one source of reagent and reagent droplet is to be routed to all the unit arrays, it should be placed first and making this placement as a constraint, all the remaining ports and devices are then placed that results a placement graph as shown in Fig. 6(c), which is isomorphic to the placement graph shown in Fig. 6(b).

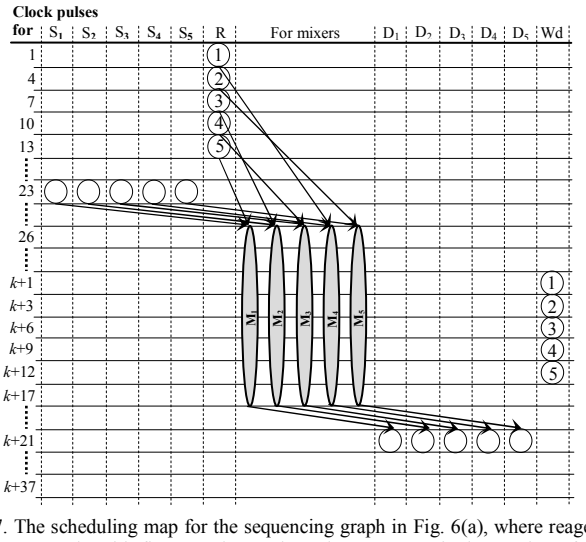

Fig. 7. The scheduling map for the sequencing graph in Fig. 6(a), where reagent R mixes separately with five samples S_1 through S_5. Here m is the number of clock pulses required for mixing and $k = 25+m-17$ after which wash droplets are dispensed. Here at the (k+23)rd clock pulse, the mixed droplets are disposed from the array after detections are made at the (k+21)st clock pulse in parallel. Next 14 clock pulses are needed for washing the whole array before starting a new assay.

Here we have assumed a case where the same reagent droplet reaches to all the respective mixers where mixing is performed

with different samples, the droplets must move mostly in parallel in the true sense, to complete the whole assay. Here as there is no crossing of edges in the placement graph, there is no need of scheduling of intra-washing during the assay is performed; rather, inter-washing is necessary to execute two parallel assays of ten assignments using the restricted sized biochip of capacity 15×15 with cross contamination avoidance. Now, as per the scheduling of the said assay, the scheduling map obtained is shown in Fig. 7.

D. Experimental Results

In this section, we compare the three biochips, one in existing article [2,5,15,18], one in the form of manuscript [8], and the one introduced in this paper, from their structural and functional characteristics. The primary differences are whether the bioassay operations are performed sequentially or in parallel, what are the sizes of mixers used, utilization of cells in the array, number of tasks carried out, number of assignments executed, etc. These are included in Table I and thus explained in brief as follows.

Table I. A table of comparison that assesses two existing arrays and the array introduced in this paper of size 15×15 each from their pattern and practical viewpoint. Here *m*, *d*, *w*, and (*w*) are the number of clock pulses applied for mixing, detection, inter-assay washing, and intra-assay washing, respectively.

Features \ Array size	15×15 (Fig. 2) [5,6,15,18]	15×15 [8]	15×15 (Fig. 5)
Mode of operation	Sequential	Parallel	Parallel
# of tasks	Six	Eight	Nine
# of mixers	One	Two	Five
Mixer size	2×3	2×4	1×3
Pin count	25	21	44
# of active cells	58	83	78
# of guard cells	91	96	116
# of unused cells	76	46	31
Wash droplets	No	Yes	Yes
# of clock pulses (for two assays)	$2 \times (12 + 19 + m + d + w)$	$2 \times (7 + 8 + m + d + (w))$	$2 \times (25 + 4 + m + d + w)$
# of assignments	Two	Four	Ten

We may note that the foremost biochip is very much under-utilized as herein 33.78% cells are unused and [8] claims that it fails to use 20.44% cells, whereas this value is only 13.78% in our design. In our biochip we accomplish 400% more assignments by sacrificing only 76% more pins, where the mixer we introduce may operate in splitting-merging mode of operation and also in to-and-fro routing of mixed droplet. Here as the unit arrays are quite smaller in size, and mixer and detection sites are much closer, the average routing time is greatly smaller in comparison to both the earlier two cases. Hence the number of clock pulses we require in performing two assays of ten assignments is $2\times(25+4+m+d+w)$, which is comparable in contrast to its two earlier designs.

In this design we use pin 36, below each mixer, as the decision point, which is activated only when the mixing is ensured, and pin 39 as detection site. Here, we may introduce intra-array wash droplets to wash the mixers and detection sites only, when in a second assay operation the same reagent is used. Of course, in the next assay, if a different reagent is dispensed, inter-assay washing is carried out as a mandatory task in between.

VI. Conclusion

In this paper we have considered a restricted sized biochip with capacity 15×15 cells. In existing literature, such an array is used only for one bioassay operation at a time as there is only one mixer of size 2×3. This chip is underutilized and subsequently a 15×15 array is introduced with two mixers of size 2×4 each, where the assay operation is executed in parallel in the true sense. In all these respects we have configured a pin assignment where five mixers of size 1×3 each have been introduced and hence the pin count is enhanced by 76% though a multiple assay operation with five times gain in comparison to the primary assay is assured using almost the same number of clock pulses as this assay operation is achieved in parallel. Here in certain cases, only intra-assay washing is sufficient while doing successive multiple parallel assay operations and in these cases we may reduce the inter-assay washing time too before starting a new assay. Mixers we introduce are used for to-and-fro mixing of mixed droplets or splitting-merging mode of operation. Here the pin configuration is so brilliant that the crossing of two different droplets does not occur, and hence the problem of cross contamination is eventually avoided to achieve a novel design; additional cost and time for routing wash droplets are abandoned. Even then our next target is to design a more productive restricted sized array that requires even fewer pins, if possible, in realizing an utmost useful biochip.

References

[1] http://www.tutorgig.com/encyclopedia

[2] Advanced Liquid Logic, http://www.liquid-logic.com

[3] K. F. Böhringer, "Towards optimal strategies for moving droplets in digital microfluidic systems," *ICRA*, pp. 1468-1474, 2004.

[4] K. F. Böhringer, "Modelling and controlling parallel tasks in droplet based microfluidic systems," *TCAD*, vol. 25, no. 2, pp. 329-238, 2006.

[5] K. Chakrabarty and F. Su, "*Digital Microfluidic Biochips: Synthesis, Testing, and Reconfiguration Techniques*," CRC Press, 2007.

[6] K. Chakrabarty and T. Xu, "*Digital Microfluidic Biochips Design Automation and Optimization*," CRC Press, 2010.

[7] K. Chakrabarty, "Digital microfluidic biochips: A vision for functional diversity and more than Moore," *VLSI Design*, pp. 452-457, 2010.

[8] D. Dhal, P. Datta, A. Chakrabarty, G. Saha, and R. K. Pal, "An algorithm for parallel assay operations in a restricted sized chip in digital microfluidics," *IEEE ISVLSI Conference*, pp. 142-147, 2014.

[9] R. B. Fair, "Digital microfluidics: Is a true lab-on-a-chip possible?" *Microfluid Nanofluid*, Springer, vol. 3, pp. 245-281, 2007.

[10] M. R. Garey and D. S. Johnson, "*A Guide to the Theory of NP-Completeness*," San Francisco, 1979.

[11] W. L. Hwang, F. Su, and K. Chakrabarty, "Automated design of pin-constrained digital microfluidic arrays for lab-on-a-chip applications," *DAC*, pp. 925-930, 2006.

[12] P. Paik, V. K. Pamula, and R. B. Fair, "Rapid droplet mixers for digital microfluidic systems," *Lab on a Chip*, vol. 3, pp. 253-259, 2003.

[13] P. Paik, V. K. Pamula, M. G. Pollack, and R. B. Fair, "Electrowetting based droplet mixers for microfluidic systems," *Lab on a Chip*, vol. 3, pp. 28-33, 2003.

[14] F. Su and K. Chakrabarty, "Architectural-level synthesis of digital microfluidics based biochips," *ICCAD*, pp. 223-228, 2004.

[15] F. Su and K. Chakrabarty, "High-level synthesis of digital microfluidic biochips," *ICCAD*, vol. 3, no. 4, Article 16, 2008.

[16] F. Su, W. Hwang, and K. Chakrabarty, "Droplet routing in the synthesis of digital microfluidic biochips," *DATE*, pp. 323-328, 2006.

[17] V. Srinivasan, V. K. Pamula, M. G. Pollack, and R. B. Fair, "A digital microfluidic biosensor for multianalyte detection," *IEEE MEMS Conference*, pp. 327-330, 2003.

[18] T. Xu and K. Chakrabarty, "Droplet-trace-based array partitioning and a pin assignment algorithm for the automated design of digital microfluidic biochips," *IEEE/ACM ICH/SCSS*, pp. 112-117, 2006.

[19] T. Xu and K. Chakrabarty, "A cross-referencing based droplet manipulation method for high-throughput and pin-constrained digital microfluidic arrays," *DATE*, pp. 552-557, 2007.

[20] T. Xu and K. Chakrabarty, "Broadcast electrode-addressing for pin-constrained multifunctional digital microfluidic biochips," *DAC*, pp. 173-178, 2008.

[21] T. Xu and K. Chakrabarty, "A droplet-manipulation method for archiving high throughput in cross-referencing based digital microfluidic biochips," *TCAD*, vol. 27, pp. 1905-1917, 2008.

[22] T. Xu, W. L. Hwang, F. Su, and K. Chakrabarty, "Automated design of pin-constrained digital microfluidic biochips under droplet-interference constraints," *ACMJ ETCS*, 2007, vol. 3, no. 3, Article 14, 2007.

[23] J. Zeng and T. Korsmeyer, "Principles of droplet electro-hydrodynamics for lab-on-a-chip," *Lab on a Chip*, vol. 4, pp. 265-277, 2004.

An Improved Hierarchical Cluster Based Routing Approach for Wireless Mesh Network

Tapodhir Acharjee
Dept of CSE
Assam University
tapacharjee@gmail.com

Sukanya Rajkonwar
Dept of CSE
Assam University
rajkonwarsukanya@gmail.com

Sudipta Roy
Dept of CSE
Assam University
Sudipta.it@gmail.com

***Abstract*—Applications of Wireless Mesh Network(WMN) are now visible everywhere in the world ranging from battle field to community networking and satellite constellation to university networking . Routing on WMN is one of the most sought research topic these days. Many routing protocols have been proposed by the researchers and works are being done in different dimensions. For better scalability Hierarchical Cluster based routing methods have been studied. These protocols group the nodes into clusters which consist of a cluster head(CH) and cluster members. Gateway nodes connect one cluster to another cluster. Nodes are assigned different functionalities in hierarchical order. The performance will not be impacted if the network is large. In the existing hierarchical cluster based routing protocols the CH is heavily loaded, so it increases end to end delay. In this paper, we propose an improved hierarchical cluster based approach in WMN which reduces the load on CH by using Assistant CH and a node clustering algorithm is proposed which works with varying cluster heads. The results are compared with two other important routing protocols for WMNs.**

Keywords—Wireless Mesh Network; Scalability; Hierarchical Cluster based routing ; Cluster Head ; Assistant Cluster Head; Node Clustering Algorithm

I. INTRODUCTION

Wireless mesh networks are dynamically self-organized and self-configured, with the nodes in the network automatically establishing an ad hoc network and maintaining the mesh connectivity [1]. It is said to be a promising wireless technology that can overcome the limitations of WLAN[2].WMNs have received widespread use and attention over the last years. The number of installations of WMN is growing rapidly. Mesh networks can be used for providing "last mile" IP connectivity to a number of users without the need of any infrastructure. The wireless nodes can be added as and when required. The mesh network acts as a common backhaul network which provides a link between different types of networks and eventually access to the Internet.

WMNs architecture has been classified into three categories namely, Infrastructure WMNs, client/Infrastructure-less WMNs and Hybrid WMNs. In infrastructure WMNs, mesh routers create an infrastructure for mesh clients, whereas in client WMNs nodes make peer-to-peer network among them and perform mesh functions, such as routing and self-configuration. Hybrid WMNs are a combination of the previous two methods where the Mesh clients can connect to the network through mesh routers and can also directly mesh with other mesh clients [3].

Scalability is an important issue for Wireless Mesh Network. Cluster base and Hierarchical routing protocols are quite helpful in this case. End to end delay, bandwidth consumption, energy consumption, throughput, and scalability all these performance metrics may be improved with efficient clustering techniques [4]. In this paper we are proposing one clustering algorithm and introduce an Assistant Cluster Head(ACH) to reduce the load on the CH among some other modifications to hierarchical cluster based routing. Ultimately, we analyze the scalability performance of our proposed method and compare the results with BATMAN and HWMP protocols by simulations in ns-3 considering packet delivery ratio (PDR), throughput and delay.

The remaining sections of the paper are structured as follows: In section II, Cluster based routing protocols are discussed. Section III discusses the proposed method. In section IV, Simulation results are presented and analysed. Finally, a conclusion is drawn in section V.

II. CLUSTER BASED ROUTING PROTOCOLS

There are a number of cluster based routing protocols proposed in the literature. The Cluster-head Gateway Switch Routing(CGSR) [5], The Hierarchical State Routing (HSR) [6], Hierarchical Cluster-Based Link State Routing(L-HCLSR)Protocol [7] etc. Some are used for MANETs and some may be implemented in WMNs also. But, we mainly focus here on the following two routing protocols as these are particularly focused on WMN.

A. Cluster Based Routing Protocol (CBRP)[8][9]

CBRP is based on cluster formation of mesh points and the communication between Mesh Portal Points(MPPs) and Cluster heads(CHs).MPP assigns one node as a CH of each cluster group and stores the CH and CH's neighbors information in its own table. The cluster formation algorithm is initialized by the new node which sends a CH query to its one hop neighbor. At the same time, the new node also initializes its topology data table and inserts a table entry at level 0 which indicates that it is a member of a cluster which

978-1-4673-6680-9/16/$31.00 ©2016 IEEE

does not have any CH until now. If no reply comes within a specified time interval, the node promotes itself as cluster leader. Many criteria may be used to select a CH or refuse the inclusion of a member in a cluster. Polling is performed from the CH periodically, to inform the members that the CH is active and also to know that all the members are active or not. When a CH is promoted, it initializes a list of all cluster members' addresses. In CBRP , the path establishment process is completed in 4 steps: setup of the cluster head, path creation, path reply, and path setup. CHs maintain two tables, one for neighboring CHs and another for MPs under it. Every cluster member stores the information on its CH. The Path creation process is started when a normal cluster member wants to communicate with a destination node. The source MP sends a path request (PREQ) message to its CH which checks its own member list first. If the information is available with CH, it sends a path reply, otherwise it forwards the PREQ to the MPP. The MPP multicasts a PREQ message to all of the cluster heads and the CH under which the destination node belongs, will respond with a path reply (PREP)which is forwarded to the source CH and ultimately to the source node. In this way, the path between the source and destination nodes is established. So, in CBRP two kinds of routing, viz, Intra-cluster routing and inter-cluster routing are performed. In CBRP, when the CH fails, then broadcasting is required.

The drawbacks of CBRP are that the load on MPP is quite high here and also, even when destination MP is in the same cluster, the Mesh Points (MPs) must communicate with the CH for communicating with the other MP.

B. Hierarchical Cluster Based Routing For Wireless Mesh Networks Using Group Head[10]

This approach is an extension of the cluster based routing scheme for wireless mesh networks . Here, WMNs are divided into different domains of Mesh Points(MPs) which are further subdivided into different clusters. One MP is regarded as a Group Head (GH) in each domain and one MP as a Cluster Head (CH) in each cluster. Almost all mesh points are distributed into clusters. MPP maintains the information about all the GHs. As shown in figure 1, MPP, GHs and CHs are all staying in fixed positions and only MPs may be mobile. An MP cannot be CH and GH at the same time. Here, MP9 and MP10 are group heads and maintain two clusters each. Big circle is denoting one cluster and every cluster is having one cluster head(CH) .Here MP1, MP3, MP5 and MP7 are cluster heads. The functioning of MP,CH, GH and MPP are shown in the flowcharts.

The Hierarchical cluster based routing approach works following the hierarchy i.e., MP-> CH -> GH -> MPP with mesh points on the bottom of the hierarchy and mesh point portal on the top. So, if an MP needs to communicate with an MP which is its neighbor in the same cluster, the RREQ need not be forwarded to the CH. The MP itself will find the entry for the neighbors in its routing table. But, if the destination MP is not a neighbor the RREQ will be forwarded to CH and CH finds out the route if its entry is there in its routing table. The REEP will be forwarded to source MP. If the destination MP's entry is not there in the CH's table, the CH forwards the RREQ to its GH which in turn forwards the RREQ to all CHs(except the source CH) under it.

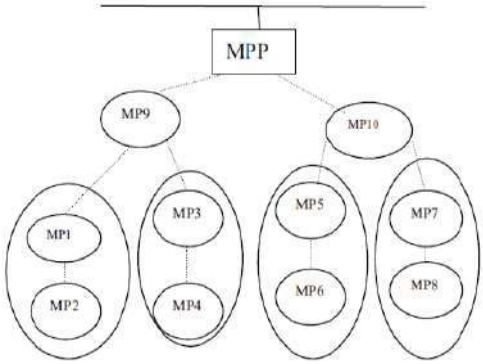

Fig 1:Wireless Mesh Network divided in Domains

If any CH is having that entry in its routing table, it will respond, otherwise will do nothing .If any RREP is received from any CH, it will be forwarded to the CH and ultimately to the source MP. If the GH is unable to find the route, it will forward the RREQ to the MPP, which forwards the RREQ to all its GHs(except the source GH) under it. Accordingly, the GHs will forward the RREQ to all their CHs and if the route is found by any GH, the RREP response will come to the MPP. The MPP forwards the RREP to the source GH which forwards it to source CH and lastly from GH to source MP. If the MPP is not able to find the route within a timeout interval, it will send a RERR message back to the source. Thus, CH, GH and MPP are sharing the loads hierarchically.

III. PROPOSED ROUTING PROTOCOL

In the hierarchical cluster based routing for wireless mesh networks using group head we have noted following drawbacks:

i) If the destination is two-hops neighbor node but is in another cluster, there can't be a direct communication between these two neighbor nodes. The routing path has to pass through their two CHs if the CHs are in the same group or else path should pass through their GHs. So it increases path length.

ii) Addition of GH reduces the load on MPP but there is still load on cluster head. Due to this reason end to end delay is increased.

To improve the performance of the previous protocol discussed we add some new features and propose a cluster based approach which may be used to reduce load on the CH.

In the previous algorithm the CH, GH and MPP are fixed. In our algorithm we take changing CH so that if CH fails the algorithm can work with new CH. For these reasons we have made the following changes in the proposed method -

1) An Assistant Cluster head (ACH) is introduced which share the load of CH.

2) A Cluster formation algorithm is proposed.
3) Each node in the network contains neighbor table which contains information about neighboring nodes and cluster adjacency table contains information about CH and ACH.
4) CH and ACH node contain cluster adjacency table.It contains information about cluster member nodes and gateway nodes.
5) GH stores information about CH/ACH of all clusters under it.
6) MPP stores information about all GHs under it.
7) GH, MPP are fixed but CH and ACH shall not be fixed.

A. Proposed cluster formation algorithm

Step 1: Initially each node is in undecided (Un) state.
node → Un
Step 2: Each node broadcasts hello message to 1 hop away nodes which contains
hello={ id, state, Sn, no. of neighbors}
//id=node id state=node's state Sn=Signal strength
Step 3: The receiving node send reply_hello message if sender(Sn)>receiver(Sn)
Step 4: The node will elect itself as CH if connectivity is highest and in case of tie of highest connectivity the node will elect itself as a CH(Cluster head) if Sn is higher than other node.
Step 5: CH will elect a node as ACH if connectivity of CH > connectivity of that node but higher than others or in case of tie elect the one with Sn or in case of tie of Sn elect the one with lower id .
Step 6: CH broadcast announcement message to the neighbor nodes along with ACH which contains
Announcement ={CH id, ACH id ,cluster id}
Step 7: The receiver node -> CM
if it received one announcement message
else receiver node ->GW
//CM=Cluster member GW=gateway
Step 8: The CM and GW reply with register message which contains
Register = {id, state, list_of_neighbors}
Step 9: CH forward register message to ACH.
Step 10: CH/ACH include CM and GW in its cluster adjacency table and form the cluster.
Step 11: End

Initially each node is in undecided state. For cluster formation each node sends hello message which contains node id, node's signal strength (Sn), state (Un/CH/CM/GW) and no. of neighbors. The receiving node checks its Signal strength with sender's Signal strength, if it is less than sender's Signal strength then send reply for hello message it received otherwise do nothing. The node with highest connectivity will elect itself as a CH. CH selects the node with next highest connectivity as an assistant cluster head (ACH) or in case of tie select the one with more signal strength or in case of tie of signal strength select the one with lower id as an ACH and broadcast announcement message which contains CH id, ACH id and cluster id to the neighbor nodes along with ACH. The receiving node sends one announcement message to set its state as cluster member (CM) and the node with more announcement message will set itself as gateway node (GW).The CM and GW nodes reply with register message which contains its id, state and its neighbor nodes. CH forwards the register message to ACH. CH and ACH then include these nodes in its cluster adjacency table and form the cluster. There is a need of re-election of CH/ACH if connectivity of CH is beyond the maximum threshold value or is below the minimum threshold value.

B. Routing in proposed approach

1. Source node (S) checks destination (D) in neighbor table (N) .
2. If (D in N)
Begin
S sends packet to D;
End
3. S unicasts RREQ to CH.
4. If (CH is not overloaded)
Begin
5. CH check D in cluster adjacency table (C)
6. If (D in C)
Begin
CH unicast the RREQ to D
D Send RREP to S through the path where RREQ was sent
End
7. Else if (D not in C)
Begin
8. CH multicasts RREQ to gateway nodes
End
End if
9. Else
Begin
CH forward RREQ to ACH
End
End if
10. ACH check D in C table
If (D in C)
Begin
ACH unicasts RREQ to D
D sends RREP to S using the path where RREQ was sent
End
11. Else
Begin
ACH multicasts RREQ to gateway nodes.
End
End if
End if
12. The receiving gateway nodes forward RREQ to CH.
13. Repeat step 4.

14. Repeat step 5.
15. Repeat step 6.
16. Repeat step 7.
17. If after certain timeout source CH doesn't get any reply forward RREQ to GH.
18. GH multicasts RREQ to all CH of clusters under it.
19. For all clusters
Begin
Repeat step 5;
Repeat step 6;
Repeat step 7;
CH discards RREQ;
Repeat step 9;
Repeat 10;
ACH discard RREQ
End
20. If after certain timeout GH doesn't get any reply
Begin
Forward RREQ to MPP
End
End if
21. MPP multicasts RREQ to all GH under it
22. For all receiving GH
Begin
Repeat step 18;
Repeat step 19;
End
23. End

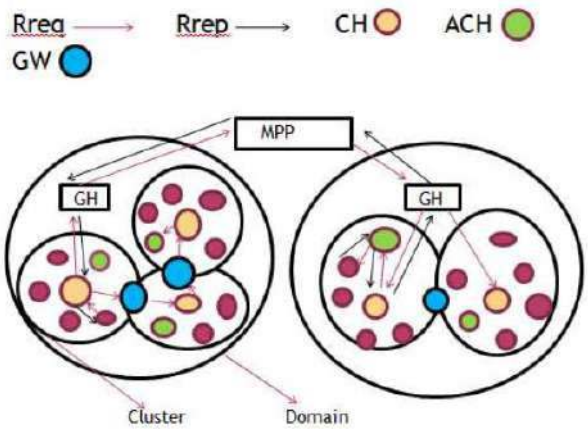

Fig 2: Routing in Proposed method

If a node needs to send packet to other node then the sender node checks if the destination node is in its neighbor table, if it is there, source MP sends the packet directly to that node. If it is not in the neighbor table then it sends Rreq message to CH.CH will check if the destination node is in its cluster adjacency table, if it is there, the CH forwards the Rreq to that node otherwise multicast it to 48 gateway nodes. If the CH is overloaded i.e. number of Rreq received exceeds the threshold value (THload) then it forwards the Rreq to ACH.ACH does the same thing as CH did. Gateway (GW) node will forward the Rreq message to CH of the clusters to which it is associated except the sending CH. Same procedure will be repeated by these CHs like source CH .If the destination node gets the Rreq message, it sends Rrep using the reverse direction of the same path it got Rreq message. If after certain time period if CH/ACH does not get any reply then it forwards the packet to GH.GH will forward Rreq to MPP.MPP will multicast to all the GHs under it.GH will multicast Rreq message to all the CHs of the clusters under it. If CH is not overloaded, it will check its cluster adjacency table, if it contains the address, it forwards the Rreq message to the destination, otherwise forwards Rreq message to ACH.ACH does the same thing as CH did. When the destination node gets the Rreq message , it replies with Rrep message using same path in reverse direction through which Rreq came. Thus a bidirectional path will be established between source and destination. Using that path both the MPs can communicate with each other.

IV. SIMULATION RESULTS AND DISCUSSION

This section presents the results obtained from different simulation scenarios described in previous section. In Figure 3, 4 & 5 , we compare the performance of our proposed modified Hierarchical Cluster Based Routing Protocol with BATMAN((Better Approach to Mobile Ad-hoc Networking)[11] and HWMP(Hybrid Wireless Mesh Protocol) [12] routing protocol. The comparison between these two protocols from the scalability point of view is already discussed in our previous work[13].Here, we performed the simulation in ns-3[14].

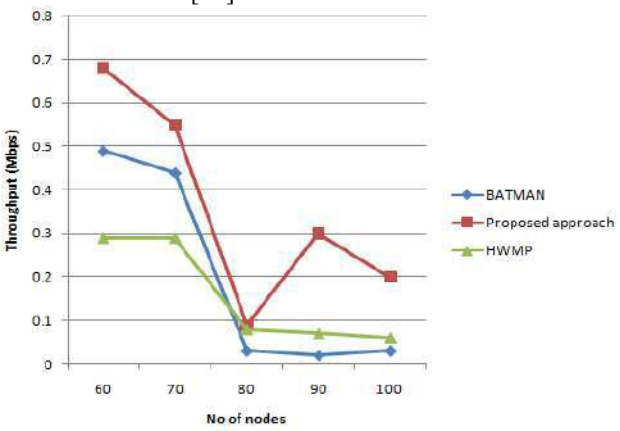

Figure 3: Variations of Throughput and Number of Nodes

Figure 3 shows that the performance of proposed modified hierarchical cluster based routing protocol in terms of throughput is better than HWMP and BATMAN. Up to 30 nodes, throughput (in kbps) of the proposed approach decreases but when the number of nodes is higher than 30 throughput increases .After 40 nodes throughput of the proposed approach again decreases, but the overall performance is better than HWMP and BATMAN. Throughput of HWMP is higher than that of BATMAN if number of node is small, i.e., less than 40. However, if the number of node is large, i.e., more than 40, throughput of the

BATMAN is increased but that of HWMP remains nearly constant. When number of nodes is large, the least number of control packets (e.g., RREQ, RREP or ORG) are successfully received from the clients to choose the routes in HWMP, so its throughput degrades in larger network.

Figure 4 shows end-to-end delay (in seconds) of proposed approach is lower than BATMAN up to 50 nodes. After 50 nodes end to end delay of proposed approach increases and becomes higher than BATMAN. End-to-End Delay of proposed approach is higher than HWMP.A distance-vector tree rooted at a single root mesh point is proactively selected by HWMP, so as to quickly select a routing path. On the other hand, BATMAN divides the information about the best possible end-to-end paths between nodes in the mesh to all

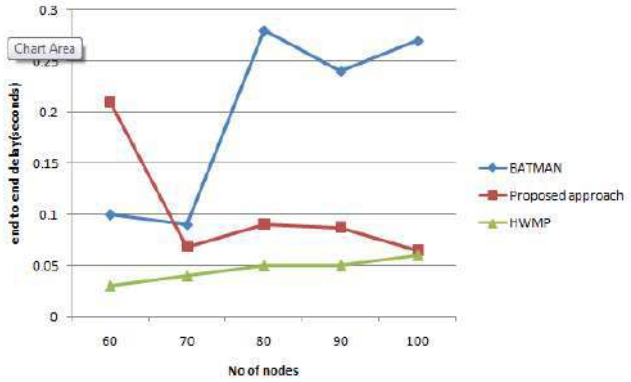

Figure 4 : Variations of End to end delay and Number of Nodes

participating nodes. Therefore, more time is required to select the routing path. In the proposed approach, path selection takes some time if destination is in other cluster or domain but congestion of packets is decreased using this clustering technique.

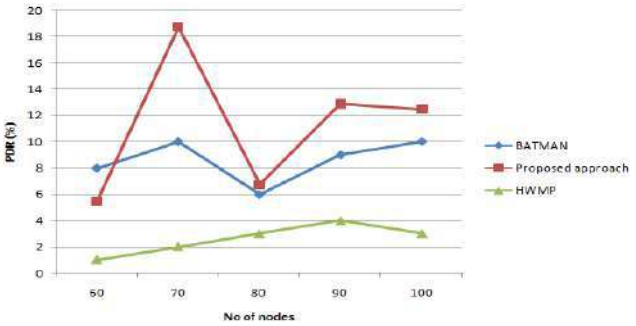

Figure 5 : Variations of Packet Delivery Ratio and Number of Nodes

Figure 5 shows packet delivery ratio (%) of proposed approach is lower than HWMP if number of nodes is small, i.e., less than 20 but higher than BATMAN when the number of nodes is less than 60. Increase in number of nodes cause much collision in the proposed hierarchical cluster based routing protocol, BATMAN and HWMP, which is caused by the following two reasons. Firstly, there is more number of nodes contending for the channel to send their data packets. Secondly, to choose routes, the clients have to send control packets, such as the RREQ, RREP or ORG message. Although these packets are very small in size, the nodes have to contend for the channel again and again to send these control packets. This leads to more packet loss.

Thus, Packet error rate(PER) in our proposed approach may be more than the other two protocols. This may be reduced by introducing better clustering approach which may also explore other alternative paths when there is more PER in the current route

V. CONCLUSION

In this paper, we presented a modified hierarchical cluster based routing approach for wireless mesh networks to reduce the drawbacks of previous approach. Although this approach creates an extra load on the mesh point portal and group heads, but reduces loads on cluster heads by introducing assistant cluster head. In this approach, hierarchical clustering is used and if source mesh points and destination mesh points are in same domain, the MPP does not participate in the route discovery which reduces the burden of the mesh point portal by group head. In the proposed approach cluster formation algorithm is proposed so that even if cluster head fails, the algorithm still works with new cluster head. In a large network the proposed Hierarchical Cluster Based Routing Protocol gives higher throughput than the other two protocols. Packet delivery ratio of proposed approach is lower than HWMP if number of nodes is small but when the number of nodes is large it provides lower PDR than BATMAN. When more numbers of node are added, there is a significant decrease in packet delivery ratio (PDR) in all the protocols. The proposed Hierarchical Cluster Based Routing Protocol gives higher delay than HWMP but gives lower delay than BATMAN when the number of nodes is small. Further improvements with introducing even better clustering algorithm may give better results in terms of scalability.

REFERENCES

[1] I. F. Akyildiz, X. Wang, and W. Wang, Wireless mesh networks: a survey. Computer Networks, vol. 47, no. 4, March 2005.

[2] S. Misra, S. Chandra Misra and I. Woungang, Guide to Wireless Mesh Networks,Springer, 2009, pp. 369-370.

[3] Z. Yan, L. Jijun and H. Honglin, “Wireless Mesh Networking, Architectures Protocols and Standard”, USA: Auerbach Publications, 2007.

[4] S. Chinara an S. K. Rath “A Survey on One-Hop Clustering Algorithms in Mobile Ad Hoc Networks” J Netw Syst Manage (2009):183– 207 DOI 10.1007/s10922-009-9123-7

[5]C. C. Chiang, T. C. Tsai, W. Liu and M. Gerla. “Routing in clustered multihop, mobile wireless networks with fading channel, The Next Millennium”, The IEEE SICON, pp.197–211 1997.

[6]A. Iwata, C.C. Chiang, G. Pei, M. Gerla, and T.W. Chen.“Scalable routing strategies for ad hoc wireless networks”.IEEE Journal on Selected Areas in Communications, Special Issue on Ad-Hoc Networks, pp 1369-1379, 1999.\

[7] B. Guizani,.B. Ayeb and A. Koukam ,Hierarchical Cluster-Based Link State Routing Protocol for Large Self-Organizing Networks, IEEE 12th International Conference on High Performance Switching and Routing (HPSR), pp 203 - 208 ,2011

[8] M. Singh, S.G. Lee, T. W. Kit and L.J. Huy,“ Clusterbased routing scheme for Wireless Mesh Networks,” *Advanced Communication Technology (ICACT),* 2011 13th International Conference, Publication Year: 2011 , Page(s): 335 – 338.

[9] M. Singh, S.G. Lee and D. Singh, A Simulation-Based Performance Analysis of a Cluster-based Routing Scheme for Wireless Mesh Networks,

International Journal of Multimedia and Ubiquitous Engineering, Vol.8, No.5 ,2013, pp.283-296.
[10] D. Kaushal, G. Niteshkumar, B. Prasann K. and V. Agarwal. Hierarchical cluster based routing for wireless mesh networks using group head, International Conference on Computing Sciences (ICCS), Phagwara, pp. 163-167, 2012.
[11]Neumann, C. Aichele, M. Lindner, and S. Wunderlich, Better Approach To Mobile Ad-hoc Networking (B.A.T.M.A.N.), Internet-Draft, pages 1-24, 2008. Network Working Group
[12] S. M. S. Bari, F. Anwar, M. H. Masud, Performance Study of Hybrid Wireless Mesh Protocol (HWMP) for IEEE 802.11s WLAN Mesh Networks, International Conference on Computer and Communication Engineering ,July 2012, pp. 712-716.
[13] A H Mozumder, T Acharjee, S Roy, Scalability performance analysis of batman and HWMP protocols in wireless mesh networks using ns-3, International Conference On Green Computing Communication and Electrical Engineering (ICGCCEE), 2014 , pp. 1–5.
[14] NS-3, The ns3 network simulator, *Online+. Available: http://www.nsnam.org/, 2014.

An Ontology Based Context Aware Protocol in Healthcare Services

Anirban Chakrabarty and Sudipta Roy

Abstract Interpretation of medical document requires descriptors to define semantically meaningful relations but due to the ever changing demands in healthcare environment such information sources can be highly dynamic. In these situations the most challenging problem is frequent ontology search keeping with user's interest. To manage this problem efficiently the paper suggests an ontology model using context aware properties of the system to facilitate the search process and allow dynamic ontology modification. The proposed method has been evaluated on Cancer datasets collected from publicly accessible sites and the results confirm its superiority over well known semantic similarity measures.

Keywords Ontology mapping · Context awareness · Search personalization · Healthcare

1 Introduction

Most Healthcare systems contain a large collection of related documents which necessitates a semantic search system to swiftly and accurately identify documents which satisfy user's needs. It has been found that keyword based search engines most often fail to give the expected results relevant to the query context. One of the key factors for personalized information access is the user context [1]. Context can be defined as the user's objective for seeking information [2]. In this paper, context is defined through the notion of ontological profiles which are updated over time to reflect changes in user interests. Ontology consists of a formal conceptualization in a particular field of interest that can be easily visualized or can be considered as a

Anirban Chakrabarty (✉) · Sudipta Roy
Assam Central University, Silchar, India
e-mail: chakrabarty.anirban@redffmail.com

Sudipta Roy
e-mail: Sudipta.it@gmail.com

J.K. Mandal et al. (eds.), *Proceedings of the First International Conference on Intelligent Computing and Communication*, Advances in Intelligent Systems and Computing 458, DOI 10.1007/978-981-10-2035-3_15

description of the elements it contains and when aligned with other ontologies it can help in forming a community of such elements or concepts [3, 4].

The major contributions suggested in this paper is mentioned as follows: (1) It provides an ontology for cancer patients containing both medical and socio economic conditions (2) to search for an optimal treatment plan suited to the patient (3) The ontology can be extended by healthcare experts based on changing treatment options, different disease symptoms and missing information with minimum involvement from external sources. (4) An ontology mapping strategy has been suggested that exploits contextual information of source ontology and supplements it in linguistic and structural similarity to enhance the strength of match with the target ontology.

2 Related Work

Most retrieval systems suffer from keyword barrier phenomenon which refers to the inability of information retrieval systems to convey semantic context of documents [5]. Related work developed a framework for Formal Concept Analysis which extended the Tf-Idf weighting model by introducing ontology dependent concepts [6]. Most search engines do not include user preferences and search context but provide users with a generalized search facility [7]. A related study shows that little work has been done on contextual retrieval to combine search technologies and ontology alignment using context in a single framework to provide the most accurate response for a user's information requirement [8].

A popular method to facilitate information access is through the use of ontology. Researchers have attempted to utilize ontology for improving navigation effectiveness as well as personalized Web search and browsing for generating user profiles [9]. An innovative approach for Ontology based on Concept merging was suggested were first the horizontal technique checks all relationships between concepts at the same level of two ontologies and merges them as defined by WordNet, then the vertical approach completes the merging of concepts at different levels but placed on same branch of the tree [10].

The notion of concept similarity calculation using ontology is that two concepts have a semantic correlation, and there exists a path in class hierarchy diagram. In a pioneering work, Resnik measures the semantic similarity of two words according to the maximum amount of information of their common ancestor node [11]. Leacock and Chodorow proposed a semantic similarity model based on distance which is an easy and natural approach but is heavily dependent on the ontology hierarchy already established [12]. Study of related work shows the use of RIMOM: a dynamic multi strategy ontology alignment framework which uses both linguistic and structural similarity to map source and target ontologies but it is suitable for only for 1:1 mapping [13]. The ontologies can be expressed in various ways. The most common language used to model ontologies is the Web Ontology Language (OWL), which is a form of RDF and is written using a subset of XML [14].

Unfortunately, most of these systems can provide little support in support for knowledge sharing and context reasoning because of their lack of ontology. Recent study focus on the use ontology based personalization system for assisting healthcare industry in patient diagnosis and intervention plans [15].

3 Methodology

In this work ontology has been developed to organize the terms of cancer disease, its symptoms, diagnosis, treatment options, intervention plans, patient condition and other social issues related to disease. On top of this a search algorithm based on context information stored in Ontology has been suggested which extracts all correlated words of the search string and can map from one ontology to another (Figs. 1 and 2).

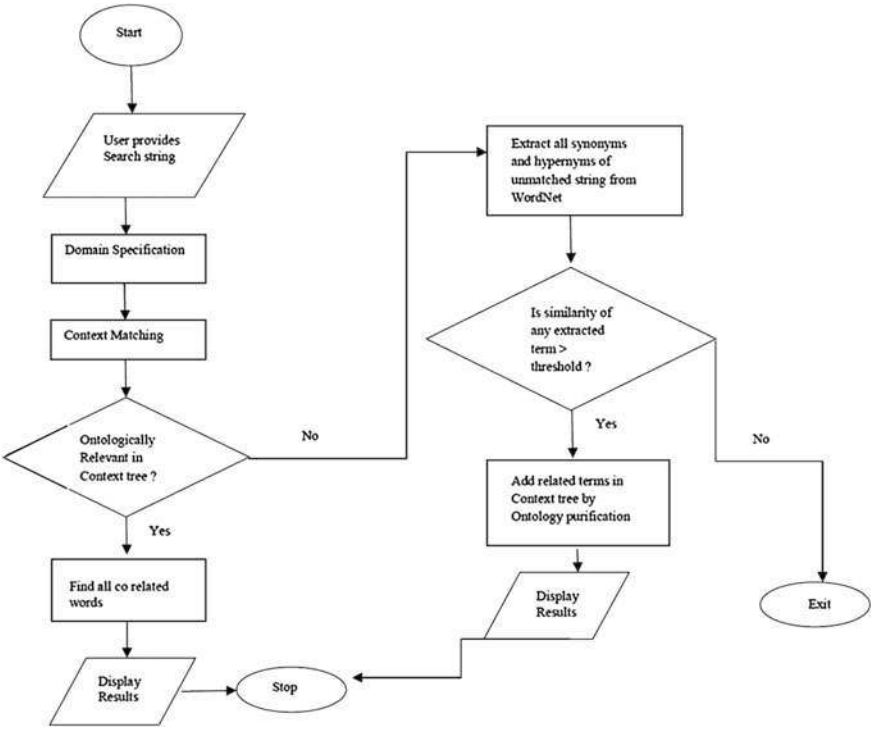

Fig. 1 Flowchart of context matching using an ontology framework

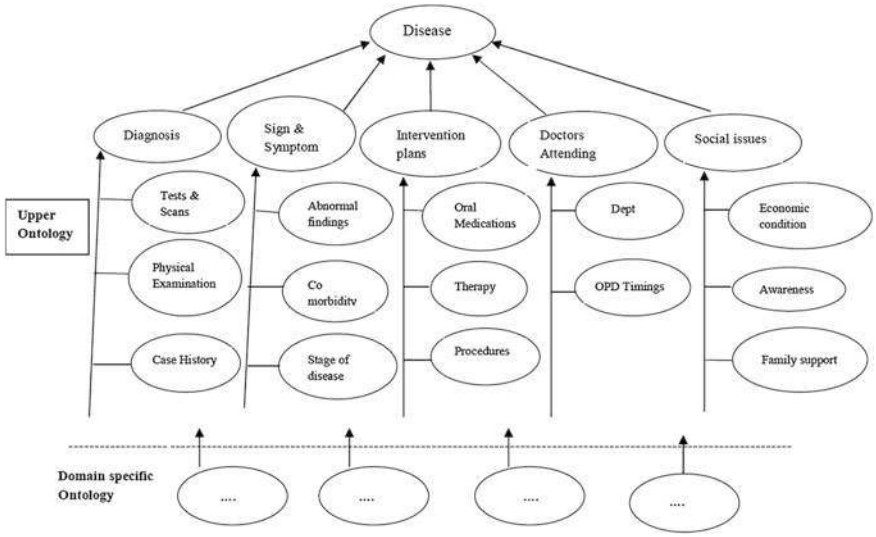

Fig. 2 Ontology hierarchy for cancer patients

4 Ontology Used

There are many existing ontology, but since critically ill patients need accurate and urgent medical intervention we have developed Cancer related Ontology containing medical and social concepts to assist in searching information and decision making.

5 Explanation of Proposed Algorithms

5.1 Context Search Technique

Step 1 Perform linguistic match between search string and the one present in target ontology based on Word Net. If direct match is found then display output and exit.
If no direct match found then based on the similarity results the pairs are sorted into three buckets: (a) above the upper threshold—provisionally similar (b) between the upper and lower threshold—uncertain bucket and (c) below the lower threshold—no match. Add all composite matches to the "uncertain bucket" along with the concepts between the upper and lower threshold (selected based on experimentation).

Step 2 Structural matching: For concepts whose similarity values are in uncertain bucket, perform the following:

(a) for each pair of concept, compare their parent nodes (when matching is between two ontology) to determine the total parental similarity for updating the original pairs similarity value. If match is found increment the score by 0.1.
(b) for each pair of concepts, compare their grandparent nodes to determine the total similarity for updating the original pairs similarity value. If match is found increment the score by 0.05.

Step 3 Use Word Sense disambiguation on the set of terms in 'Uncertain' and 'Provisionally similar' buckets to select the words actually representing the given context. The WSD method used here takes average of similarity values for each concept searched to show its relatedness to the ontology.

5.2 Ontology Modification

This procedure is called when the context is not found in the ontology tree but the searched context has a comparable relation then the context is dynamically added as a node in the ontology tree in appropriate location. Each ontology node is associated with an Id for comparison.

Pseudo code:

```
Modify (Root,Id,mi,N,M,Left,Right,Par)
Set Ptr = Root, Id= TRUE.
 Apply Algorithm-2 to find the similarity or relevance of searched  area.
 [If Node found] Set Ptr=Node.
Else if [node was not found but has to be added based on relevance threshold of the
domain set then check immediate ancestor. ]
{ Id[NodeO1]->Par=Id [NodeO2]->Par

Add new node.
If{ Id [NodeO1]<Id [NodeO1]->Par
Set Left[Par]=New
Else Set Right[Par]=New.
Set Id of new node.}
Print Updation Successful.
}}
[Else Updation Not Possible. ]
}
```

6 Experiment

6.1 Data Set

The experimental data used in this work has been collected from different cancer related websites which allows open access and made publicly available for research and study purposes [16–21]. The training data set comprising of 2721 documents was used for the representation of the cancer ontology indexing 204 concepts in the hierarchy.

6.2 Experimental Metrics

To perform a comparison of the improvement of proposed method with other established semantic search algorithms used in contemporary literature like k-NN, Resnik similarity, Rocchio based methods [22, 23].

The similarity measure suggested by Resnik, gives the information content (IC) of the Least Common Subsequence (LCS) for two concepts:

$$\text{SimRes} = \text{IC}(\text{LCS}) \tag{6}$$

where IC is defined as:

$$\text{IC}(c) = -\log\, p(c) \tag{7}$$

here p(c) is the probability of encountering a context c in a corpus.

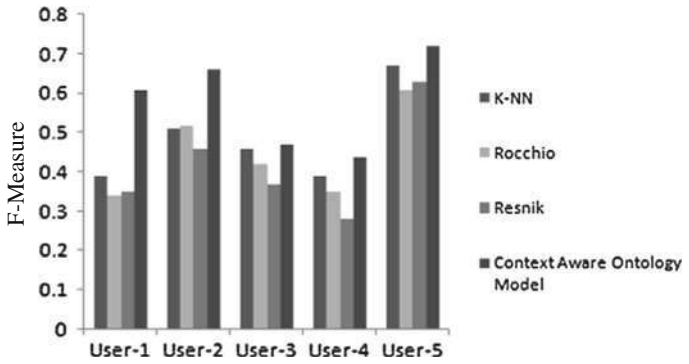

Fig. 3 Comparison of F-measure with other similarity measures for five users

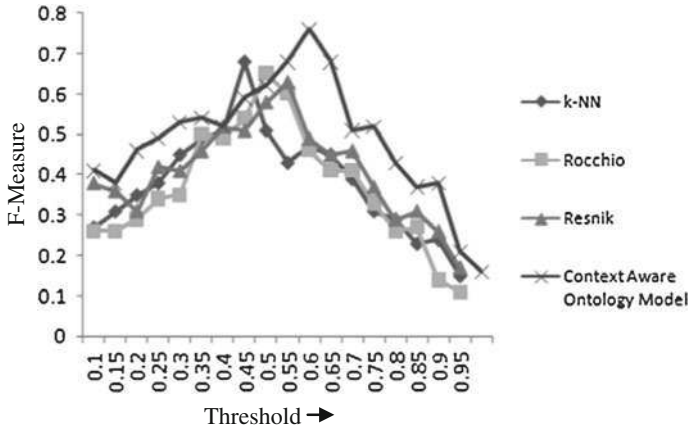

Fig. 4 Comparison of F-measure with varying threshold

The effectiveness of search was measured in terms of Top-n Recall and Top-n Precision [24]. The F-measure defined as $F = 2 * P * R/(P + R)$ is a balanced mean between precision and recall metrics and was used for comparing searches made by five different users.

6.3 Results

See Figs. 3, 4, 5 and 6.

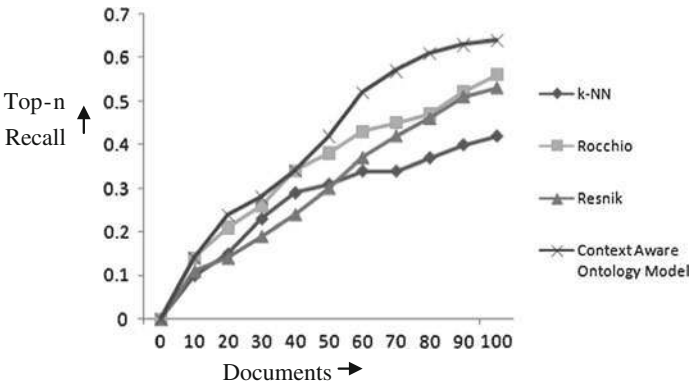

Fig. 5 Variation of average top-n recall in top-n documents using overlap queries

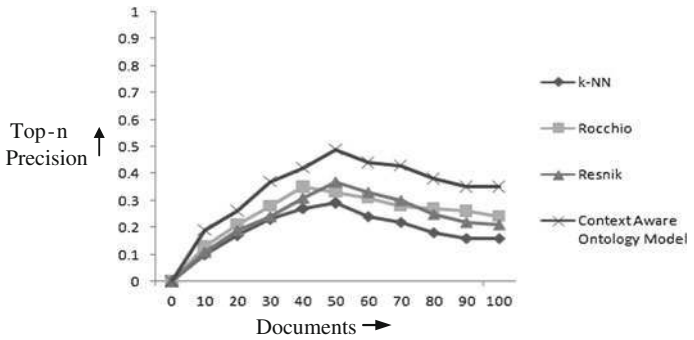

Fig. 6 Variation of average top-n precision in top-n documents using overlap queries

6.4 Discussion of Experimental Results

The comparison of F-measure with other semantic search techniques like k-NN, Rocchio and Resnik methods is depicted in Fig. 3. For all such users there has been improvement in F-measure values in case of our Context Aware Ontology model. Since the value of similarity depends to some extent on the threshold considered in the function so a variation of threshold with F-measure for different similarity techniques have been studied for same set of five users. The highest F-measure value was reached for a threshold of 0.6 in our context aware ontology model as shown in Fig. 4. Figures 5 and 6 gives the comparison of precision and recall values for top-n search results for all similarity techniques as shown above.

7 Conclusion

The work presents a framework for contextual information access using ontologies and demonstrated that the semantic knowledge embedded in cancer ontology can efficiently assist in search process and facilitate dynamic ontology modification. A comparison with other semantic search techniques shows that if contextual information present in ontology is retrieved effectively it can improve the search results based on user's requirements. This search technique can be extended to compare two separate ontologies as well.

It may be noted that the experimental results reported here is based on usage of randomly selected users, a few hundred queries, and a limited number of relevant documents. Future research in this area will consists of much larger scale of experiments and optimization parameters.

References

1. Pei-Min Chen, Fong-Chou Kuo , An information retrieval system based on a user profile, *The Journal of Systems and Software*, vol. 54, pp. 3–8, 2000.
2. Dey, A.K., Salber, D. Abowd, G.D., "A Conceptual Framework and a Toolkit for Supporting the Rapid Prototyping of Context-Aware Applications", *Human-Computer Interaction Journal*, Vol. 16(2–4), pp. 97–166, 2001.
3. Cimiano, P., Ontology Learning and Population from Text: Algorithms, Evaluation and Applications. Springer-Verlag New York, Inc., Secaucus, NJ, USA, 2006.
4. Gargouri, Y., Lefebvre, B., Meunier, J. Ontology Maintenance using Textual Analysis. Proceedings of the Seventh World Multi-Conference on Systemics, Cybernetics and Informatics (SCI). Orlando, USA (2003).
5. M-Y. Chen, H-C. Chu, Y-M. Chen, Developing a semantic enable information retrieval mechanism. *Expert Systems with Applications*, 37:322–340, 2010.
6. Rohana K. Rajapakse, Michael. Denham, Text retrieval with more realistic concept matching and reinforcement learning. *Information Processing and Management.* 42(5), 1260–127, September 2006.
7. Ashraf, J., Khadeer Hussain, O., Khadeer Hussain, F.: A Framework for Measuring Ontology Usage on the Web. In: The Computer Journal. Oxford University Press, 2012.
8. J. Allan, et al. Challenges in information retrieval and language modeling. ACM SIGIR Forum, 37(1):31–47, 2003.
9. Fang Liu, Clement Yu, Personalized Web Search for Improving Retrieval Effectiveness, *IEEE Transactions on Knowledge and Data Engineering*, Vol. 16, No. 1, January 2004.
10. Miyoung Cho, Hanil Kim, and Pankoo Kim. A new method for ontology merging based on concept using wordnet. In Advanced Communication Technology, 2006. ICACT 2006. The 8th International Conference, volume 3, pages 1573/1576, February 2006.
11. Philip Resnik, "Using Information Content to Evaluate Semantic Similarity in a taxonomy", In Proceedings of the *14th International Joint Conference on Artificial Intelligence*. Monte real, Canada, pp. 448–453, 1995.
12. C. Leacock, M. Chodorow. "Combining Local Context and WordNet Similarity for Word Sense Identification", *Computational Linguistics*, vol. 24, no. 1, pp. 147–165, 1998.
13. Juanzi Li, Jie Tang, Yi Li, and Qiong LuoRiMOM: A Dynamic Multistrategy Ontology Alignment Framework, *IEEE Transactions on Knowledge and Data Engineering*, Vol. 21, No. 8, August 2009.
14. Ashraf, J., Khadeer Hussain, O., Khadeer Hussain, F.: A Framework for Measuring Ontology Usage on the Web. In: The Computer Journal. Oxford University Press, 2012.
15. David Riano; Francis Real; Joan Albert Lopez; Fabio Campana; Sara Ercolani; Patrizia Mecocci; Roberta Annicchiarico & Carlo Caltagirone. An Ontology based personalization of Healthcare knowledge to support clinical decisions for chronically ill patients, Journal of Biomedical Informatics, Elsevier, 429–446, 45 (2012).
16. http://www.cancer.org/research/index [Last accessed on 12th October, 2015].
17. http://www.cancercare.org/accessengagementreport [Last accessed on 12th October 2015].
18. http://www.oncolink.org/resources [Last accessed on 7th October, 2015].
19. http://med.stanford.edu/cancer.html [Last accessed on 25th September, 2015].
20. http://www.ncbi.nlm.nih.gov/pubmed [Last accessed on 21st September, 2015].
21. http://www.cdc.gov/cancer/ [Last accessed on 16th September, 2015].
22. Oh-Woog Kwon, Jong Hyeok Lee. Text categorization based on *k*-nearest neighbor approach for Web site classification, *Information Processing and Management* Volume 39, Issue 1, Pages 25–44, January 2003.

23. Guanyu Gao, Shengxiao Guan. Text categorization based on improved Rocchio algorithm. In Proc. of Systems and Informatics (ICSAI) IEEE International Conference, pp. 2247–2250, 2012.
24. Paulo Cremonesi, Yehuda Koren, Roberto Turrin. Performance of recommender algorithms on top-n recommendation tasks. In Proc. of the fourth ACM conference on Recommender Systems, pp. 39–46, ACM New York, USA, 2010.

Classification and Performance Analysis of Intra-domain Mobility Management Schemes for Wireless Mesh Network

Abhishek Majumder
Tripura University
Suryamaninagar, Agartala
abhi2012@gmail.com

Subhrajyoti Deb
Tripura University
Suryamaninagar, Agartala
subhrajyotideb1@gmail.com

Sudipta Roy
Assam University
Silchar, Assam
sudipta.it@gmail.com

ABSTRACT

Nowadays Wireless Mesh Networks (WMNs) has come up with a promising solution for modern wireless communications. But, one of the major problems with WMN is the mobility of the Mesh Clients (MCs). To offer seamless connectivity to the MCs, their mobility management is necessary. During mobility management one of the major concerns is the communication overhead incurred during handoff of the MCs. For addressing this concern, many schemes have been proposed by the researchers. In this paper, a classification of the existing intra domain mobility management schemes has been presented. The schemes have been numerically analyzed. Finally, their performance has been analyzed and compared with respect to handoff cost considering different mobility rates of the MCs.

Categories and Subject Descriptors

C.2.1 [**Network Architecture and Design**]: Wireless communication

General Terms

Numerical Analysis

Keywords

Wireless Mesh Networks, Mobility Management, Intra-domain, Mesh Client, Handoff, Classification

1. INTRODUCTION

Recently Wireless Mesh Networks (WMNs) has become a prominent solution for modern wireless communications. In WMN nodes can be classified as mesh client (MC), mesh router (MR) and gateway (GW). The mobile users are MCs. MRs are the wireless routers to route the Internet as well as intranet packets. An MR having a wired interface to the Internet is called GW. Because of the random mobility behavior of the MC maintenance of seamless network connectivity becomes a challenging issue. In last few years some broad surveys on mobility management in cellular networks have been carried out and various models have already been established for analysis of performance. But due to architectural difference the proposed schemes are generally not relevant for WMNs [1]. In [1] I.F. Akyildiz et al explained that because of distributed nature of the WMN the mobility management designed for centralized cellular network cannot be used in WMN. The mobility management schemes designed for ad-hoc network does not work well in WMN because in WMN the MRs are generally static and the MCs are mobile. In case of ad-hoc network all the nodes are mobile. This gap creates the opportunity of development of mobility management schemes for WMN considering its unique feature of almost static MRs. For providing seamless connectivity to the MCs in WMN many mobility management schemes have been developed. Some of the intra-domain mobility management schemes discussed in this paper are: MEsh networks with MObility management (MEMO) [2], Mesh Mobility Management (M3) [3], and Wireless mesh Mobility Management (WMM) [4], ANT [5], Infrastructure Mesh (iMesh) [4], SMesh[7], Static Anchor Scheme [8] and Dynamic Anchor Scheme [8] have been discussed. The schemes have been classified considering the approach they use to route the packets. Finally, the schemes are numerically analyzed to observe the effect of mobility rate of MCs on handoff cost.

Organization of the paper is as follows. Section 2 discusses the classification of intra-domain mobility management. In section 3 System model and assumptions have been discussed. The mobility management schemes have been numerically analyzed in section 4. Section 5 compares the performance of the schemes. Finally, conclusion has been presented in section 6.

2. INTRA-DOMAIN MOBILITY MANAGEMENT

In mobility management there are two parts: location management and handoff management [1]. Location management manages the location registration and this issue has been comprehensively researched for cellular networks. Mobile terminals periodically send the information to the system that update new location details in location database [9]. On the other hand, handoff management is a mechanism where terminals carry all its connections active or alive while shifting to another access pint (AP) from its current AP. A comprehensive literature study of mobility management in wireless mesh networks has discussed in [1, 10, 11]. There are two types of mobility management schemes in WMN: intra-domain mobility management scheme and

ICTCS'16 March 4-5, 2016, Udaipur, Rajasthan, India.

http://dx.doi.org/10.1145/2905055.2905173.

inter-domain mobility management scheme. In this section classification of intra-domain mobility management scheme for WMN has been discussed.

Intra-domain mobility management schemes have been classified into three categories: tunnel based, routing based and multicast based. Figure 1 shows the taxonomy of mobility management schemes in WMN.

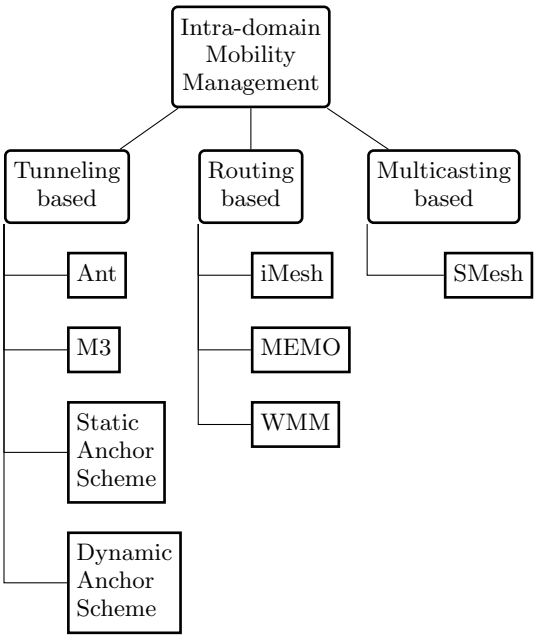

Figure 1: Taxonomy of mobility management scheme

2.1 Tunneling based Schemes

In tunnel based schemes mobile terminals register their location information to location database servers. In case of downstream internet packet, the GW tunnels the packets to the MC through the host MR. The upstream internet packets are sent to the GW by the MC without tunneling. The downstream as well as upstream intranet packets are tunneled by the host MR of source MC to host MR of destination MC. Some of the intra-domain mobility management schemes are: ANT, M3, Static and Dynamic Anchor Scheme.

The advantage of tunnel based scheme is that, no broadcast control message is used while the MC changes its point of attachment. The disadvantage is that, an extra IP header is added with each and every data packet to route the packet to the serving MR of destination MC.

2.1.1 Ant

Wang et. al proposed Ant [5] mobility management scheme. In Ant when a MC changes its point of attachment, a location update message and handoff confirmation message is sent to the location database server and old Routing Access Point (RAP) respectively by the new RAP. A location update acknowledgement is sent back by the location server to the new RAP acknowledging the update of MCs location in its database. Previous RAP establishes a temporary bidirectional tunnel toward new RAP to send buffered packets. It also sends tunnel request to the new RAP and all the RAPs of the corresponding MCs. In response, the new RAP and corresponding RAPs send back tunnel build acknowledgement and tunnel update acknowledgement to the old RAP respectively.

The advantage of this scheme is that, before link failures, RAP sends handoff association message to all its neighbors to reduce the handoff delay. Thus, the neighboring RAP gets alert of performing a handoff process in advance. But the problem with this scheme is that, signaling cost for location update is significantly large. Moreover, during each handoff location update message will be sent to the central location server which will increase the load on the location server.

2.1.2 M3

M3 [3] is another hybrid routing scheme. In M3 the GW maintains the location information of the MCs. A location update message is sent periodically to the GW by the MC. When a MC enters into the vicinity of a new MR, its old MR adds a forward pointer to the new MR. This process continues till the MC sends location update message to the GW. When location update is sent to the GW the forward chain length is reset to 0 and the GW sets host MR as serving MR of the MC in its location database. GW tunnels downstream Internet packets to the serving MR of the MC. If destination MC is within its coverage area, the packets are delivered to the MC. Else packets are delivered through the forward chain of MRs. On the other hand, upstream Internet packets are directly sent to the GW by the current MC without tunneling. The intranet traffic are sent to the GW by the source MC. The GW then sends he packet to the MC using tunnel.

The advantage is that, M3 is its simplicity. But, the problem with this scheme is that periodic location update of the MC make the system very static which is not good in an environment where different MCs have different mobility behavior. When the MCs are moving at higher speed forward chain length will be large.

2.1.3 Static Anchor Scheme

In Static Anchor Scheme [8] location server is maintained at the GW. As MC moves out from the coverage area of a MR and enters into the vicinity of a new MR, the old MR adds a forward pointer to the new MR. MC sends location update message to GW and the corresponding MCs when the forward chain length becomes equal to k. Thus the forward pointer gets reset. The GW tunnels downstream Internet packets to serving MR of the MC. MR then forwards the packets to destination MC directly if it is within serving MRs coverage area. Else packets will be forwarded to current MR of MC through forward chain. The current MR directly sends upstream Internet packets to the GW. In case of intranet packets, source MC sends the packets to the serving MR of destination MC which in turn is forwarded to current MR of destination MC.

Advantage of Static Anchor Scheme is, optimal value of k is determined for each mobile node depending on the service and mobility behavior of the MC. But, the problem with this scheme is that for calculating the optimal value of k periodically MCs has to perform computation which is not desirable for a battery powered MC. Moreover, all the queries for a MC are sent to the GW which increases its network and computation load.

2.1.4 Dynamic Anchor Scheme

This scheme is similar to the Static Anchor Scheme but here only difference is that in addition to the previous condition the forward pointer will be reset due to arrival of new intranet or Internet session. When the new Internet session arrives, the GW sends location query message to the MC through the serving MR of the MC. The current MR of the MC sends back response to the GW and the forward chain gets reset. In case of arriving intranet session, the source MC ends location query message for the destination MC to the GW. The GW performs the same location query process as it has done in case of Internet session arrival. After the location of the MC is updated in the GW, the GW sends back the response to the source MC. The source MC the then send packet directly to the serving MR of the destination MC.

The advantage of this scheme is that, the schemes is behaves more dynamically in different network conditions. The problem with this scheme is that the load on the GW increases heavily.

2.2 Routing based Scheme

Routing based schemes combine routing protocol with mobility management. MCs location information is propagated all through the WMN using routing scheme. Some of the routing based intra-domain mobility management schemes are: iMesh, MEMO and WMM.

In general the advantage routing based scheme is that no extra IP header is necessary for routing of data packets to destination MCs. Problem with this type of scheme is route update message is broadcasted in entire WMN.

2.2.1 iMesh

In iMesh [6] when MC enters into the vicinity of new MR, its route information is broadcasted in entire WMN through Host and Network Association (HNA) message. OLSR routing protocol is used for this broadcast. On receiving HNA all the MRs update MCs routing information.

Advantage of this scheme is that use of OLSR for broadcasting HNA message reduces the propagation of control messages. The problem with this scheme is that, HNA message is broadcasted after every handoff.

2.2.2 MEMO

In MEMO [2] scheme, as MC changes its point of attachment route error message is broadcasted in entire WMN by old MR. New MR proactively sends route reply message to GW for Internet communication. To maintain ongoing intranet connectivity the new MR broadcasts route request message to find a path to the corresponding MCs. In response, MRs of corresponding MCs send back route reply. This scheme uses routing table entries for routing of Internet and intranet packets.

The advantage of this scheme is that for maintaining continuous Internet connectivity a route reply message is proactively sent to the GW by the MC. Moreover, routing process is straight forward in this scheme. But the problem with this scheme is that excessive propagation of control message for removal of old route and setting up of new route.

2.2.3 WMM

Huang et al. introduced WMM scheme [4]. In WMM, MR maintains two types of table: routing table and proxy table. In this scheme no location update message is used. The options field of IP header of the data packet is divided into four parts: IRS (IP address of receivers host MR), RST (timestamp of senders host MR), ISS (IP address of senders host MR) and SST (timestamp of senders host MR). The ISS stores the IP address of MCs current MR. While forwarding data packets the intermediate MRs store the address of source MCs current MR in its proxy table. When a MC enters into the vicinity of a new MR, the old MR adds a forward pointer towards new MR.

The advantage of this scheme is that unlike other routing based scheme it does not suffer from excessive propagation of control message for route management. The problem of this scheme is that, each data packet has to carry extra bytes for storing IRS, RST, ISS and SST in its IP header.

2.3 Multicasting based Schemes

In Multicast based scheme a MC may be associated with a multiple MRs at a time. Data packets destined to MCs are copied and multi-casted to all the MRs in MCs data group.

The advantage of this type of scheme is that, this scheme reduces the handoff latency by associating MC with multiple MRs. On the other hand it suffers from routing overhead because of multicasting of the packets.

2.3.1 SMesh

In SMesh [10] there are two groups of MRs associated with a MC: data group and control group. A MR which believes that it can serve a MC the best, it joins the data group of that MC. The MRs of the control group will keep track of the MCs current location. When there is some packet to be delivered to the MC, it is multicasted to all the MRs which are in the data group of the MC. On receiving those packets, the MRs forward the packets to the MC.

The advantage of this scheme is that, because of multicasting possibility of packet is low. But, before the MC moves to the neighboring MR, the current MR establishes tunnel to all the neighboring MRs. This requires significant number of control packet transfer. Moreover, for maintenance of multicast group huge routing overhead is involved.

3. SYSTEM MODEL

This section presents system model and assumptions for carrying out the numerical analysis. Let, residence time of the MC in a MRs coverage area follows exponential distribution with rate (t_s) [12]. Therefore, the number of associations of an MC with MRs in a time unit follows Poisson distribution with rate λ_s [12]. In addition to the above mentioned assumptions some more parameters are used for numerical analysis of the schemes. Table 1 shows the parameters used for mathematical modeling and their interpretations.

4. NUMERICAL ANALYSIS

In this section handoff cost of intra-domain mobility management schemes discussed in section 2 will be discussed. In Ant scheme, when the MC moves from one RAP (Routing Access Point) to another, new RAP sends location update message towards location server. When location server receives location update message, it updates its location database and sends back location update acknowledgement. Old RAP sends tunnel setup request to the new RAP and

Symbol	Interpretation
M	Total number of MRs in the WMN.
α	Average distance between an arbitrary MR and the GW.
β	Average distance from an arbitrary MR to another arbitrary MR in WMN.
γ	Communication latency per hop.
t_{M3}	Time interval between two consecutive location updates in M3.
N_{active}	Average number of corresponding MCs of any arbitrary MC.
k	Threshold forward chain length for reset of forward chain in Static and Dynamic Anchor Scheme.
c_{move}	Average displacement of MC per MR association.
P_r	Probability that the MR broadcasts network control message to its neighborhood.

Table 1: Parameters and their interpretations.

the RAPs of corresponding nodes. The new RAP and corresponding RAPs sends tunnel build ACK and tunnel update ACK to the old RAP. So handoff cost per time unit of the scheme is,

$$C_{hANT} = \{(2 \times \alpha + 2 \times \beta \times N_{active} + 2) \times \gamma\} \times \lambda_s \quad (1)$$

In SMesh as client moves from old mesh node to a new mesh node, it joins the data group of the client and the local spines deamon informs all the other nodes of the mesh network through flooding. The old mesh node sends leave request to the control group of the client. The mesh node believing that it has the best connection with client sends back an acknowledgement. The local spines deamon informs other mesh node about its leave information from the data group of client. Therefore, the handoff cost per time unit is,

$$C_{hsMesh} = (2 \times M \times P_r + 2 \times \gamma) \times \lambda_s \quad (2)$$

In case of static anchor scheme [8] and dynamic anchor point scheme [8] location update message of the mesh client is sent to the Location server when the forward chain length is k. The cost of the procedure is $(\alpha + N_{active} \times \beta) \times \gamma$.Else, old Anchor Mesh Router adds a forward pointer to new Anchor Mesh Router costing $2 \times \gamma$. Therefore, handoff cost per time unit is,

$$C_{hstatic} = C_{hdynamic} = \{2 \times \gamma \times \left(\lambda_s - \frac{\lambda_s \times C_{move}}{k}\right) + (\alpha + N_{active} \times \beta) \times \frac{\lambda_s \times C_{move}}{k} \times \gamma\} \quad (3)$$

In iMesh as MC moves from one MR to another, HNA message is broadcasted using OLSR. So, handoff cost per time unit is,

$$C_{hiMesh} = \{P_r + M\} \times \lambda_s (4)$$

In MEMO scheme when MC changes its point of attachment from one MR to different MR, route error message is broadcasted in entire network by the old MR. A proactive route reply is sent towards GW by the MC. If MC wishes to extend the communication with corresponding MC, the new MR broadcasts route requests in WMN for finding corresponding MC. The host MR of corresponding MC responds by sending back route reply. Therefore, the schemes handoff cost per time unit is [12],

$$C_{hMEMO} = \{M + \alpha \times \gamma + N_{active} \times (M + \beta \times \gamma)\} \times \lambda_s \quad (5)$$

In M3 scheme location update message is sent by the MC to GW every t_{M3} time unit. Else, old MR adds a forward pointer to new MR. So the per time unit handoff cost is [12],

$$C_{hM3} = \{2 \times \gamma \times \frac{t_{M3}-1}{t_{M3}} + \alpha \times \gamma \times \frac{1}{t_{M3}}\} \times \lambda_s (6)$$

In WMM scheme there is no separate location update message. As MC changes its point of attachment, old MR adds a forward pointer to new MR. So, per time unit handoff cost is computed as [12],

$$C_{hWMM} = \{2 \times \gamma\} \times \lambda_s (7)$$

5. PERFORMANCE COMPARISON

In this section, the handoff cost of all the schemes which are numerically analyzed in section 4 has been compared. Table 2 shows the typical values of parameters used for comparison.

Parameter	Value
M	1000
α	50
β	30
γ	0.1
k	10
t_{m3}	1200
c_{move}[12]	0.4
P_r	0.4

Table 2: Value assign for handoff cost calculation

Figure 2 shows the effect of increase in mobility rate on handoff cost. Here, the value of N_{active} is considered as 30 and the value of λ_s is varied between 0.05 and 0.5. From figure 2 it can be observed that handoff cost per time unit

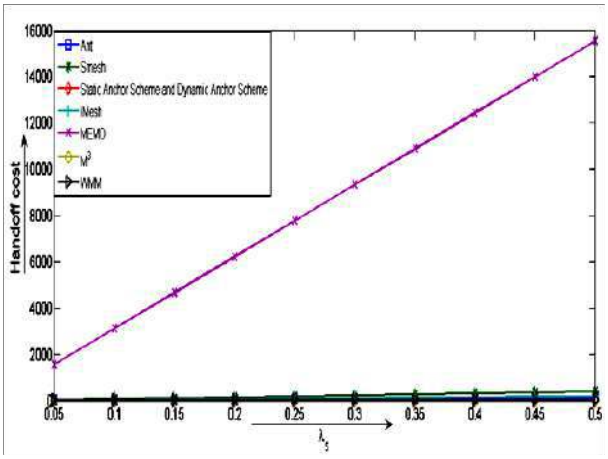

Figure 2: Impact of mobility rate on handoff cost per time unit

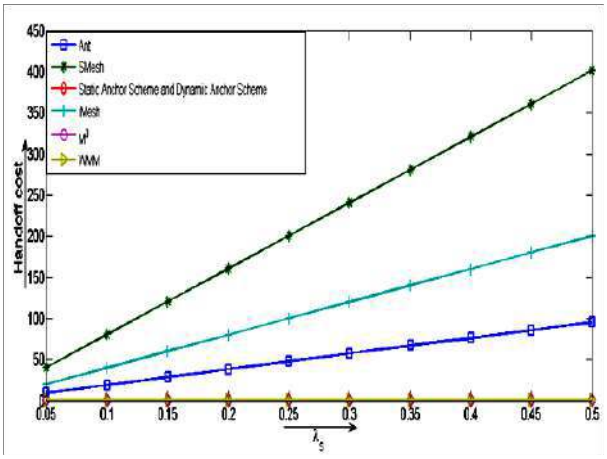

Figure 3: Impact of mobility rate on handoff cost per time unit (Subplot of figure 2)

of MEMO is the highest among all the schemes. This is because in MEMO during every handoff route error and route request messages are broadcasted. Figure 3 shows a subgraph of figure 2 to highlight the effect of mobility rate on handoff cost per time unit of Ant, Static Anchor Scheme, iMesh, M3 and WMM. SMesh has significantly high handoff cost. The reason behind this is, broadcast of join and leave information in the entire network by the new and old MR respectively. In iMesh since message is broadcasted in the entire network only by the new MR during every handoff, the handoff cost is less than SMesh. In case of ANT, only unicast message are sent by the old and new MR to the GW and corresponding MR during every handoff. Therefore, its handoff cost per time unit is less than that of iMesh. In Static and Dynamic Anchor Scheme, when the forward chain length becomes equal to k location update message is sent to the GW as well as corresponding MRs. Since here $k = 10$ the frequency of sending the location update message is very less which results in a handoff cost very less than that of ANT. In M3 location update message is sent every t_{M3} time unit. Since, t_{M3} is set to 1200, MC sends route update message towards GW less frequently. Therefore, location update cost is less than that of M3. In WMM there is no location update message. Only old MR adds a forward pointer to new MR. Therefore, handoff cost per time unit of WMM is the lowest. With the increases in mobility rate, handoff cost per time unit of all schemes increases because frequency of sending location update message increases. Increase rate of MEMO is very high because, the scheme uses AODV for flooding of route request and the number of route request and route error broadcasts increases with increase in node mobility rate. SMesh increases at lower rate than MEMO, because here link state routing protocol is used for broadcasting leave and join information of MRs in the entire WMN. Rate of increase in handoff cost of iMesh is less than SMesh because here only HNA message is broadcasted in WMN using OLSR. Handoff cost per time unit of Ant increases at lower rate than iMesh because it uses unicasting of location update message instead of broadcasting. The increase rate of Static Anchor Scheme, Dynamic Anchor Scheme, M3 and WMM is very low because the frequency of sending unicast location update message is very less.

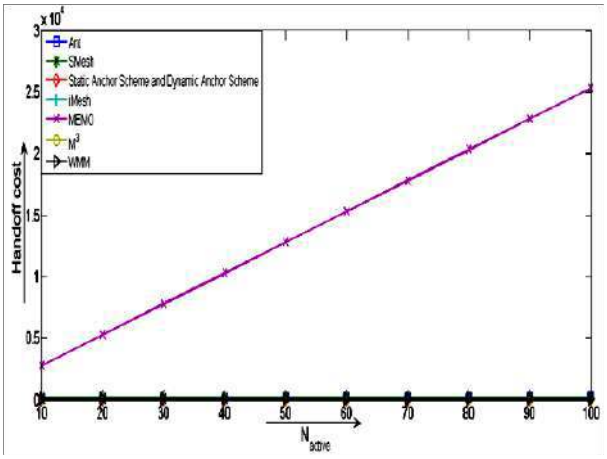

Figure 4: Impact of number of corresponding nodes on handoff cost per time unit

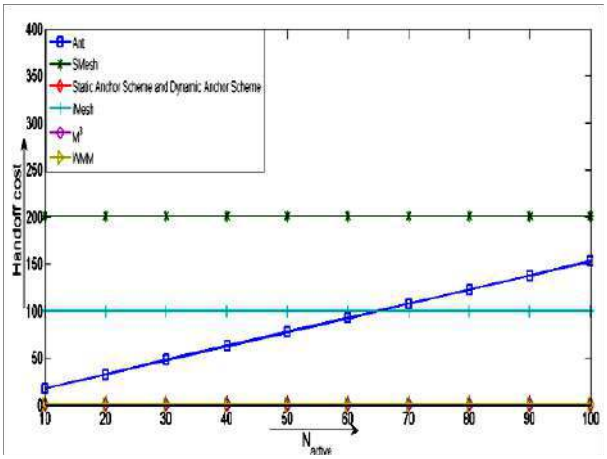

Figure 5: Impact of number of corresponding nodes on handoff cost per time unit (Subplot of figure 3)

Figure 4 shows the impact of increase in number of corresponding nodes (N_{active}) on handoff cost per time unit. Figure 5 shows the subplot of figure 4 highlighting the handoff cost for Ant, SMesh, Static Anchor Scheme, Dynamic Anchor Scheme, iMesh, M3 and WMM. Here, the value of λ_s is set to 0.25 and the number of corresponding MCs are varied between 10 to 100. With the increase in N_{active} handoff cost per time unit increases because route request message is broadcasted in the entire network for more number of corresponding MCs. The handoff cost of Ant increases with the increase in N_{active} because tunneling request is sent to more number of MRs. In case of Static and Dynamic Anchor Scheme since location update message sent to the corresponding MRs is infrequent, handoff cost per time unit increases at very low rate. Handoff cost of iMesh, M3 and WMM is independent of increase in N_{active} because location update message is not sent individually to corresponding MCs.

6. CONCLUSION AND FUTURE WORK

This paper presents classification of mobility management schemes. Different mobility management schemes have been discussed in brief. Handoff cost per time unit of the mobility management schemes have been calculated. A comparative study of the mobility management schemes with respect to handoff cost has been performed. From the comparison it was found that MEMO and WMM has the highest and lowest handoff cost per time unit respectively. Study of query cost and packet delivery cost of these schemes remains as future work. Moreover, simulation of the mobility management schemes for comparison will also be done in future.

7. ACKNOWLEDGEMENT

The work is funded by Department of Electronics and Information Technology (DeitY), Ministry of Communications and Information Technology, Electronics niketan, 6 CGO Complex, Lodhi Road, New Delhi-110003, Government of India, Vide no. 14(8)/2014-CC&BT, Dated: 03.09.2015.

8. REFERENCES

[1] I. F. Akyildiz, X. Wang, and W. Wang, "Wireless mesh networks: A survey," Computer Networks, vol. 47, no. 4, pp. 445-487, Mar. 2005.

[2] M. Ren, C. Liu, H. Zhao, T. Zhao, and W. Yan, "MEMO: An applied wireless mesh network with client support and mobility management," IEEE GLOBECOM 2007-2007 IEEE Global Telecommunications Conference, Nov. 2007.

[3] R. Huang, C. Zhang, and Y. Fang, "A mobility management scheme for wireless mesh networks," IEEE GLOBECOM 2007-2007 IEEE Global Telecommunications Conference, Nov. 2007.

[4] D.-W. Huang, P. Lin, and C.-H. Gan, "Design and performance study for a mobility management mechanism (WMM) using location cache for wireless mesh networks," IEEE Transactions on Mobile Computing, vol. 7, no. 5, pp. 546-556, May 2008.

[5] H. Wang, Q. Huang, Y. Xia, Y. Wu, and Y. Yuan, "A network-based local mobility management scheme for wireless mesh networks," 2007 IEEE Wireless Communications and Networking Conference, 2007.

[6] V. Navda, A. Kashyap, and S. R. Das, "Design and evaluation of iMesh: An infrastructure-mode wireless mesh network," Sixth IEEE International Symposium on a World of Wireless Mobile and Multimedia Networks.

[7] Y. Amir, C. Danilov, M. Hilsdale, R. Musaloiu-Elefteri, and N. Rivera, "Fast handoff for seamless wireless mesh networks," Proceedings of the 4th international conference on Mobile systems, applications and services - MobiSys 2006, 2006.

[8] Y. Li and I.-R. Chen, "Design and performance analysis of mobility management schemes based on pointer forwarding for wireless mesh networks," IEEE Transactions on Mobile Computing, vol. 10, no. 3, pp. 349-361, Mar. 2011.

[9] I. F. Akyildiz, J. Xie, and S. Mohanty, "A survey of mobility management in next-generation all-iP-based wireless systems," IEEE Wireless Communications, vol. 11, no. 4, pp. 16-28, Aug. 2004.

[10] Z. Zhang, R. W. Pazzi, and A. Boukerche, "A mobility management scheme for wireless mesh networks based on a hybrid routing protocol," Computer Networks, vol. 54, no. 4, pp. 558-572, Mar. 2010.

[11] J. Xie and X. Wang, "A survey of mobility management in hybrid wireless mesh networks," IEEE Network, vol. 22, no. 6, pp. 34-40, Nov. 2008.

[12] A. Majumder and S. Roy, "Design and analysis of a dynamic mobility management scheme for wireless mesh network," The Scientific World Journal, vol. 2013, pp. 1-16, 2013.

Personalizing Healthcare Services to support Decision making in treatment of Cancer patients using Ontology Alignment

Anirban Chakrabarty, Dr.Sudipta Roy
Computer Science and Engineering Department
Assam Central University
Silchar, India
chakrabarty.anirban@rediffmail.com, sudipta.it@gmail.com

***Abstract*— The foremost medium of information exchange has been text since ages but with the swift increase in volume of documents it has become a tedious task to organize and retrieve relevant information without the use of text-mining applications. Ontologies are a formal way of representing conceptual knowledge and can be related to text data to assist in this task. There is always a need for accurate interpretation of medical records of cancer patients in deciding intervention plans for proper treatment. However due to the ever changing demand in healthcare services such information sources can be highly variable and may not be suitable for all patients. In this situation the most challenging problem is personalizing healthcare treatment adapted to the patient's medical, social and economic conditions. To manage this problem efficiently the work suggests an ontology alignment model using context aware properties of the system and the patient to facilitate decision making. A patient ontology is mapped to the disease ontology to dynamically transform general treatment options into individual intervention plans most suitable for the patient. The proposed method can be used by medical professionals in recognizing incorrect diagnosis, preventive actions or in identifying co- occurring diseases in the patient.**

Keywords— Ontology alignment; Context awareness; Personalization; Cancer treatment

I. INTRODUCTION

With the widely increasing critical diseases Healthcare Industry have to provide lifesaving services within budget of consumers avoiding over treatment and comorbidities. Personalized healthcare service based on patient's actual requirement is need of hour and can be referred as patient context. Context can be defined as the set of concepts pertaining to a particular domain of information [1]. Ontology provides a formalized way of conceptualizing knowledge in a particular field of interest that can be easily comprehensible or can be considered as a description of the elements it contains and when aligned with other ontologies it can help in forming a community of such elements or concepts [2]. Ontology can be applied easily in medical support system because they not only capture healthcare knowledge in an incremental way but also can be integrated with the analyzing process performed by such system. In critical healthcare systems, particularly where there is variable set of patients with different disease syndromes and with different comorbidities and economic status, there is a high necessity to personalize the knowledge involving both patient conditions and intervention plan. In such situations an ontology mapping framework for aligning both the patient and disease can prove to be beneficial [3].

With this context, the work developed an ontology to organize the terms related to cancer disease and possible treatment options. This is called the disease ontology and it is mapped to the patient profile ontology which considers patient past and present medical history his social and economic conditions as well. An ontology alignment model is suggested which can map these ontologies to generate intervention plans suited for personalized treatment considering different context rather than providing over or wrong treatment.

The major contributions suggested in this paper is mentioned as follows: (1) It provides an ontology for cancer patients containing both medical and socio economic conditions (2) provides medical practitioners option to search for an optimal treatment plan suited for the patient (3) Health care experts can apply this system for identifying comorbid diseases, incorrect diagnosis and in taking decisions most customized for patient (4) An ontology mapping strategy has been suggested that exploits contextual information of source ontology to enhance the strength of match with target ontology.

II. REVIEW OF RELATED WORK

Medical ontologies can provide a feasible solution for representation of knowledge embedded in healthcare industry to provide improved services to its customers but no single ontology is sufficient for this purpose [4]. Rather, multiple ontologies must be integrated before they can support meaningful data analysis. Interoperability is necessary in healthcare for effective communication and prompt access to medical records for generating intervention plans to ensure patient care [5]. However most healthcare access engines do not include user preferences and search context but provide users with a generalized search facility [6].

A related study shows that little work has been done on contextual retrieval to combine search technologies and ontology alignment using context for efficient information retrieval as per users interest [7]. Study of related work reveals

978-1-4673-6984-8/16/$31.00

that effort has been made to utilize ontology for improving navigation effectiveness and web search to generate user interest area [8]. An innovative Ontology based concept merging was suggested using both horizontal and vertical approach for identifying relations between concepts of two different ontologies [9]. A class hierarchy model using the notion of concept similarity correlation was proposed [10]. A dynamic multi strategy ontology alignment framework RIMOM was used for exploiting both semantic and structural similarity to map source and target ontologies but it was only suitable for 1:1 mapping [11].

The ontologies can be expressed in various ways. The most common language used to model ontologies is the Ontology Web Language (OWL), which is a form of RDF and is written using a subset of XML [12]. Several ontology alignment algorithms have been developed over the past years were attempts have been made to develop matchers that perform large scale ontology alignments in minimum amount of time. Still, a great deal of work remains in creating a universally capable alignment tool that can map multiple ontologies [13]. A review shows the use of MaasMatch which was used to compute the similarity between the concepts in ontologies and an algorithm was used for extraction and elimination of faulty alignments from the result [14]. Another technique for ontology matching was developed that simulates the behavior of manually matching terms without having any expertise in the field [15]. Ontologies have been previously applied in bio medicines and ontology editors like Protégé has contributed to the development of biomedical ontologies[16][17].

III. Methodology

In this work a disease Ontology has been developed to map the concepts associated with cancer disease- its syndromes, lab tests and diagnosis, intervention plans, comorbidities. The patient case Ontology considers the patient condition including his medical history both past and recent economic conditions, which governs the choice for package of treatment in hospitals and also social issues related to disease. A search algorithm based on context information stored in Ontology has been suggested which extracts all correlated words from both aligned ontology and generates a personalized intervention plan for treating the patient. Smart recommendations are suggested by user based on this ontology alignment. Fig.1 shows the alignment of two ontologies using a mapping relation that identifies exact, broader, and narrower or no match. Such ontology hierarchy consists of concepts with properties and instances. The mapping function extracts the matching concepts from two ontologies and generates the target ontology which in this case is a personalized treatment plan for a patient.

IV. Ontology Alignment

There are many existing ontology, but since critically ill

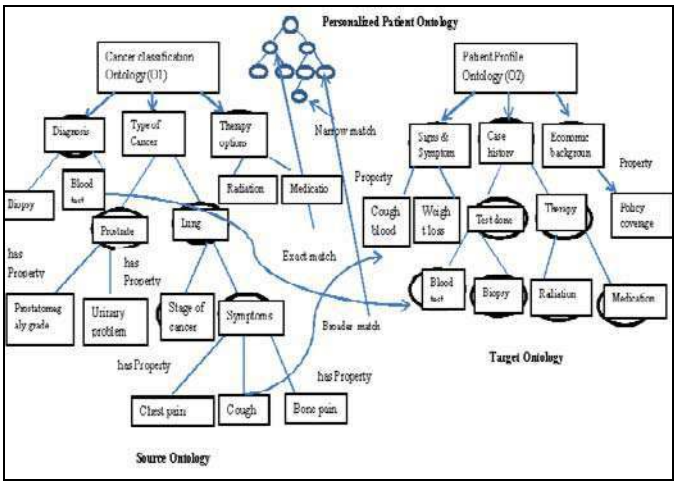

Fig.1. Ontology Alignment for personalized patient profile generation

patients need accurate and urgent medical intervention we have developed Cancer related Ontology containing medical and economic concepts to assist in searching information and decision making. In this work ontology is defined as a 5-tuple: O={C,P,Rc,Rp,I} where C and P are the set of concepts and properties respectively. Rc defines the hierarchical relationships (ci,cj) were ci is the sub concept of cj. Similarly, Rp defines the hierarchical relationships between each property and its sub properties, I denotes the instances of concepts.

We define Ontology Alignment with respect to to a patient to provide personalized services by matching concepts between patient and cancer ontology as defined below:

Align(O1,O2) = {patientid, ci1, ci2, relation_i, simscore_i}
here patientid is a unique system generated id for each patient, ci1 € O1, ci2 € O2 ; relation_i €{exactmatch, broad, narrow, conflict}; simscore_i €[0..1] here simscore provides the alignment score of two concepts in the ontology and is explained in Equation-1 in next section. Each tuple in Align(O1,O2) represents that concept ci1 in O1 is mapped to concept ci2 in O2 with score_i and the alignment type relation_i.

A Concept(c) in this ontology is represented as 4-tuple {Meta(c), Hier(c), Co-related(c), ,Inst(c),} were meta(c) gives the set of words describing metadata of concept like labels, comments ; Hier(c) is a vector that provides the sub and super concepts of c; Co-related(c) is a vector storing words that indicate synonym, hyponym of concept c; Similarly property of a concept is defined as a 4-tuple {Meta(p),Hier(p),Domain(p),Inst(p),} were Domain(p) is the set of concepts that have property p and Inst(p)gives the set of instances for this property. A personalized intervention plan is dynamically generated after ontology alignment and integrating with patient profile shown in Table-1 below.

TABLE I. A PORTION FROM ONTOLOGY ALIGNMENT

Patientid	Concepts accessed in Cancer Ontology	Concepts accessed in Patient ontology	Relation type	Score
P1	Cough	Cough with blood	Broader	0.87
P2	Prostrate cancer	Prostrate cancer	Exact	1
P3	Biopsy	Age	Conflict	0
P4	Blood test	PSA	Narrow	0.76

V. EXPLANATION OF PROPOSED ALGORITHMS

A. Algorithm for Ontology Alignment

The objective of aligning among different domain ontology is to enable the use of ontology A to search resources annotated with concepts from another ontology B [18]. The patient profile ontology hierarchy generated consists of matched concepts from two ontologies along with their scores.

Step-1: Contextual Match- Perform matching between concepts (including properties) from source and target ontologies using (1) shown below. Initially the pairs are sorted into three buckets: above the upper threshold - similar, between upper and lower threshold – uncertain bucket and below the lower threshold-conflicts. The threshold is selected based on experimentation.

$$Sim(c1,c2)=|p(c1)\cap p(c2)|\div|p(c1)\cup p(c2)| \quad (1)$$

here p(c) denotes the property p of concept c and |p(c)| gives the no. of properties belonging to concept c. Equation-1 shows the similarity of ontology concepts c1 € O1, c2 € O2 and it can be interpreted that more the properties match in two concepts, higher the similarity score of two concepts.

The similarity of two instances is determined by the percentage of similar properties in both instances. The expression for similarity between two instances I1 € O1 and I2 € O2 is given in (2) below.

$$Sim(I1,I2)=|IP(I1)\cap IP(I2)|\div|IP(I1)\cup IP(I2)| \quad (2)$$

Where IP(I) denotes property set of instance I

And | IP(I) | denotes no.of properties of instance I.

Step-2: Subtree Matching - For concepts falling in the uncertain bucket do the following using (3).

(a) for each pair of concept from two ontologies, compare their parent nodes to determine the parental similarity and use it to increment or decrement the original similarity score for concepts.

(b) for each pair of concept compare their child nodes to determine the child similarity and use it to update the original similarity score for the concepts.

$$Sim(c1,c2)=2*Depth(LCS)/[Depth(c1)+Depth(c2)] \quad (3)$$

here LCS indicates the least common subsumer(same parents for two concepts) and Depth(c) denotes the shortest distance from root node to a node c in the ontology where the synset of c is located.

Step-3: Generate Intervention plan - Continue matching concepts to identify type of match for identifying the symptoms of disease, co morbidities and test conducted patientwise. The intervention plan is generated by integrating the aligned dataset with the patient profile to predict the personalized plan for the patient. The intervention plan can be generated based on weights assigned by medical experts to different factors in (4) below.

$$\text{Intervention Plan} = \alpha\times\text{MatchedConcepts} + \beta\times\text{Cancerstage} + \gamma\times\text{Economicstatus}+\zeta\times\text{SocialFactors}) \div(\eta*\text{Patientage}+£*\text{comorbiddisease}) \quad (4)$$

here α,β,γ are weights assigned to no.of matched concepts,Stage of Cancer{Stage-I, Stage-II, Stage-III, Stage-IV}, and Economic status of patient considered in the range {Individual without policy, Individual with Policy, Corporate Policy, VIP} were numeric values has been assigned in increasing order of weight were higher values indicate better package of treatment as per patient economic status. The weightage ζ indicates weight given to social factors associated with cancer, like the one considered here is that whether the patient lives or works in radioactive sensitive environment stored as {1,0}. Severity of intervention decreases to a great extent with increasing age and presence of co morbid disease. Here there is a scope of assigning variable weights to the concepts based on its importance instead of assuming uniform weights for all. The Intervention plan shown in (4) has to be quatified in ranges with higher values suggesting intense treatment and lower values relying more on observation tests and Oral medication. Factors relating to Social issues of the patient for eg. type of job, awareness, habits affecting treatment of cancer can also be included in intervention plan provided data regarding the same is available. A comparative result for generalized and personalized intervention plan based on ontology alignment is depicted in Table II.

TABLE II. A COMPARISON OF GENERALIZED AND PERSONALIZED INTERVENTION PLAN GENERATED FROM ONTOLOGY ALIGNMENT

Patientid	Primary disease identified	Stage of cancer	General Intervention plan for cancer disease	Co occurent disease based on alignment	Age of patient in yrs	Economic status	Intervention Plan customized for patient
1	Locally advanced Prostate cancer	Stage-III	Chemotherapy followed by observatory test	Fatty liver	57	Corporate policy	Chemotherapy followed by Radical prostatectomy
2	Local Prostate cancer	Stage-II	radiation therapy followed by hormone therapy	Myocardial ischemia	72	Individual policy	Hormonal therapy and observation
3	Non small cell Lung cancer	Stage-III	Chemotherapy cycles with intermediate medication and radiation.	Frequent Vomiting and chest pain	21	Individual without policy	Chemotheray cycles with and thoracentesis
4	Squamous cell lung cancer	Stage-II	Radiation	Shortness of breath and cough, fatigue	46	Corporate policy	Lobectomy followed by radiation

B.Pseudo code for Personal Recommendation based on Ontology alignment

The patient and cancer ontologies are aligned to compute the matches in identifying the primary, co-occurring diseases, tests to be conducted. Based on these, medical professionals are provided smart recommendations while accepting any character for search. The pseudo code is provided below:

Step-1: Initialization

```
alphabet1=array(alphabets);
number1=array(prime numbers);
datanum1=array(random numbers);
data=array("PSA","bonescan","turp biopsy","CT scan,
"Radiation","Uroflowmetry"); // concepts associated with
  lab test for prostrate  cancer.
String1 array stores the search made by user
searchitem=1;
arrlength = count(alphabet1);
```

Step-2: Matching -If any character entered matches with stored alphabets then search multiplied with corresponding prime number.

```
for(i=0;i<strlen(string1);i++)
{       for(j=0;j<arrlength;j++)
        {
        if(string1[i]==alphabet1[j])
        {
searchitem = searchitem * number1[j];
        }
}
```

Step-3: Search Recommendation for user

```
c=0;
 for(i=0,j=0;i<count(datanum1);i++)
{
   if(datanum1[i]%searchitem==0)
{
possibleval[j]=data[i];
                j++;
                c++;
}
   }
          for(t=0;t<c;t++)
                {
        Display possibleval[t];
                }
          }
```

VI. EXPERIMENT AND RESULTS

A. Data Set

The experimental data used in this work has been collected from different cancer related websites which allows open access and has been made publicly available for research and study purposes [19-24]. The training data set comprising of 2721 documents was used for the representation of the cancer ontology indexing 204 concepts in the hierarchy. The testing was done selecting fifty patients randomly who have different types and stages of cancer. The software used for this work is jdk1.7, Html, CSS, and Protégé

4.1.Results

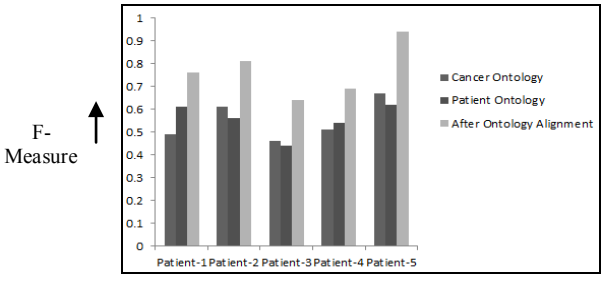

Fig. 2. Comparison of F-measure for selected users

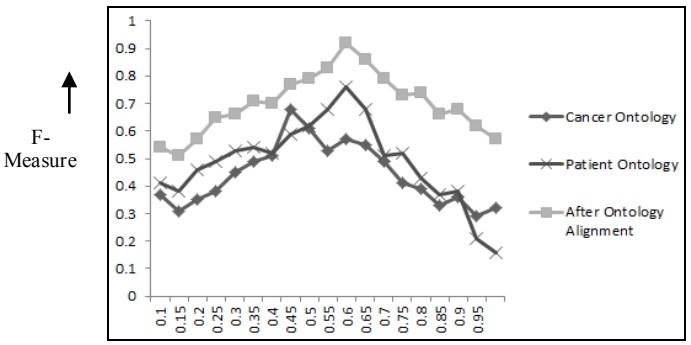

Fig. 3. Comparison of F-measure with varying threshold

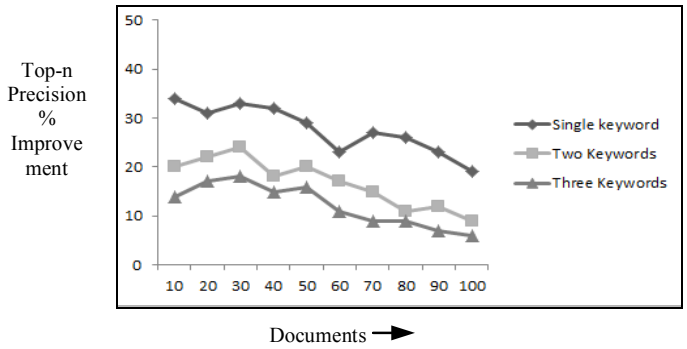

Fig. 4. Percentage of Improvement in Precision with Ontology Alignment Search using single and multiple words

B. *Analysis of Experimental Results*

The experimental evaluation was designed to retrieve the precision, recall and F-measure values and to study its variation with change in threshold [25]. A comparison of our ontology alignment based search has been evaluated using one, two and three keywords for top-n documents [26].The comparison of F-measure for intervention plans of five patients suffering from cancer is provided in Fig.2. The results confirm that there is a sharp improvement in F-measure values in case of our Ontology Alignment model. The variation in F-measure values with changing threshold has been plotted in Fig.3. It has been observed that peak value for F-measure has been obtained at a threshold of 0.63. Fig.4 and Fig.5 provides the percentage in improvement in top Precision and Recall values for ontology alignment search results using one, two and three keywords. Both results show that there is a significant rise in precision and recall values using single keyword in our ontology alignment approach when compared with individual ontology search results. The improvement however decreases with the increase in keywords.

VII. SUMMARY AND FUTURE SCOPE

The work demonstrates use of Ontology alignment to generate intervention plans suitable for patients, integrating

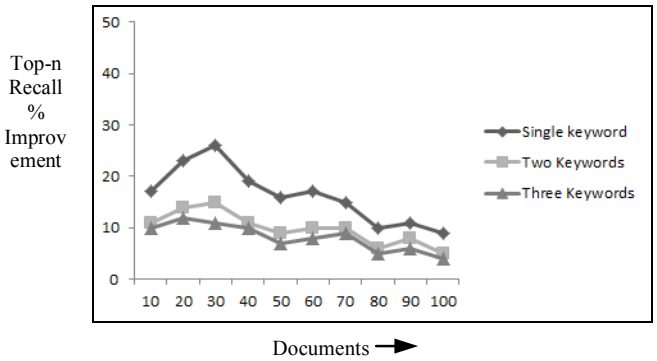

Fig. 5. Percentage of Improvement in Recall with Ontology Alignment Search using single and multiple words

the medical, personal and economic factors. The work uses contextual matching, and sub tree matching to accurately identify matches thus eliminating the ones not required for the patient. Smart recommendations are suggested to user based on searched domain which can be provided when the user inputs any search character for eg. tests required for lung cancer. The experimental results provided here are based on usage of randomly selected users, a few hundred queries, and a limited number of relevant documents. Future research in this area will consists of much larger scale of experiments and optimization parameters.

This heterogeneous ontology alignment can be applied to search among Digital libraries for plagiarism check of research papers submitted by authors. Another application of this work can be used by Software Development companies to archive the source code and components in an ontology framework which can be reused later for searching suitable codes and components applicable for specific projects.

REFERENCES

[1] Shady Shehata, Fakhri Karray, and Mohamed S. Kamel, An Efficient Concept-Based Mining Model for Enhancing Text Clustering, IEEE Transaction on Knowl. and Data Engineering, Vol. 22, No. 10, October 2010

[2] Lorena Otero-Cerdeira , Francisco J. Rodríguez-Martínez,,Alma Gómez- Rodríguez, Ontology matching: A literature review, Elsevier J. of Expert Systems with Applications, 42, 949–971, 2015.

[3] David Riano, Francis Real , Joan Albert Lopez-Vallverdu, Fabio ampana , Sara Ercolani, Patrizia Mecocci , Roberta Annicchiarico, Carlo Caltagirone, An ontology-based personalization of health-care knowledge to support clinical decisions for chronically ill patients, Elsevier J. of Biomedical Informatics, 45, 429–446, 2012.

[4] Scheuermann RH, Ceusters W, Smith B. Toward an ontological treatment of disease and diagnosis. In: Proceedings of the 2009 AMIA summit on translational bioinformatics, San Francisco (CA), p. 116–20, 2009.

[5] Healthcare Information exchange and interoperability www.citl.org/research/hiei.htm, Center for Information Technology leadership, 2004. Last accessed on December 2015.

[6] Fang Liu, Clement Yu, Personalized Web Search for Improving Retrieval Effectiveness, IEEE Transactions on Knowl. and Data Engineering, Vol. 16, No. 1, January 2004.
[7] Rohana K.Rajapakse, Michael.Denham, Text retrieval with more realistic concept matching and reinforcement larning. Information Processing and Management.42(5),1260-127, September 2006.
[8] Ashraf, J., Khadeer Hussain, O., Khadeer Hussain, F.: A Framework for Measuring Ontology Usage on the Web.In: The Computer Journal. Oxford University Press, 2012.
[9] Miyoung Cho, Hanil Kim, and Pankoo Kim. A new method for ontology merging based on concept using Wordnet. In Advanced Communication Technology, 2006. ICACT 2006. The 8th International Conference, volume 3, pages 1573/1576, February 2006.
[10] M-Y.Chen, H-C.Chu, Y-M.Chen, Developing a semantic enable information retrieval mechanism. Expert Systems with Applications, 37:322-340, 2010.
[11] Juanzi Li, Jie Tang, Yi Li, and Qiong LuoRiMOM: A Dynamic Multistrategy Ontology Alignment Framework, IEEE Transactions on Knowledge and Data Engineering, Vol. 21, No. 8, August 2009
[12] Ontology Web Language, http://www.w3.org/TR/owl-features/ 2008. [Accessed on 20th December 2015]
[13] P. Lambrix and H. Tan, A Tool for Evaluating Ontology Alignment Strategies, J. of Data Semantics, Vol. 8, pp. 182-202, 2007.
[14] Schadd, F. C., & Roos, N. (2012). MaasMatch results for OAEI 2012. In P. Shvaiko, J. Euzenat, A. Kementsietsidis, M. Mao, N. F. Noy, & H. Stuckenschmidt (Eds.), OM, CEUR-WS.org. (pp. 160–167).
[15] Paulheim, H., Hertling, S., & Ritze, D. (2013). Towards evaluating interactive ontology matching tools. Lecture notes in computer science LNCS, Vol. 7882, pp. 31–45.
[16] Brochhausen M, Spear AD, Cocos C, Weiler G, Martn L, Anguita A, et al. The ACGT master ontology and its applications – towards an ontology driven cancer research and management system. J Biomed Inform 2011;44(1): 8–25.
[17] http://protegewiki.stanford.edu
[18] P. Shvaiko, J. Euzenat: Ontology matching: state of the art and future challenges, IEEE Transactions on Knowledge and Data Engineering, 2013.
[19] http://www.cancer.org/research/index
[20] http://www.cancercare.org/accessengagementreport
[21] http://www.oncolink.org/resources
[22] http://med.stanford.edu/cancer.html
[23] http://www.ncbi.nlm.nih.gov/pubmed
[24] http://www.cdc.gov/cancer/
[25] Yuan-chao Liu , Chong Wu, Ming Liu, Research of fast SOM clustering for text information, Elsevier J. of Expert Systems with Applications 38 (2011) 9325– 9333.
[26] Paulo Cremonesi, Yehuda Koren, Roberto Turrin. Rerformance of recommender algorithms on top-n recommendation tasks. In Proc. of the fourth ACM conference on Recommender Systems, pp.39-46, New York, USA, 2010.

Comparison of Performance Metrics of ModAODV with DSDV and AODV

Mrinal Kanti Deb Barma, Rajib Chowdhuri, Sudipta Roy and Santanu Kumar Sen

Abstract In this paper, an adaptive routing in Mobile Adhoc Network (MANET) is presented using special neighbors on different routes. The routing table of each node is computed and stored in a metric. The path with the minimum cost is selected as the primary routing path among all feasible paths. The Adhoc On—Demand Distance Vector (AODV) Routing protocol is modified in such a way that only the destination node will respond to a route request which greatly reduces the transmission of control data packets in a network. The performance of modified AODV is evaluated based on metrics such as throughput, packet delivery ratio, and normalized routing overhead.

Keywords MANET · Throughput · Packet delivery ratio · Normalized routing overhead

1 Introduction

The primary motivation toward the design and development of a Distance Vector Routing (DVR)-based hybrid protocol for Mobile Adhoc Network (MANET) and WSN kind of networks is mainly because of the simplicity and elegance of the DVR algorithm, which is a traditional routing protocol based on Bellman Ford's

M.K.D. Barma (✉) · Rajib Chowdhuri
Department of Computer Science and Engineering, NIT Agartala, Jirania, Tripura, India
e-mail: mkdb06@gmail.com

Rajib Chowdhuri
e-mail: rjbchwdhri@gmail.com

Sudipta Roy
Department of Computer Science and Engineering, Assam University, Silchar, India
e-mail: sudipta.it@gmail.com

S.K. Sen
Department of Computer Science and Engineering, GNIT Kolkata, Kolkata, India
e-mail: santanu.sen@ieee.org

R. Singh and S. Choudhury (eds.), *Proceeding of International Conference on Intelligent Communication, Control and Devices*, Advances in Intelligent Systems and Computing 479, DOI 10.1007/978-981-10-1708-7_11

algorithm that later on got rejected mainly because of the Count-To Infinity (CTI) problem of the DVRA. The second motivation forwards the development of DVR-based routing algorithm for MANETs because of its neighbor exchange-based routing technique, through which a route can view its whole world only through a neighbor, and hence, need not to keep track of the whole network, thereby reducing the burden of bandwidth and battery supply. Routing is the heart of a network and optimality and reliability are the keen requirements for the success of such routing protocol.

The goal of this paper is to modify the routing table of original Adhoc On—Demand Distance Vector (AODV) protocol based on special neighbors of each route to obtain a modified version of AODV protocol termed as ModAODV whose performance is compared with that of AODV and DSDV in terms of throughput, packet delivery ratio, and normalized routing overhead.

2 Comparison of ModAODV Protocol with DVR Protocol

The important disadvantages of DVR protocol is as follows:

Slow Convergence Problem: When there is an increase in the cost of any link or there is a link failure between two neighboring nodes in a network or internetwork, the algorithm, in the worst case, may require an excessive number of iterations to converge or to terminate. The slow convergence phenomenon actually results from the propagation of a bad news which implies a loss or increased distance of a route. In the DVRA, the bad news travels slowly unlike the good news [1, 2].

Count to Infinity problem: DVR Algorithm suffers from the serious problem of CTI [1, 3–5] which sometimes occurs following a link or router failure, due to unending routing loops involving two or more routers. IP packets going round in loops are ultimately dropped after expiry of the Time-to-Live (TTL), but they generate considerable amount of unproductive traffic before being dropped.

Oscillation Problem: Because of the need to always use the shortest path, there may be frequent switching of routes caused by even small increase or decrease in the link costs. This frequent route switching gives rise to instability in routing and this problem is known as the route oscillation problem [2].

3 Identification and Utilization of Special Neighbors

Distance Vector Routing Table (DVRT) is primarily used for identifying special neighbors which are used in making ModAODV efficient and practical with fast convergence and no CTI problem. The procedure of identification of special neighbor and its method of utilization in case of both topological and traffic change is based on the example network shown in Fig. 1.

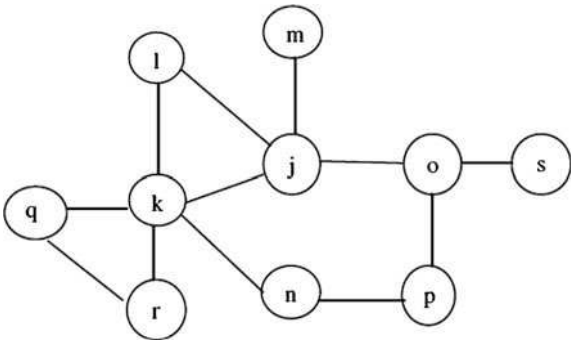

Fig. 1 Sample network with special neighbors of router *j*

3.1 Forwarding Neighbor (FN)

Identification—A router R_j identifies its current FNs for different destinations by processing the entries in its own routing table $DVRT_j$. If, in the *i*th entry in $DVRT_j$, R_j finds that $DEST_i = R_i$ but Next Hop $NH_i = R_k$ where $R_k \neq R_i$, then R_j identifies R_k as its FN for reaching R_i and notes it down in its Neighbor Table NT_j. However, if R_j finds that $DEST_i = R_i = NH_i$, then it identifies R_i as a neighboring router.

3.2 Dependent Neighbor (DN)

Identification—If a router R_k presently reaches a destination R_i via its neighbor R_j, i.e., if R_k depends on R_j for reaching R_i, then R_k is a Dependent Neighbor (DN) of R_j for reaching R_i. The routers R_k, R_l, and R_m, but not R_n, in Fig. 1 are all DNs of R_j for reaching the destination R_i.

Utilization—Router R_j utilizes its DNs in the ModAODV protocol when R_j is unable to find an alternative shortest path to destination. In such scenario, it permits some time to R_k to discover and advertise a new route (not via R_j) to reach destination. Only, thereafter, R_j considers that route as a contender for becoming the alternative shortest path to reach Destination.

3.3 Co-Neighbor (CN)

Identification—If three routers R_j, R_k, and R_l, form a triangle in a network graph, then any two of the three routers are mutual CNs of each other for the third one, e.g., in Fig. 1, R_k is a CN of R_j for R_l, R_l is a CN of R_j for R_k, R_j is a CN of R_k for R_l, and so on.

Utilization—The utility of a CN is enormous because it can help to isolate a link failure from a router failure to yield an extremely rapid convergence. In case R_j ever

loses its direct communication with a Multi Connected Neighbor (MCN) R_k, and has at least one CN say, R_l, then, R_j can statistically decide, with the help of its CN R_l, whether the router R_k itself has failed or the connecting link R_j, R_k has failed. Thus if R_j, being unable to communicate directly with its MCN neighbor R_k, discovers that R_l, its CN for R_k, is also unable to communicate with R_k, then both R_j as well as R_l, conclude that R_k itself has failed. On the other hand, if R_l can still communicate with R_k, then R_j concludes that its link R_j, R_k has failed. In the former case, both R_j and R_k will recognize the failed router R_k as a Lost Destination and will quickly disseminate this vital information throughout the network to achieve an extremely fast convergence. In the latter case, R_j will simply choose to reach R_k indirectly via its CN R_l and this indirect route to R_k will be shortest if the distance metric is hop count.

ModAODV is implemented based on the following general assumptions:

(i) Each router maintains an interval timer called Periodic Update Interval Timer that will periodically interrupt it for performing the periodic update of its DVRT and for sending copies of this updated DVRT to all neighbors.
(ii) Each router has, one interval timer called the Neighbor Interval Timer for all its neighbors to check that at least one DVRT is received from that neighbor within each Periodic Update Interval.
(iii) Each router has one Echo Timer for each neighbor which times out if any neighbor fails to send back an ECHO RESPONSE packet in response to an ECHO REQUEST packet sent by the router to that neighbor.
(iv) A DVRT has N entries where each entry corresponds to each known router in the N-node network. Each entry has 3 fields, namely, the identity of a destination router, the estimated distance (metric) of this router and, finally, the identity of the Next-Hop (NH) router, i.e., the FN in case of any remote router, for reaching that destination.

4 Results and Analysis

We use network simulator ns-2.34 [6, 7] and the simulations were performed with a minimum of 11 nodes to a maximum of 30 nodes and the nodes were of unicast type. The maximum number of packets in an interface queue which is known as Interface Queue Length (IFQLEN) is varied from 10 to 50 (Table 1).

4.1 Measuring Throughput

Throughput = (Total number of successfully received data packet/(Time of received data packet − Time of sent data packet)).

Table 1 Parameters used in simulation

Parameter	Value
Area of the network	500 m × 400 m
Simulation time	150 s
Packet size	512 Bytes
MAC type	IEEE 802.11
Interface queue type	Queue/DropTail/Priqueue
Mobility model	Random waypoint
Traffic type	CBR

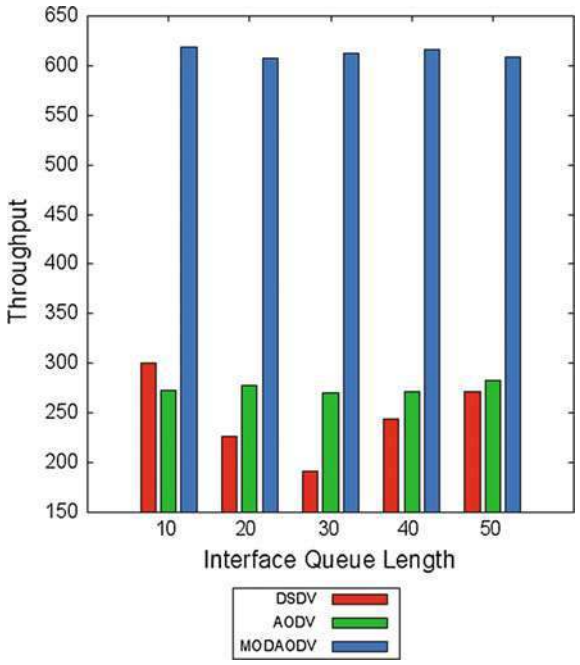

Fig. 2 Measurement of throughput with increase in interface queue length

In the first experiment, 5 (five) simulations were performed for each routing protocol to obtain the values of throughput by varying the size of IFQLEN from 10 to 50.

Figure 2 shows the impact of increasing IFQLEN on throughput. The number of nodes used in this experiment was 11. The maximum speed was V_m = 20.0 m/s and pause time was 2.0 s and it is observed that throughput of modified AODV doubles the throughput of original AODV and DSDV with increase in the number of packets in the interface queue.

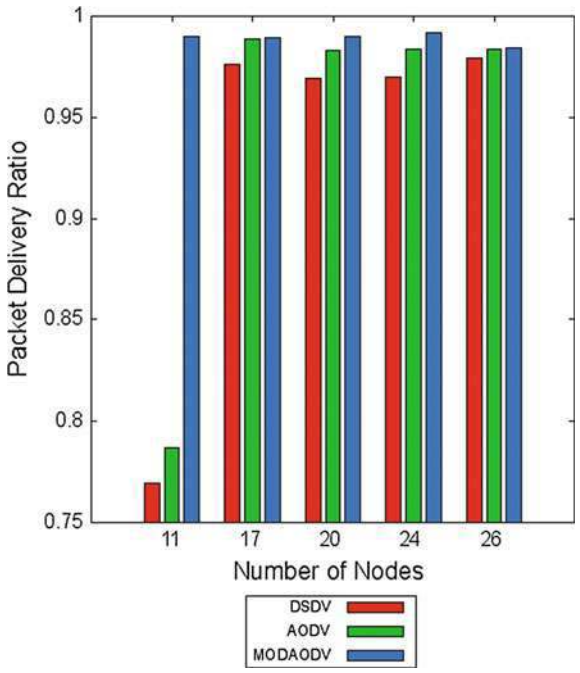

Fig. 3 Measurement of packet delivery ratio with increase in number of nodes

4.2 Measuring Packet Delivery Ratio

PDR = $\sum$ (Number of packets received by all sinks)/$\sum$ (Number of packets send by all sources).

In the second experiment, 5 (five) simulations were conducted for each routing protocol to obtain the values of PDR by varying the number of nodes from 11 to 26 and in the third experiment, the speed of nodes was varied from 40 to 90 m/s.

Figure 3 shows the impact of increasing the number of nodes on PDR. ModAODV delivers much higher data packets which is almost 5.62 % higher than that of AODV and by 4.38 % higher than DSDV. In this experiment, pause time was 2.0 s and the speed of nodes was 20 m/s.

Figure 4 shows the impact of increasing the speed of nodes on PDR. ModAODV delivers higher data packets which is almost 2.22 % higher than original AODV and 1.14 % higher than DSDV. In this experiment, 30 (thirty) nodes were taken and pause time was 20 m/s.

4.3 Measuring Normalized Routing Overhead

Normalized Routing Load (NRL) = (Amount of routing-related transmission)/(Total amount of data-related transmission).

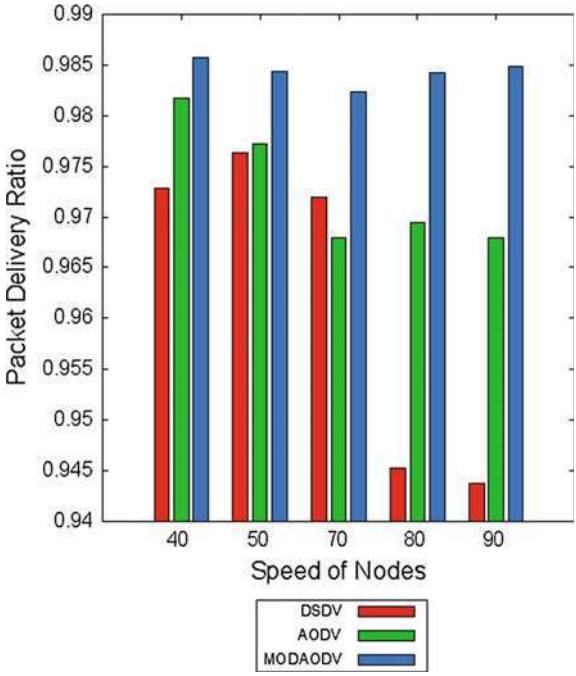

Fig. 4 Measurement of packet delivery ratio with increase in speed of nodes

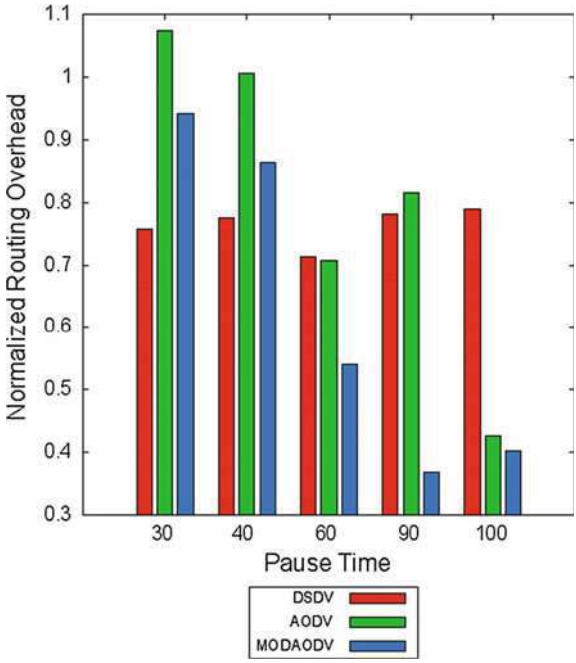

Fig. 5 Measurement of routing overhead with increase in pause time

In this experiment, 5(five) simulations were performed for each routing protocol to obtain the values of NRL by varying the pause time of nodes from 30 to 100 s.

Figure 5 shows the impact of increasing pause time of nodes on NRL which clearly depicts that the routing overhead of ModAODV is much lower than that of original AODV and DSDV except when pause time were 30 s and 40 s, overhead of ModAODV is a bit higher compared to DSDV. In this experiment, 30 (thirty) nodes were taken, speed of nodes was 20 m/s, and the size of IFQLEN was 50.

5 Conclusion

This paper compares the performance of a new routing protocol called ModAODV with two foremost routing protocols DSDV and AODV using ns-2 simulations. The results show that throughput of ModAODV doubles the throughput of original AODV and DSDV with increase in IFQLEN. The impact of increasing the number of nodes and speed of nodes depicts that ModAODV delivers much higher data packets compared to AODV and DSDV. The impact of increasing the pause time of nodes depicts that original AODV and DSDV has highest routing overhead compared to ModAODV. Throughput decreases in case of DSDV since it needs to advertise both periodic and event-driven updates but throughput of AODV remains stable. Thus DSDV consumes more bandwidth compared to DSDV.

As our future work, we will try to include one more additional feature to this ModAODV protocol like acknowledgement of data by the destination to the source.

References

1. A.S. Tenenbaum, “Computer Networks”, 5th Ed., Pearson Education Asea, 2010.
2. D.E. Comer, “Internetworking with TCP/IP”, 4th Ed., Pearson Education, Singapore, 2005.
3. S. K. Ray, S. K. Paira and S. K. Sen, “Modified Distance Vector Routing Avoids Counting - To-Infinity Problem”, Proc. Intl. Conf. CODIS 2004, Kolkata, pp. 31–34, 2004.
4. S. K. Ray, J. Kumar, S. K. Sen and J. Nath, “Modified Distance Vector Routing Scheme for a MANET”, Proc. Of the 13th National Conference on Communications (NCC), IIT Kanpur, pp. 197–201, 2007.
5. A. Leon-Garcia and Indra Widjaja, “Communication Networks”, 2nd Ed., Tata McGraw-Hill, 2004.
6. K. Fall and K. Varadhan, “The NS Manual, (formerly ns Notes and Documentation)”, The VINT Project: A Collaboration between Researchers at UC Berkeley, LBL, USC/ISI and Xerox PARC, 2011.
7. Yan Li, “Mobile Ad Hoc Network Simulation: Analysis and Enhancements”, PhD thesis, Heriot-Watt University, Edinburgh, UK, 2008.

Mammogram Classification using Gray-Level Co-occurrence Matrix for Diagnosis of Breast Cancer

Ranjit Biswas
Department of CSE
Assam University
Silchar, India
ranjit_tb@yahoo.co.in

Abhijit Nath
Department of CSE
Assam University
Silchar, India
abhijitnath2007@gmail.com

Sudipta Roy
Department of CSE
Assam University
Silchar, India
sudipta.it@gmail.com

***Abstract*— Breast cancer is one of the most common forms of cancer in women worldwide. Most cases of breast cancer can be prevented through screening programs aimed at detecting abnormal tissue. So, early detection and diagnosis is the best way to cure breast cancer to decrease the mortality rate. Computer Aided Diagnosis (CAD) system provides an alternative tool to the radiologist for the screening and diagnosis of breast cancer. In this paper, an automated CAD system is proposed to classify the breast tissues as normal or abnormal. Artifacts are removed using ROI extraction process and noise has been removed by the 2D median filter. Contrast-Limited Adaptive Histogram Equalization (CLAHE) algorithm is used to improve the appearance of the image. The texture features are extracted using Gray Level Co-occurrence Matrix (GLCM) of the region of interest (ROI) of a mammogram. The standard Mammographic Image Analysis Society (MIAS) database images are considered for the evaluation. K-Nearest Neighbor (KNN), Support Vector Machine (SVM) and Artificial Neural Network (ANN) are used as classifiers. For each classifier, the performance factor such as sensitivity, specificity and accuracy are computed. It is observed that the proposed scheme with 3NN classifier outperforms SVM and ANN by giving 95% accuracy, 100% sensitivity and 90% specificity to classify mammogram images as normal or abnormal.**

Keywords—Mammogram; ROI; GLCM; Confusion Matrix; 3NN classifier.

I. INTRODUCTION

Breast cancer grows in the breast cells usually in the lobules (glands which produce milk) and in the milk ducts (that carry milk to the nipple). In 2015, 40290 women death reported due to breast cancer [1]. The best way to identify the presence of breast cancer at an early stage is by interpreting mammogram images. Though mammography is an effective screening tool used by the radiologist for breast cancer detection at an early stage [2], however by visual interpretation it's very difficult for the radiologist to classify the affected tissue whether it is cancerous or not. Sometimes, the mammography test can give negative results in the presence of tumor by not detecting the exact ROI where tumor is present. In such cases, further tests are required which can be expensive and time-consuming. Also, abnormal tissue region may also be missed in visual (manual) interpretation of a mammogram image. In recent years Computer Aided Detection (CAD) system are being used to solve the problem of interpretation of the mammogram image. (The mass or calcifications in the breast tissue which may get unnoticed in visual interpretation by radiologists are easily and effectively being detected using CAD systems. The development and fine tuning of the CAD system has become more crucial for early and effective detection of abnormal tissues in the given digital mammogram image [3]. Thus, the main objective of CAD system is to increase diagnosis accuracy and enhancing the mammogram interpretation. Thus, CAD system can reduce the variability in judgments among radiologists by providing an accurate diagnosis of digital mammograms.

Rest of the paper is organized as follows: section 2 discusses about computer aided breast cancer detection systems; a new automated system is proposed and discussed in section 3; section 4 depicts the experimental results; conclusion and future work is discussed in section 5.

II. RELATED WORK

A CAD system was proposed in [4] for automatic detection and classification of breast cancer where noise and pectoral region removed from the breast using morphological operations and histogram based methods respectively. Using intuitionistic FCM based clustering, ROI is extracted and that ROI is transformed into four sub bands with the help of discrete wavelet transform (DWT). Wavelet energy features and 13 gray level co-occurrence features are computed form these sub bands. Then the self-adaptive resource allocation network (SRAN) classifier is used for classification. In 2013, tumor cut algorithm was proposed by Maanasa et al. for segmentation of mammogram image for detection of breast cancer [5]. Noise and artifact is removed using Gabor filter. Then from segmented image, geometrical and textural features are extracted. The optimal features are calculated using anova test calculator. With the help of optimal features, the mammogram image is classified into normal, benign and malignant using support vector machine (SVM) classifier.

S. Deepa et al. in [6] proposed a method for classification of mammogram image. According to abnormality given in the MIAS database, the ROI of size 256x256 is extracted. From the decomposed image, contourlet co-efficient is computed using contourlet transform and from that, co-efficient, co-occurrence matrix is generated. With the help of co-occurrence matrix, optimal features are selected using sequential floating forward selection (SFFS) algorithm. Probabilistic neural network is used for classification.

978-1-5090-3411-6/16 $31.00 © 2016 IEEE
DOI 10.1109/ICMETE.2016.85

In 2014, Puneeth et al. [7] proposed a method for classification of mammogram image based on textural features, which is calculated using gray level co-occurrence matrix. K-Nearest Neighbors (KNN) classifier is used for classification.

In 2015, K. Vaidehi et al. [8] developed an intelligent system for retrieval of content-based mammogram image. In their proposed method, the features are calculated from the ROI. Using support vector machine image is classified and top 10 image is retrieved using KNN algorithm.

In 2015, Subashini et al. [9] developed a method where ROI is extracted from each mammogram image and from the ROI textural features are calculated using gray level co-occurrence matrix. Hybrid genetic algorithm-particle swarm optimization is used to select best features from the set of extracted features. With the help of optimal features, the image is classified using KNN algorithm.

In 2016, F Shirazi et al. in [10], presented a breast cancer detection system by combining mixed gravitational search algorithm (MGSA) and support vector machine (SVM). The authors used MIAS database and the features are extracted using gray level co-occurrence matrix (GLCM). In the experimental setup, the authors have use 70% of the dataset (out of 100 ROIs) as training dataset which includes normal and abnormal tissues. The rest of the 30% of the dataset is used as test objects and the results are computed upon that. By using only SVM with 24 features the performance was reported to be 86% whereas by the combination of MGSA – SVM with 12 features the performance was reported to be 93.1%.

III. PROPOSED SYSTEM

In this section, mammogram image classification system is proposed. The proposed system for classification of mammogram images is built based on GLCM by applying different classifiers. The system is divided into five stages to classify mammogram images. First step is the data set collection, second is ROI extraction process, third is the pre-processing steps which is again divided into two steps filtering and enhancement, fourth is the feature extraction from GLCM and last stage is classification. The architecture of the proposed system is shown in Fig. 1.

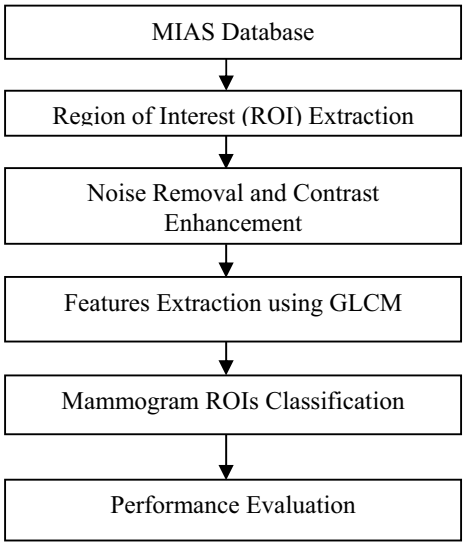

Fig. 1: Architecture of Proposed Method

A. Dataset collection

In this experiment, the mammogram images were obtained from the MIAS [11] data set. MIAS is an organization of UK research groups interested in the understanding of mammograms and has generated the digital mammograms dataset for their research. It consists of 322 images of left and right breast from 161 patients, which contains normal and abnormal images, and abnormal images are again classified into benign and malignant. The dataset provides the details, about the location and radius of the abnormalities marked by expert radiologists. In the MIAS dataset, the mammogram originally was of the size of 1024×1024 pixels.

B. Region of Interest (ROI) Extraction process

Original mammogram images have different types of noises, artifacts in their background, pectoral muscles etc which are unwanted for feature extraction and classification. Hence a cropping operation has been applied on mammogram image to extract the ROIs which contains the abnormalities, apart from the unwanted portions of the image. MIAS database gives all the details about each mammogram image, viz., size in pixels, character of background tissue, class of abnormality, *Xc* and *Yc* coordinate value of centre of abnormality, *'r'* radius of circle enclosing the abnormality by the radiologists. ROIs extraction performed by manual cropping operation considering the centre of the abnormal area as the centre of ROI and taking the approximate radius (in pixels) of a circle enclosing the abnormal area as shown in Fig. 2. For the extraction of normal ROI, the same cropping procedure has been performed on normal mammographic images with random selection of location. In this work, all the ROIs are resized in to 128 x 128 for uniformity. In this phase, the rectangular ROIs are extracted and the ROIs are free from the background information and artifacts, which is defined by equation (1) [12].

$$I_{ROI} = I[X_c - r, (1024 - Y_c) - r, 2r, 2r] \quad (1)$$

C. Pre-Processing

A mammogram is an X-ray image of the breast. It may contain noise and image quality may be poor. So preprocessing step is mostly needed to make the image suitable for classification. Thus, filtering technique is used to

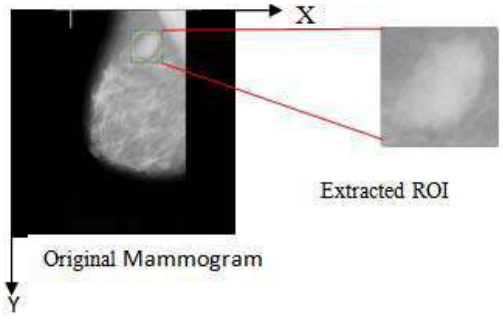

Fig. 2: Cropping of ROI

remove noise and the enhancement technique is used to improve the image quality [13].

In this work, median filter is used as it preserves the information while removing noise. PSNR and MSE [14] values of the median filter are calculated and compared with two other filter techniques. Median filter performs better by giving highest PSNR value and lowest MSE value shown in table 1. Contrast of each pixel relative to its local neighborhood is adaptively enhanced during this process which is known as Contrast Limited Adaptive Histogram Equalization and to improve the appearance of the image contrast-limited adaptive histogram equalization (CLAHE) [15] is used here. Fig. 3 shows the result of contrast enhancement process.

D. Feature Extraction

In image processing, processing of large data is time consuming and less efficient for classification. For reducing time, the input data is transformed into reduced set of feature vector. This transformation process is called feature extraction process. This feature vector contains relevant information and is used as input vector for classification.

Features can be classified based on color, texture and shape. In this work, we are mainly concerned about texture features and for extraction of features; Gray Level Co-occurrence Matrix (GLCM) is used since it has been proven as a powerful tool for feature extraction [16]-[17]. In this work four textural features namely contrast, correlation, Energy, homogeneity are extracted with $d = 1$ and $\theta = 0^0, 45^0, 95^0, 135^0$ and then take the average of these four direction.

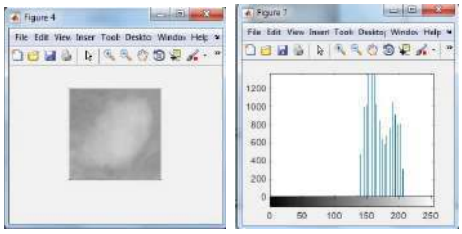

(a) (b)

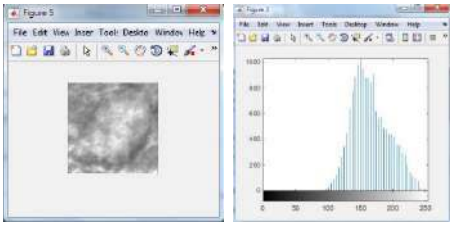

(c) (d)

Fig. 3: (a) De-noised image; (b) Histogram of (a); (c) Contrast enhanced image (d) Histogram of (c)

TABLE 1: PSNR AND MSE VALUE OF MAMMOGRAM SAMPLES

Image	*Averaging filter*		*Wiener filter*		*Median filter*	
	PSNR	***MSE***	***PSNR***	***MSE***	***PSNR***	***MSE***
Mdb015	3.52	28929.74	26.63	141.23	**37.28**	**12.17**
Mdb145	3.28	30543.91	26.64	140.84	**38.86**	**8.46**

E. Gray Level Co-occurrence Matrix (GLCM)

Grey level co-occurrence matrices (GLCM) are introduced in [18]-[19]. It explains the occurrence of certain grey levels in relation to other grey levels using statistical sampling. The process statement is reproduced as it is from [18]-[19] in the following paragraph.

Assume that an image to be analyzed is rectangular and has N_X rows and N_y columns. The gray level appearing at each pixel is quantized to N_g levels. Let, $L_x = \{1,2,....,N_x\}$ be the rows, $L_y=\{1,2,....,N_y\}$ be the columns and $G=\{0,1,2,....N_g\text{-}1\}$ is the total number of gray levels quantized up to N_g levels. The set L_xxL_y is the set of pixels of the image ordered by their row-column designations. Then, the image I can be represented as a function of co-occurrence matrix that assigns some gray level in L_xxL_y as I: L_xx$L_y \rightarrow G$.

The texture-context information is specified by the matrix of relative frequencies $p_{i,j}$ with two neighbouring pixels separated by distance$d$, one with gray level i and the other with gray level j. Such matrices of gray-level co-occurrence frequencies are a function of the angular relationship θ and distance d between the neighbouring pixels. By using a distance of one pixel and angles quantized to 45^0 intervals, four matrices of horizontal, first diagonal, vertical, and second diagonal (0, 45, 90 and 135 degrees) are used. Then, the un-normalized frequency in those four directions is defined by equation (2).

$$p(i,j,d,\theta) = \#\left\{\begin{array}{c}((k,l),(m,n)\epsilon\left|(L_x\,X\,L_y)\,X\,(L_xXL_y)\right| \\ (k-m=0,|l-n|=d)\;or\;(k-m=d,l-n=-d) \\ or\;(k-m=-d,l-n=d)\;or\;(|k-m|=d,l-n=0), \\ or\;(k-m=d,l-n=d)\;or\;(k-m=-d,l-n=-d), \\ I(k,l)=i,\quad I(m,n)=j\end{array}\right. \quad (2)$$

Where # is the number of elements in the set, *(k, l)* the coordinates with gray level *i, (m, n)* the coordinates with gray level *j*.

Consider $p(i,j)$ be the $(i,j)^{th}$ entry in a normalized GLCM. G is the number of gray levels range from 0 to N_g-1. μ is the mean value of *p*. $\mu_x, \mu_y, \sigma_x, \sigma_y$ are the means and standard deviations of p_x and p_y and presented in Equations (3), (4), (5) and (6) respectively.

$$\mu_x = \sum_{i=0}^{N_g-1}\sum_{j=0}^{N_g-1} i.p(i,j) \quad (3)$$

$$\mu_y = \sum_{i=0}^{N_g-1}\sum_{j=0}^{N_g-1} j.p(i,j) \quad (4)$$

$$\sigma_x = \sum_{i=0}^{N_g-1}\sum_{j=0}^{N_g-1}(i-\mu_x)^2.p(i,j) \quad (5)$$

$$\sigma_y = \sum_{i=0}^{N_g-1}\sum_{j=0}^{N_g-1}\left(j-\mu_y\right)^2.p(i,j) \quad (6)$$

In this paper, four textural features namely contrast, correlation, Energy, homogeneity are extracted from mammogram ROIs using GLCM as formulated in [18]-[19]

Contrast:

$$F1 = \sum_{n=0}^{N_g-1} n^2\{\sum_{i=1}^{N_g}\sum_{j=1}^{N_g} p(i,j)\}, |i-j| = n \quad (7)$$

Contrast is a relative measure of the intensity between a pixel and its neighbours over the whole image and is presented in equation (7). It is the quantity of local variation present in an image.

Correlation:

$$F2 = \sum_{i=0}^{N_g-1} \sum_{j=0}^{N_g-1} \frac{(ij)p(i,j)-\mu_x\mu_y}{\sigma_x\sigma_y} \quad (8)$$

How a pixel is correlated to its neighbor over the whole image is known as correlation and is presented in equation (8). Feature values range from -1 to 1, these extremes indicating perfect negative and positive correlation respectively.

Energy:

$$F3 = \sum_{i=0}^{N_g-1} \sum_{j=0}^{N_g-1} \{p(i,j)\}^2 \quad (9)$$

Energy also known as uniformity or angular second moment (ASM). Energy measure the sum of squared elements in the GLCM as presented in equation (9). Basically the property of energy is provide how uniform the texture image. The range of energy is [0 1], where Energy is 1 for a constant image.

Homogeneity:

$$F4 = \sum_{i=0}^{N_g-1} \sum_{j=0}^{N_g-1} \frac{p(i,j)}{1+(i-j)^2} \quad (10)$$

It measures the closeness of the distribution of the elements in the GLCM to the GLCM diagonal and is defined in equation (10). The range of homogeneity is [0 1], where homogeneity is 1 for a diagonal GLCM. It is high when local gray level is uniform and inverse GLCM is high.

F. Classification

Last step of the proposed method is the classification of the mammogram image into normal or abnormal. Here, the classification is done mainly with the help KNN algorithm and compared with SVM and ANN classifiers.

KNN is a supervised learning that has been used in many applications in the field of data mining and pattern recognition. This classifier computes the distance from the unlabeled data to every training data point and selects the best k-neighbor with the shortest distance. This classifier implementation is very simple since there is no need of explicit training step. The input to the classifier is the k-closest training samples and the output is the class name or a class membership. The output is decided by majority vote of its neighbours, where the input is being assigned to the class most frequent among its k-nearest neighbours. When k is considered as 1, then the input is just allocated to that class.

In this present study 1NN and 3NN are considered and Euclidean distance is used for calculating the distance between the new samples and training samples. Different k values give different results.

IV. EXPERIMENTAL RESULT AND DISCUSSION

To carry out the research, 208 mammogram images are considered out of which 188 images are used as a training set and 20 (10 normal and 10 abnormal) images are taken as testing set. From the de-noised and contrast enhanced ROI based mammogram images, the four texture features are calculated with the help of gray level co-occurrence matrix. These features are used as an input to the KNN classifier for training and testing.

TABLE 2: GLCM FEATURES VALUE FOR TEST DATASET

Image	***Contrast***	***Correlation***	***Energy***	***Homogeneity***
mdb190	0.1606	0.9073	0.2173	0.9225
mdb193	0.1313	0.8719	0.3492	0.9366
mdb199	0.1493	0.8560	0.2947	0.9282
mdb204	0.1768	0.9293	0.1929	0.9134
mdb208	0.1354	0.9616	0.2595	0.9347
mdb209	0.1510	0.9518	0.1814	0.9267
mdb212	0.1527	0.9180	0.2150	0.9255
mdb214	0.1868	0.9414	0.1504	0.9083
mdb219	0.1919	0.9470	0.1537	0.9060
mdb226	0.1868	0.9507	0.1382	0.9101
mdb234	0.2052	0.9331	0.1580	0.9000
mdb245	0.1767	0.8382	0.2810	0.9150
mdb246	0.0784	0.8818	0.5188	0.9639
mdb252	0.1616	0.9620	0.1402	0.9206
mdb257	0.1307	0.8268	0.3763	0.9362
mdb264	0.1496	0.9113	0.2591	0.9281
mdb272	0.1812	0.8195	0.2968	0.9122
mdb282	0.1501	0.7991	0.3470	0.9270
mdb302	0.1571	0.8367	0.3081	0.9236
mdb304	0.1476	0.9099	0.3128	0.9288

To evaluate the performance of the proposed system the following parameters are used which is defined by the equations (11),(12) and (13)[20].

$$\text{Accuracy} = \frac{TP+TN}{N} \times 100\% \quad (11)$$

$$\text{Specificity} = \frac{TN}{TN+FP} \times 100\% \quad (12)$$

$$\text{Sensitivity} = \frac{TP}{TP+FN} \times 100\% \quad (13)$$

Where, True positive (TP) = the mammogram image predicted with abnormal when actually the mammogram image is abnormal.

True negative (TN) = the mammogram image predicted with normal when the mammogram image actually normal.

False positive (FP) = the mammogram image predicted with abnormal when the mammogram image is normal.

False negative (FN) = the mammogram image predicted with normal when the mammogram image is abnormal.

Accuracy defines the overall correctness of the classifier, specificity defines true negative rate and sensitivity defines true positive rate. The higher values of both sensitivity and specificity show better performance of the system. Tables 3, 4, 5 and 6 show the classification result using 1NN, 3NN, SVM and ANN respectively with the help of confusion matrix. The overall performance of the proposed method is shown in table 7. The performance of the four classifiers are compared and represented graphically in fig. 4.

From the graphical representation of fig. 4, it is revealed that 3NN classifier outperforms other three in terms of accuracy and specificity whereas in terms of sensitivity 3NN outperforms SVM and ANN clearly and equals with 1NN. Thus, 3NN can be considered as a more efficient classifier for the classification of the mammogram ROIs images than 1NN, SVM and ANN.

TABLE 3: CONFUSION MATRIX FOR 1NN

Target class	**Predicted class**	
	Normal	***Abnormal***
Normal	7(TN)	3(FP)
Abnormal	0(FN)	10(TP)

TABLE 4: CONFUSION MATRIX FOR 3NN

Target class	**Predicted class**	
	Normal	***Abnormal***
Normal	10(TN)	0(FP)
Abnormal	1(FN)	9(TP)

TABLE 5: CONFUSION MATRIX FOR SVM

Target class	**Predicted class**	
	Normal	***Abnormal***
Normal	6(TN)	4(FP)
Abnormal	3(FN)	7(TP)

TABLE 6: CONFUSION MATRIX FOR ANN

Target class	**Predicted class**	
	Normal	***Abnormal***
Normal	7(TN)	3(FP)
Abnormal	2 (FN)	8(TP)

TABLE 7: CLASSIFICATION RESULS

Methods	**Accuracy %**	**Sensitivity %**	**Specificity %**
1NN	85	100	70
3NN	95	100	90
SVM	65	70	60
ANN	75	80	70

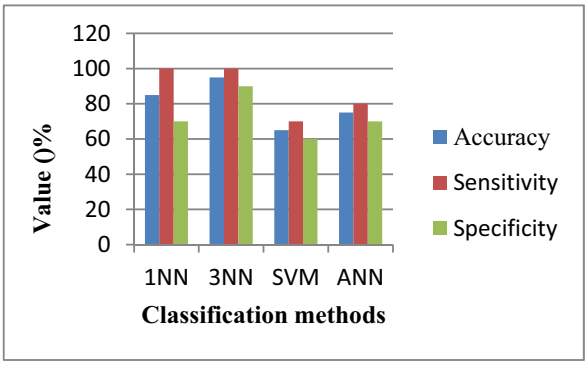

Fig. 4: Performance comparison of 1NN, 3NN, SVM, ANN classifiers

V. CONCLUSION AND FUTURE WORK

The CAD system is developed and presented here for the classification of mammogram into normal and abnormal breast tissues with the aim to support the radiologists in visual diagnosis. The experimental results show that 3NN gives the maximum accuracy rate for normal and abnormal classification (96%) compared to other classifiers.

The present work can be extended to the whole MIAS database with 322 mammogram images or other mammogram databases too. In future, more number of other statistical movement features may be considered with proper feature selection technique and accuracy may be improved further. A new mammogram database can be created by collecting mammogram images from different clinics and hospitals and this proposed method may be tested on that database.

REFERENCES

[1] American Cancer Society, "*Breast cancer facts & figures 2015-2016*," Atlanta, American Cancer Society, Inc. 2015.

[2] L. Tabar, P.Dean, *"Mammography and breast cancer: the new era,"* International Journal of Gynecology and Obstetrics, vol. 82, Issue 3, September 2003, pp. 319-326.

[3] H. Cheng, X. Shi, R. Min, L. Hu, X. Cai, H. Du, "*Approaches for automated detection and classification of masses in mammograms,"* Pattern recognition, vol. 39, 2006, pp. 646-668.

[4] S. Shanthi, and V. Murali Bhaskaran,"*Computer aided system for detection and classification of breast cancer,"* International Journal of Information Technology, Control and Automation,vol. 2, no. 4, October 2012, pp. 87-98.

[5] Maanasa N A S, V Gowri, "*Segmentation of mammogram using tumor-cut algorithm,*" International Journal of Engineering and Innovative Technology, vol. 2, Issue 10, April 2013, pp. 172-175.

[6] S. Deepa, V. Subbiah Bharathi, *"Textural feature extraction and classification of mammogram images using CCCM and PNN,"* IOSR Journal of Computer Engineering, vol. 10, Issue 6, 2013, pp. 07-13.

[7] Puneeth L., Krishna A.N. "*Classification of mammograms using texture features,*" International Journal of Innovative Research & Development, vol. 3, Issue 7, July 2014, pp. 373-377.

[8] K. Vaidehi, T. S. Subashini, *"An intelligent content based image retrieval system for mammogram image analysis,"* Journal of Engineering Science and Technology, vol. 10, 2015, pp.1453 – 1464.

[9] Subashini Sundaravinayagam, Bhavani Sankari. S, "*Detection and classification of masses in mammograms using a hybrid GA-PSO-KNN approach,*" International Journal of Advanced Research Trends in Engineering and Technology, vol. 2, May 2015.

[10] F. Shirazi, E. Rashedi, "*Detection of cancer tumors in mammography images using support vector machine and mixed gravitational search algorithm*," In proceedings of IEEE 1st Conference on Swarm

Intelligence and Evolutionary Computation, Bam, March 2016, pp. 98-101, doi:10.1109/CSIEC.2016.7482133.

[11] S. A. J Suckling, D Betal, N Cerneaz, D R Dance, S-L Kok, J Parker, I Ricketts, J Savage, E Stamatakis and P Taylor, "*The mammographic image analysis society digital mammogram databaseExerpta medica,*" International Congress Series 1069, 1994, pp. 375-378.

[12] R. N. Panda, M. A. Baig, B. K. Panigrahi, M. R. Patro "*Efficient CAD system based on GLCM & derived feature for diagnosing breast cancer*," International Journal of Computer Science and Information Technologies, vol. 6, 2015, pp. 3323-3327.

[13] Mister Khan, Sumit Kataria and Smriti, "*Mammography based breast cancer detection using different classifiers,*" National Conference on Emerging Trends in Electronics & Communication, vol. 1, No. 2, July 2015.

[14] K. Malathi, R. Nedunchelian, "*Comparision of various noises and filters for fundus Images using pre-processing techniques*," International Journal of Pharma and Bio Sciences, vol. 5, july 2014, pp. 499-508.

[15] K. Zuiderveld, "*Contrast Limited Adaptive Histogram Equalization*," Academic Press Inc, 1994.

[16] Pradeep N, Girish H, Karibasappa K, "*Segmentation and feature extraction of tumors from digital mammograms*," Computer Engineering and Intelligent Systems, vol 3, No.4, 2012.

[17] Biswajit Pathak, Debajyoti Barooah, "*Texture analysis based on the graylevel co-occurence matrix considering possible orientations,*" International Journal of Advanced Research in Electrical, Electronics and Instrumentation Engineering, Vol. 2, September 2013.

[18] Robert M. Haralick, K. Shanmugam, and ITS'HAK Dinstein, *"Textural features for image classification,"* IEEE Transaction on system, man and cybernetics, vol.SMC-3, No.6, November 1973, pp. 610-621.

[19] L.K. Soh, and C. Tsatsoulis, "*Texture analysis of sar sea ice imagery using grey level co-occurrence matrices,*" IEEE Transactions on Geoscience and Remote Sensing, vol.37, no. 2, March 1999, pp. 780-795.

[20] R. Nithya B. Santhi, "*Classification of normal and abnormal patterns in digital mammograms for diagnosis of breast cancer*," International Journal of Computer Applications, vol. 28, August 2011, pp. 21-25.

Web Service Discovery based on IR Models: A Review

Arnab Paul
Department of Comp. Sc. & Engg.
Assam University, Silchar
Assam, India
arnab.itaus@gmail.com

Sudipta Roy
Department of Comp. Sc. & Engg.
Assam University, Silchar
Assam, India
sudipta.it@gmail.com

Monowar Hussain
Department of Comp. Sc. & Engg.
Assam University, Silchar
Assam, India
hussainmonowar83@gmail.com

***Abstract*—Web service discovery is one of the major research thrust areas in the field of computing environment. From last decade, a good number of researchers are contributing their thoughts in finding the best available service from a pool of services that can satisfy the user's requirement. Different researchers have adopted different methodologies and ideas to visualize their noble thoughts in the field of web service discovery. Information retrieval methods are one of them. Utilization of IR methods in service discovery approaches makes the discovery process efficient. In this paper, we focus on those service discovery approaches which employ information retrieval methods for the purpose of automatic discovery. This paper provides a survey of how these approaches differ from each other while discovering a service.**

Keywords*: *Web Service Discovery; Information Retrieval etc.

I. INTRODUCTION

Web services are loosely coupled, distributed and independent application components that can be published, found and used on the web[1]. W3C defines web service as: "A Web service is a software system designed to support interoperable machine-to-machine interaction over a network. It has an interface described in a machine-processable format (specifically WSDL). Other systems interact with the Web service in a manner prescribed by its description using SOAP messages, typically conveyed using HTTP with an XML serialization in conjunction with other Web-related standards"[2].

Web services runs on the technologies called WSDL (Web Service Description Language), UDDI (Universal Description, Discovery and Integration) and SOAP (Simple Object Access Protocol). WSDL[3] describes services a set of network endpoints. WSDL document provides the functionalities of a service in XML format. UDDI[4] is the universally accepted XML based standard service repository in which the services in WSDL format can be published. Services in Service Oriented Architecture (SOA) can communicate with each other through SOAP[5]. SOAP is a lightweight XML based protocol for exchange of information in a decentralized, distributed environment.

Web service discovery is one of the most popular domains in SOA. The fundamental concept is that web service providers publish their services in the service repository and web service consumers use those services; web service discovery is the process of finding the most appropriate service from the repository that satisfies the consumers' need.

Automatic discovery of web services without human intervene is a popular research area for many researchers. Researchers have suggested many methods for the automatic discovery of web services. Our paper focuses on those discovery processes which utilize information retrieval methods for the purpose of automatic discovery. The paper is organized as follows: section II provides overview of web service discovery mechanism; section III discusses some of the information retrieval methods; section IV deals with various approaches taken by many authors for web service discovery; section V concludes the study.

II. WEB SERVICE DISCOVERY

If a web service consumer wishes to avail a service but is unaware of the providers of the service, then the consumer must initiate the 'discovery' process. Discovery is "the act of locating a machine-processable description of a Web service that may have been previously unknown and that meets certain functional criteria"[1].

The web service providers publish their web service descriptions along with the associated functional descriptions of the services in the form WSLD in the service repository. In order to use some services available in the service repository, the service consumers need to provide the service requirements based on the associated functional descriptions. Based on the consumer's service criteria, the discovery unit finds the appropriate service from the service repository that fulfills the specified criteria and returns the associated service

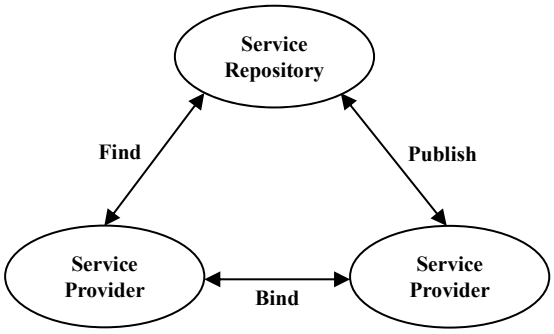

Figure 1.Web Service Discovery process

description to the consumer. If the discovery unit returns more than one services for single query, then the consumer has to select one of them based on some additional criteria. Both service provider and consumer must agree on the service description and the semantics of the interaction. And then, the provider and consumer communicates by exchanging the SOAP messages[1].

III. INFORMATION RETRIEVAL MODELS

Information retrieval is the study of finding unstructured documents from a large collection of documents with respect to a given query. IR can be broadly classified in two categories: semantic and statistical. Semantic technique extends retrieval capability by adding both syntactical and semantic analysis. Semantic analysis utilizes the contextual meaning of the user query to produce more relevant result. In statistical IR techniques, the documents which match the user query most closely are retrieved based on some statistical measures[6].

Boolean, vector space and probabilistic methods are the widely used statistical approaches in IR. The documents and the queries are often broken into words, generally referred to as terms. These terms need to undergo a number of preprocessing techniques before using them in any statistical measures [6].

Boolean IR is the oldest and simplest Information Retrieval model. In Boolean information retrieval system, any query can be expressed in terms of Boolean expression. The terms in the query are combined with the operators and, or, and not [7]. The result of a Boolean query is either true or false. A document is either relevant or irrelevant w.r.t. a query depending on whether the document satisfies the query or not[6]. For a query, this model retrieves that document for which it finds the exact match. Partial matches are not retrieved and also there is no ranking mechanism[10].

In Vector Space Model[8], each document is represented as vector of terms.

$$d_j = \{w_{1j}, w_{2j}, \ldots, w_{tj}\}$$

where, t represents the total number of terms in the document collection. If a term is present in the document, then the weight for the term in the document vector is non zero. The query is also represented as a vector of terms in Vector Space Model. There are two different techniques for computing the term weights of the terms present in the document vector and query vector: term-frequency (tf) and inverse document frequency (idf). The next step is to measure the similarity between the query vector and each of the document vectors. The similarity is generally measured using the cosine similarity[9]. The documents whose similarity values are greater than the threshold value are retrieved as a set of relevant documents. In vector Space Model, the term weights are not binary; partial matching and ranking of documents are possible. The order of appearance of the terms in the document does not coincide when represented as vector space which is one of the limitations of this model. Another limitation is that this model does not capture the semantics of the query and document[10].

Probabilistic IR model retrieves documents based on the probability of the document relevant to the query. The Probabilistic Ranking Principle[11] (PRP) is as follows:

"If a reference retrieval system's response to each request is a ranking of the documents in the collection in order of decreasing probability of relevance to the user who submitted the request, where the probabilities are estimated as accurately as possible on the basis of whatever data have been made available to the system for this purpose, the overall effectiveness of the system to its user will be the best that is obtainable on the basis of that data".

For a document vector d and query vector q, the documents are ranked according to their probability of relevance w.r.t. the query: $P(R = 1|d, q)$, where R is the indicator random variable which is either 1 or 0 based on whether d is relevant or nor relevant with respect to the query respectively.

The Binary Independence Model[7] is a probabilistic IR model which employs some basic assumptions to make feasible estimate of the probability similarity between the document and the query. One assumption is that both documents and query are represented as binary term incidence vectors. Another assumption 'independence' means that the terms in documents are independent of each other having no association between them. The probability $P(R|d, q)$ that a document is relevant is modeled based on the probability of

relevance of the term incidence vectors $P(R|\vec{x}, \vec{q})$. Then, using Bayes rule, we get

$$P(R = 1|\vec{x}, \vec{q}) = \frac{P(\vec{x}|R = 1,\vec{q})P(R = 1|\vec{q})}{P(\vec{x},\vec{q})}$$
$$P(R = 0|\vec{x}, \vec{q}) = \frac{P(\vec{x}|R = 0,\vec{q})P(R = 0|\vec{q})}{P(\vec{x},\vec{q})}$$

where $P(\vec{x}|R = 1, \vec{q})$ and $P(\vec{x}|R = 0, \vec{q})$ represent the probability of retrieving relevant or irrelevant documents respectively with document representation as $\vec{x}$. For a particular query, a document will be either relevant or irrelevant, which implies:

$$P(R = 1|\vec{x}, \vec{q}) + P(R = 0|\vec{x}, \vec{q}) = 1$$

IV. LITERATURE SURVEY

In this paper[12], they propose an algorithm based on the concept of singular value decomposition (SVD) of linear algebra to locate the similar services for a service request. For the purpose of retrieving similar services, they first collect keywords from the service descriptions of web services available in UDDI registry. These words are passed through a preprocessing stage which involves the elimination of stop words and then obtaining stemmed words. In this way, they build a collection of unique words for all the services present in the UDDI. All the words in the collection are assigned weight which is the value of inverse document frequency of the corresponding word. In the next step, vectors for all services are created where the value of each vector element for a particular service is calculated based on the weight of each word multiplied by its binary occurrence in that service. A service matrix is constructed considering all these vectors and then the singular value decomposition method of linear algebra is applied on this service matrix to find the relationship between services, define threshold for retrieving similar services and filter out the irrelevant services. To find similar services for a given service, they apply the concept of cosine similarity measurement. They present a comparison table between keyword matching technique and their SVD based proposed model which shows better result for their model.

In this paper[13], they propose a method for the analysis and discovery of Web services. They combine one of the information retrieval methods and the existing standards that describe the web services for the purpose of web service discovery. For a service request, their search engine finds the similar service/s from a collection of web services based on the information like functionalities, descriptions etc. of the services. The distributed search engine employs the concept of vector space model of information retrieval system to discover the analogous service for a specific service request. The first step in their model deals with the extraction of keywords like endpoint URLs, types and their attribute names, message names, service names and XML comments from web services that are available in the WSDL file repository. Using these extracted keywords, a vector space is created where each dimension is represented by a term. Each document (WSDL file) is represented by a vector within this vector space. Vector elements of each vector are assigned normalized term weights calculated based on the term frequency and inverse document frequency of the term. They also extend their model to work with distributed vector space. The query processor extracts keywords from the given query string and also creates the query vector. The cosine similarity value is calculated between the query vector and each document vector present in the term space. Documents are then sorted based on their similarity rating. Their model works fine in distributed environment.

In this paper[14], they propose a flexible service discovery method to discover useful services. Textual elements of the service request are compared against textual elements of all available services in the repository to discover similar services and to rank them according to their similarity. To carry out this task, they use vector space model of information retrieval system. Next, a structure matching algorithm is projected on this ranked list of services to refine and evaluate the quality of the service set. For this purpose, they develop a heuristic, domain-specific tree-edit distance algorithm. WSDL specifications describing the web services based on XML syntax are hierarchical in nature. Therefore, the tree-edit distance algorithm can calculate the similarity between two tree structures as because minimum node modifications required to match them. Comparing two web services is based on comparison of service operations which, in turn, is based on comparison of service messages which again is based on comparing the data-types of the WSDL specifications. The algorithm matches the data-types, messages and operations of the WSDL specifications respectively. Each of these three steps results in individual matrix that evaluates the similarity score of all pair-wise combinations of source and target data-types/ messages/ operations. The final similarity score is the maximum score calculated as the sum of matching scores of all individual operation pairs. Their report includes experiments on service discovery with IR methods only, with structure matching only and with IR and structure matching combined. For service discovery with IR methods only, they report a precision of 51% at 95% recall on average; with

structure matching only, they report a precision of 20% at 72% recall on average. The retrieval system with IR and structure matching combined achieves a precision of 61.5% at 90% recall with an increase in precision by 10.5% and drop in recall by 5% as compared to retrieval technique with IR method only.

In this paper[15], they propose a web-service search method to discover similar service operations given a natural language description of the desired service. Their work is almost similar to that of Wang & Stroulia[14], but they focus on semantic similarity rather than structural similarity. For a given service description, they first obtain a candidate set of service operations by using TF and IDF techniques of Information retrieval System. Web service data-types can be primitive or complex. Primitive data-types do not contain semantic information. Primitive data-types are converted to complex data-types by replacing them with their corresponding parameters to contain semantic meaning. XML schema is modeled as a tree of labeled nodes. The labeling is done as tag node and constraint node. Constraint node is further subdivided as sequence node, union node and multiplicity node. They apply bottom-up-transformation algorithm of time complexity O(n) in which they propose three transformation rules to transform all three constraint nodes to tag nodes. The service operation matching is done with the help of schema tree matching. On the candidate operations set, they use tree edit distance approach of schema matching algorithm to calculate the similarity among the operations. To measure tree edit distance between two schema trees, they introduce a new cost model to compute the cost of each edit operation which is based on weights and semantic connection of nodes. After identifying similarity of web service operations, the candidate set of service operations is clustered using agglomeration algorithm. For each cluster, operation with minimum cost will be output as search result. Since operations are associated with scores, they rank the search result based on scores of operations.

Aabhas V. Paliwal et al.[16] present an approach for web service discovery combining the concepts of ontology linking and Latent Semantic Indexing (LSI) in combination. Ontology linking is achieved by mapping domain ontology against upper merged and mid-level ontologies. LSI determines the relationship between query terms and the available documents to capture the domain semantics. After preparing the service request vector using domain ontology linking concept and service description vector from the selected WSDL documents using the LSI classifier, both the vectors are put together utilizing the cosine similarity technique to determine the similarity and to discover the relevant web services. After preprocessing of the service request, it is enhanced by associating the related upper concepts utilizing the upper ontology which helps in web service categorization. From these categorized service collections, the service descriptions are extracted and parsed to form the term-document matrix. The SVD transformation applied on term-document matrix produces reduced dimension vector for each term and each document which helps to determine the appropriate web service. Because of the categorization of services, their experimental results produce a better result.

To avoid huge number of retrieved services w.r.t. a keyword and the inability of the keywords to express semantic concepts, Jiangang Ma et al[17] propose a clustering semantic algorithm to semantically discover the web services. First they prepare a working dataset by using a clustering semantic algorithm. For a particular query, the dataset is prepared based on the relevant web services whose contents are compatible with the query. They employ K-means clustering algorithm to eliminate the irrelevant services w.r.t. a query. They use the Vector Space Model to prepare the service transaction matrix for the services in the working dataset. The working dataset is then grouped into a number of semantically related clusters by employing the concept of Probabilistic Latent Semantic Analysis approach (PLSA). This PLSA technique is used to capture the semantic concepts of the terms of the query and also the descriptions of the services which helps to determine the semantic similarity between the service and the query within the related cluster. The PLSA utilizes the Bayesian network model and an intermediate layer called hidden factor variable to associate the keywords to its corresponding documents. For each and every service of the service dataset, the PLSA computes the probability w.r.t. each latent hidden variable. Then it determines the maximum probability for each service and puts the service in the semantically related cluster. By comparing the similarity between the query and related clusters, a set of relevant services are retrieved for the query.

Ricardo Sotolongo et al.[18] propose an approach that employs the Vector Space Model of IR in combination with Vector Space Model enhanced with lexical database WordNet to efficiently discover the web services. WordNet is utilized to capture the semantics of the WSDL elements that assist in deriving the accurate similarity. They also use Linear Discriminant Function of pattern classification technique to devise the relative similarity between the term and term's synonyms and calculate the optimized weights of the terms

TABLE I. COMPARISON TABLE

Authors	Method(s) Used	Similarity Measur-ement	Advantage	Disadvantage	Distributed or Centralized	Semantic Capability
Atul Sajjanhar, Jingyu Hou, and Yanchun Zhang[12]	Singular Value Decomposition	Cosine value	Is not restricted by the tModel used by a web service during publishing	1. Poor term weighting scheme 2. No semantic issue	Centralized	No
Christian Platzer and Schahram Dustdar[13]	Vector Space Model	Cosine similarity value	Works fine in distributed environment	Does not deal with semantic search	Both	No
Yiqiao Wang and Eleni Stroulia[14]	Vector Space Model and Structure Matching Algorithm (Tree-Edit Distance Algorithm)		Inspired by signature-matching methods for component retrieval	Structural matching may be invalid when two web-service operations have many similar substructures on data types	Centralized	No
Yanan Hao and Yanchun Zhang[15]	Tree-Edit Distance Algorithm, Bottom-up-transformation algorithm		Results in better precision and recall value than keyword searching method, structure matching method and Woogle	Deals in very less semantic information	Centralized	Partial
Aabhas V. Paliwal, Nabil R. Adam and Christof Bornhövd[16]	Ontology Linking and Latent Semantic Indexing	Cosine similarity	Better result because of categorization of services	Cost of computing LSI in SVD transformation is high	Centralized	Yes
Jiangang Ma, Yanchun Zhang and Jing He[17]	Clustering Probabilistic Semantic Approach (CPLSA)	Cosine similarity and PLSA	Produces good result for using cluster based probabilistic approach over traditional keyword based search	Will function poorly for high dimensional data	Centralized	Yes
Ricardo Sotolongo, Carlos Kobashikawa, Fangyan Dong, and Kaoru Hirota[18]	Vector Space Model enhanced with WordNet	Inner product between weights of terms of WSDL and query vectors	Calculation of an optimal weight using batch perceptron algorithm of linear discriminant functions	Cost of computation is high because of calculation of relative frequency, global and relative importance, local and global similarity for both original and enhanced vectors	Decentraliz-ed	Yes

using batch perceptron algorithm. For both original vector and vector enhanced with WordNet, they calculated (i) the relative frequency of each word in each WSDL document, (ii) global importance of each word in all WSDL collection, (iii) relative importance of each word in each WSDL document. The same procedures are used for the query vector also. The local similarities between the WSDL and the query for both original and the enhanced vectors are calculated as the inner product of the relative importance of words in WSDL and relative importance of words in query. Finally, the global similarly between the WSDL and the query is calculated based on the local similarities in case of both original and enhanced vectors. They compared their algorithm with four other IR based WS discover algorithms and found that their algorithm is showing an improvement of 0.6% to 1.9% in precision and 0.7% to 3.1% in recall for the top 15 web services.

V. CONCLUSION

Finding the efficient service that satisfies the user's need is a most challenging task in the field of web service discovery mechanisms under SOA. Various techniques have been developed to answer this issue. We concentrated on the information retrieval techniques related service discovery approaches in this paper. We discussed some of the basic information retrieval methods in this paper. We also discussed the advantages and disadvantages of the approaches used for service discovery. Most of the authors have used cosine similarity to address the issue of similarity measurement. Some approaches are centralized in their nature while some others are distributed. Also some approaches focus on semantic capability to make the discovery process an efficient one. We also agree that discovery units should address the semantic capability precisely in order to find the most appropriate service.

REFERENCES

[1] Papazoglou, M. P., Georgakopoulos, D., "Service-oriented computing", Communications of the ACM, Vol. 46, No. 10, 2003, pp. 25–28.

[2] (2004, February) Web Services Architecture [Online]. https://www.w3.org/TR/2004/NOTE-ws-arch-20040211/

[3] (2001, March) Web Services Description Language (WSDL) 1.1 [Online]. https://www.w3.org/TR/wsdl

[4] (2004, October) UDDI Spec Technical Committee Draft [Online]. http://www.uddi.org/pubs/uddi_v3.htm

[5] (2000, May) Simple Object Access Protocol (SOAP) 1.1 [Online]. https://www.w3.org/TR/soap/

[6] Ed Greengrass, "Information Retrieval: A Survey", Available online at: www.csee.umbc.edu/csee/research/cadip/.../IR.report.120600.book.pdf

[7] Christopher D. Manning, Hinrich Schütze, and Prabhakar Raghavan, "Introduction to Information Retrieval", © Cambridge University Press 2008, ISBN-13 978-0-511-41405-3

[8] G. Salton, A. Wong and C. S. Yang, "A vector space model for automatic indexing", Communications of the ACM, v.18 n.11, p.613-620, Nov. 1975

[9] Sidorov, Grigori; Gelbukh, Alexander; Gómez-Adorno, Helena; Pinto, David. "Soft Similarity and Soft Cosine Measure: Similarity of Features in Vector Space Model". *Computación y Sistemas* **18** (3): 491–504. doi:10.13053/CyS-18-3-2043

[10] Joydip Datta, "Ranking in Information Retrieval", M. Tech Dissertation, Dept. of CSE, IITB, India, 2010.

[11] S.E. Robertson. The Probability Ranking Principle in IR. Journal of Documentation, 33(4):294-304, 1977. doi: 10.1108/eb026647. http://www.emeraldinsight.com/10.1108/eb026647.

[12] Atul Sajjanhar, Jingyu Hou, and Yanchun Zhang, "Algorithm for Web Services Matching", *Lecture Notes in Computer Science*, vol. 3007, pp. 665-670, © 2004, Springer-Verlag.

[13] Christian Platzer and Schahram Dustdar, "A Vector Space Search Engine for Web Services", in *Proceedings of the Third European Conference on Web Services (ECOWS'05)*, Washington, DC, USA, 2005, pp. 62 – 70, © IEEE Computer Society, doi: 10.1109/ECOWS.2005.5

[14] Yiqiao Wang and Eleni Stroulia, "Flexible Interface Matching for Web-Service Discovery", In *Proceedings of the Fourth International Conference on Web Information Systems Engineering (WISE'03)*, 2003 © IEEE Computer Society, pp. 147 – 156, doi: 10.1109/WISE.2003.1254478

[15] Yanan Hao and Yanchun Zhang, "Web Services Discovery Based on Schema Matching", In *Proceedings Thirtieth Australasian Computer Science Conference (ACSC2007)*, Ballarat, Australia, Conferences in Research and Practice in Information Technology (CRPIT), Vol. 62. Gillian Dobbie, Ed., pp. 107 – 113, ©2007, Australian Computer Society, Inc.

[16] Aabhas V. Paliwal, Nabil R. Adam, Christof Bornhovd, "Web Service Discovery: Adding Semantics through Service Request Expansion and Latent Semantic Indexing", In International Conference on Services Computing (SCC 2007), IEEEXplore, 2007.

[17] Jiangang Ma , Yanchun Zhang and Jing He, "Efficiently finding web services using a clustering semantic approach", In *Proceedings of the 2008 International Workshop on Context Enabled Source and Service Selection, Integration and Adaptation*: organized with the 17th International World Wide Web Conference (WWW 2008), p.1-8, April 22-22, 2008, Beijing, China, doi:10.1145/1361482.1361487

[18] Ricardo Sotolongo, Carlos Kobashikawa, Fangyan Dong, and Kaoru Hirota, "Algorithm forWeb Service Discovery Based on Information Retrieval UsingWordNet and Linear Discriminant Functions", *Journal of Advanced Computational Intelligence and Intelligent Informatics,* Vol.12 No.2, pp: 182-189, 2008.

Image Segmentation Using Spatial Fuzzy C Means Clustering and Grey Wolf Optimizer

[1]Th. Ibungomacha Singh, [2]Romesh Laishram
Manipur Institute of Technology
Takyelpat, Manipur, India
[1]ibomcha.2007@rediffmail.com,
[2]romeshlaishram@gmail.com

Sudipta Roy
Assam University
Silchar, Assam, India
sudipta.it@gmail.com

Abstract— **Image segmentation is one research area of image processing which has many applications in practice. In this paper we have undertaken image segmentation problem using spatial fuzzy c means (SFCM) clustering which is an unsupervised classification scheme. A good segmentation result is desirable for classification problem especially in medical image classification. Therefore SFCM clustering result is further optimized using a new colony based optimization algorithm called the grey wolf optimizer (GWO). Experiments were conducted for segmentation of magnetic resonance imaging (MRI) images. Comparative results are presented to show the effectiveness of incorporating GWO in to SFCM for image segmentation problem. Performance parameters are given in terms of clustering validity functions.**

Keywords—image segmentation; SFCM; GWO; MRI

I. INTRODUCTION

Image segmentation has been one of the thrust areas in the field of digital image processing for many years. Image segmentation [1] can be defined as the grouping of pixels into regions satisfying some criteria such that the region of interest (ROI) is well separated for detail analysis. Research in this area has revisited again particularly in medical image segmentation problem. Recently Computer aided diagnosis (CAD) is one of the main focus area of medical image processing.

Image segmentation problem can be thought of as a classification problem thereby making it suitable for the use of many machine learning based classification algorithms. Any classification algorithm can be broadly categorized into two types viz. supervised learning and unsupervised learning. One important algorithm in unsupervised learning is the fuzzy c-means (FCM) [2] clustering algorithm. In this paper we have considered the segmentation problem as a clustering in which different regions in the image are taken as clusters. The classical FCM algorithm has been used in image segmentation problem for many years and many versions of FCM were proposed and studied. In this work we have used one such variants of FCM which is called spatial-FCM (SFCM) proposed in [3]. It has proved to perform better than FCM by considering the spatial constraints in the design of FCM.

The clustering algorithm is further optimized by incorporating swarm based optimization algorithm. A swarm algorithm works on the principle of cooperation in solving a problem. There are numerous swarm algorithm which were mostly natured inspired. We have consider one recently proposed swarm algorithm called grey wolf optimizer (GWO) [4] which is a model of the hunting mechanism of grey wolves.

By combing SFCM and GWO we proposed a new image segmentation method which we called SFCMGWO. The purpose of the optimization algorithm is to further optimize the cluster centers obtained from SFCM. In medical image segmentation problem accuracy is the main criteria determining the usefulness of the algorithm rather the complexity of the algorithm. The proposed combined algorithm is tested in MRI medical image segmentation problem.

The remainder of the paper is organized as follows. Section II highlights the related works done earlier in the field of MRI image segmentation. In Section III, a brief analysis of GWO and the algorithm is presented. SFCM and SFCMGWO are explained in Section IV. Experimental analysis of the proposed algorithm on MRI image segmentation is detailed in section V and finally conclusion is drawn in Section VI.

II. RELATED WORKS

In this section some of the recent works in the field of MRI image segmentation are highlighted. A comprehensive review of the human brain MRI segmentation is given in the article [5]. MRI segmentation based on pattern recognition algorithms are presented by the authors in [6] and FCM for brain MRI segmentation is studied in [7]. A new variant of FCM i.e. SFCM is introduced by Keh-Shih Chaung et el. [3]. The spatial information is incorporated in SFCM has shown certain advantages over FCM in obtaining more homogenous regions in the segmented image. The algorithm is also less sensitive to noise. SFCM is further integrated with level set methods for automated medical segmentation as proposed in the research work [8]. A hybrid of different variants of FCM is proposed in [9], where the combination of different FCM variants is studied for brain tumor segmentation. The scheme obtained improvements by achieving computationally fast and good accuracy in segmentation results.

The optimization of FCM by incorporating nature inspired optimization algorithm is proposed [10] by using the popular genetic algorithm (GA). Since then this fusion algorithm is quite popular and extensively studied for segmentation

978-1-5090-0612-0/16/$31.00 ©2016 IEEE

problems in the works carried out by the authors in [11]-[13].The combination of other swam intelligence like particle swarm optimization (PSO) and artificial bee colony (ABC) with FCM for medical image segmentation can be found in the literatures [14-16].

In this paper a combination of SFCM and GWO i.e. (SFCMGWO) is proposed for undertaking the problem of image segmentation in medical images and especially MRI images.

III. SPATIAL FCM (SFCM)

A brief description of clustering based on the most popular FCM algorithm and its variant SFCM are presented.

The FCM algorithm assigns pixels to different cluster based on the fuzzy membership function of the pixels to belong in a particular cluster. It is an optimization algorithm that minimizes an objective function iteratively.

Let us consider an image arranged in a one dimensional matrix as $X=[x_1,x_2,.....x_N]$, where x_i represents pixel intensity value or feature value and N is the total pixels in the image. The aim of FCM is to partition the pixels in to c clusters. In the standard FCM the cost function is defined in (1).

$$J = \sum_{j=1}^{N}\sum_{i=1}^{c} u_{ij}^{m} \cdot \left\| x_j - v_i \right\|^2 \tag{1}$$

The membership value of pixel x_j to belong in i^{th} cluster is denoted as u_{ij}, v_i is the cluster center and m is a parameter that controls the partition result. The membership values and the updation of cluster centers are done according to equation (2) and (3) respectively.

$$u_{ij} = \frac{1}{\sum_{k=1}^{c}\left(\frac{\left\| x_j - v_i \right\|}{x_j - v_k}\right)^{\frac{2}{(m-1)}}} \tag{2}$$

$$v_i = \frac{\sum_{j=1}^{N} u_{ij}^{m} x_j}{\sum_{j=1}^{N} u_{ij}^{m}} \tag{3}$$

The information of neighborhood pixels is exploited in SFCM. It is highly possible that the neighborhood pixels possesses same feature value and belong to the same cluster. This concept is not considered in the standard FCM. The spatial information is exploited in SFCM by defining a spatial function [3] as in (4).

$$h_{ij} = \sum_{k \varepsilon NB(x_j)} u_{ik} \tag{4}$$

Where $NB(x_j)$ is a window define on the image centered on the pixel x_j. The size of the window can 3x3 or 5x5 but in this we have considered only 5x5 window. The spatial h_{ij} is defined as the probability that a pixel x_j belongs to the i^{th} cluster. A higher value indicates that the most of the neighborhood pixels of a center pixel under consideration belongs to that cluster. The standard FCM is modified by incorporating the spatial function in the membership function. The modified membership function is defined in (5) which is reproduced from [3].

$$u_{ij} = \frac{u_{ij}^{p} h_{ij}^{q}}{\sum_{k=1}^{c} u_{kj}^{p} h_{kj}^{q}} \tag{5}$$

where p and q are parameters that decides the impact of the original membership function and the spatial function respectively in the calculation of new membership functions. The notation used for spatial FCM with parameters p and q is $SFCM_{p,q}$. When p=1 and q=0 SFCM degenerates to conventional FCM.

The spatial FCM operates in two phase iteration. In the first phase the membership values are determined using the conventional FCM. This membership values are utilized in the calculation of the spatial function. In the second phase new membership function is calculated using (2). After the condition for convergence is achieved the iteration is over. The threshold for the convergence can be set when there is no change between two cluster centers in last two successive iterations. After the iteration is completed defuzzification process is initiated in which a pixel whose membership function is maximal is assigned to that cluster.

IV. GREY WOLF OPTIMIZER (GWO)

The Meta-heuristic based optimization algorithm has been successfully applied in many engineering and other related problems. Over the last many years research effort in this direction saw developing many popular algorithms like Genetic algorithm (GA), particle swarm optimization (PSO), artificial bee colony (ABC) etc. In this paper we focus on a newly proposed meta-heuristic algorithm called Grey Wolf Optimizer (GWO) proposed in [4]. It is inspired by the behaviour of grey wolves (Canis lupus) which maintains a hierarchy among them and follows unique steps in hunting. To mathematically model the hierarchical structure, four types of grey wolves are defined such as alpha (α), beta (β), delta (δ) and omega (ω). The leader is the alpha and most of the decisions are taken by alpha.The alpha is also called dominant wolf. Beta grey wolves are the second group in the hierarchy.They support alpha in decision making and act as subordinates of alpha. The lowest in the hierarchy is the omega. They always have to submit to all other dominant woves. If a wolf is not alpha, beta and omega they are called

delta. Deltas have to report to either alpha or beta but they are above omega. The hunting mechanism progresses in three steps: searching for prey, encircling prey and attacking prey. It is shown that GWO based model provides very competitive results comparison with other popular algorithms. The details of mathematical model of GWO can be found in [4] however we reproduce here the basic equations of GWO.

A. Mathematical model of GWO

The mathematical model of hunting mechanism and the hierarchical structure of grey wolves are presented here. The hunting in GWO algorithm is guided by alpha, beta and delta.

The following notations are used for the mathematical model of GWO.
α: Best solution
β: Second best solution
δ: Third best solution
ω: remaining solutions

The encircling behaviors of the grey wolves are modeled by (7) – (8).

$$\vec{D} = \left|\vec{C}.\vec{X}_p(i) - \vec{X}(i)\right| \tag{7}$$

$$\vec{X}_p(i+1) = \vec{X}_p(i) - \vec{A}.\vec{D} \tag{8}$$

Where $\vec{A}$ and $\vec{C}$ are coefficient vectors, $\vec{X}_p(i)$ is a vector representing the position (solution) of the prey at the i[th] iteration and $\vec{X}$ indicates the position vector (solution) of a grey wolf. The vectors $\vec{A}$ and $\vec{C}$ are calculated using (9) and (10).

$$\vec{A} = 2\vec{a}.\vec{r}_1 - \vec{a} \tag{9}$$

$$\vec{C} = 2.\vec{r}_2 \tag{10}$$

The elements of $\vec{a}$ are decreased from linearly during the iterations $\vec{r}_1$ and $\vec{r}_2$ are random vectors in the interval $[0-1]$.

During hunting process the position vectors of the search party are updated following the information gathered from alpha, beta and delta. The updating of next positions is done using (11) to (13).

$$\vec{D}_\alpha = \left|\vec{C}_1.\vec{X}_\alpha - \vec{X}\right|, \vec{D}_\beta = \left|\vec{C}_2.\vec{X}_\beta - \vec{X}\right|, \vec{D}_\delta = \left|\vec{C}_3.\vec{X}_\delta - \vec{X}\right| \tag{11}$$

$$\vec{X}_1 = \vec{X}_\alpha - \vec{A}_1.\vec{D}_\alpha, \vec{X}_2 = \vec{X}_\beta - \vec{A}_2.\vec{D}_\beta, \vec{X}_3 = \vec{X}_\delta - \vec{A}_3.\vec{D}_\delta \tag{12}$$

$$\vec{X}(i+1) = \frac{\vec{X}_1 + \vec{X}_2 + \vec{X}_3}{3} \tag{13}$$

From (9) and (10) we can see that as the vector $\vec{a}$ decreases the vector $\vec{A}$ will also decreases and the grey wolves approaches the prey. When $\left|\vec{A}\right| < 1$ the wolves attack the prey (the solution is reached).

The basic algorithm of GWO is summarized in Fig. 1.

Initialization phase ()
{
Initialize the solution as grey wolf population [X]
Initialize the vectors a, A and C
Calculate the fitness of each solution or grey wolf
Store X_α *= the best solution so far*
X_β *= the second best solution*
X_δ *= the third best solution*
}

Hunting phase ()

While *(i < no. of iterations)*
{
for *(each grey wolf)*
update the position vector of each wolf
end
update the fitness function
update X_α, X_β *and* X_δ
i=i+1
}
end
return X_α

Fig. 1. GWO algorithm.

V. EXPERIMENTAL ANALYSIS

The algorithm is evaluated on two brain MRI images used in the earlier works [3], [16]. For comparative analysis the segmentation is performed using the standard SFCM and the improved algorithm incorporating genetic algorithm (GA) and grey wolf optimizer (GWO) which are called GASFCM and GWOSFCM. The image is partition into 4 different regions i.e. the number of clusters is four. The performance of the algorithms are validated by three most commonly used validity functions: the fuzzy partition coefficient V_{pc}[17], the fuzzy partition entropy V_{pe} [18] and validity function V_{xb} [19] which are defined in (8) to (10).

$$V_{pc} = \frac{\sum_{j}^{N}\sum_{i}^{c} u_{ij}^2}{N} \tag{8}$$

$$V_{pe} = \frac{-\sum_{j}^{N}\sum_{i}^{c}\left(u_{ij}.\log u_{ij}\right)}{N} \tag{9}$$

$$V_{xb} = \frac{-\sum_{j}^{N}\sum_{i}^{c} u_{ij}\left\|x_j - v_i\right\|^2}{N.(\min_{i\neq k}\{\left\|v_k - v_i\right\|^2\})} \quad (10)$$

The fuzzy partition validity functions V_{pc} and V_{pe} indicate the level of fuzziness for better performance. The clustering result is good when V_{pc} is maximal or V_{pe} is minimal. The validity function V_{xb} gives the connection between fuzzy partition and feature property of the image. The inclusion feature makes V_{xb} more important than V_{pc} and V_{pe}. The clustering result achieved is best when V_{xb} is minimum.

The segmentation results are shown in Fig.2 and Fig.3 for two different sample images respectively. The result showed that the performance of GWO based SFCM is better than the standard SFCM and GASFCM. The results are further validated the validity functions as given tin table 1. GWOSFCM has the least value of V_{xb} and this value has more significance than the other two validity functions. GWOSFCM has also less utilization compared to GASFCM. This indicates that the GWO based algorithms are computationally fast yet very effective. The convergence of the fitness function of GASFCM and GWOSFCM are shown in Fig 4. The GWO has faster convergence than GA has attains minimum value of the cost function.

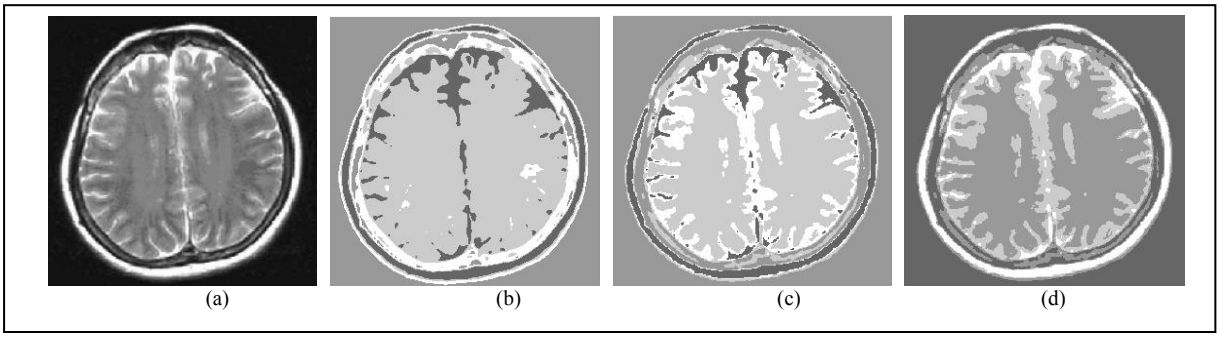

(a) (b) (c) (d)

Fig. 2. (a) Original MRI image 1(b) SFCM segmentted image (c) GASFCM segmented image (d) GWOSFCM segmented image.

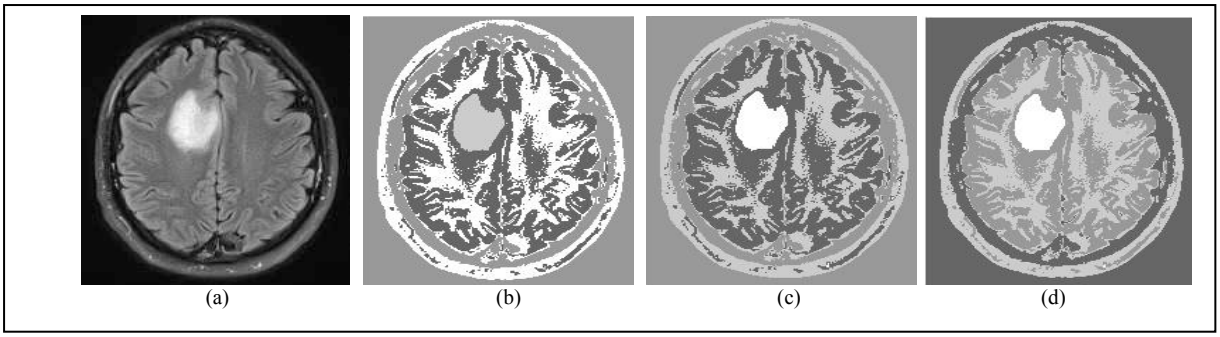

(a) (b) (c) (d)

Fig. 3. (a) Original MRI image 1(b) SFCM segmentted image (c) GASFCM segmented image (d) GWOSFCM segmented image.

TABLE I. CLUSTER VALIDITY FUNCTIONS AND TIME COST FOR DEIFFRENT ALGORITHMS

Test images	**Algorithm**	**Validity functions**			**CPU Time (sec)**
		V_{pc}	V_{pe}	V_{xb} ($x10^{-3}$)	
Image1	SFCM	**0.90**	0.074	1.3	**4**
	GASFCM	0.82	0.057	0.97	31
	GWOSFCM	0.88	**0.046**	**0.72**	29
Image 2	SFCM	**0.92**	0.063	1.7	**5**
	GASFCM	0.85	0.044	1.2	54
	GWOSFCM	0.85	**0.042**	**0.91**	52

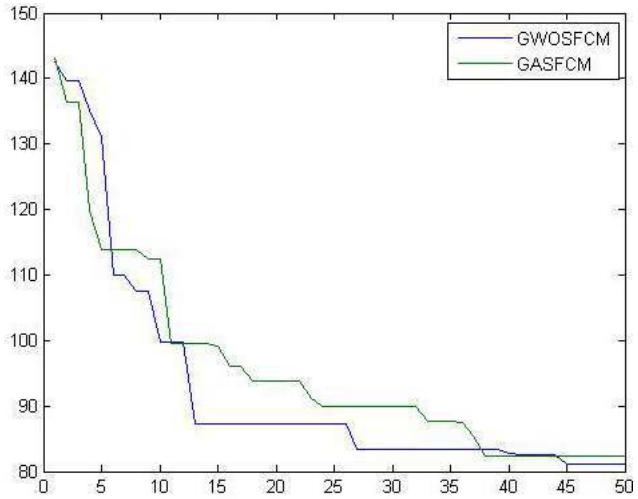

Fig. 4. Convergence of fitness function of GASFCM and GWOSFCM.

VI. CONCLUSION

The challenging problem of image segmentation is undertaken in this paper by considering segmentation as clustering problem. A recently proposed optimization algorithm i.e. grey wolf optimizer (GWO) is incorporated in the standard spatial FCM (SFCM). Experimental results on brain MRI images clearly show that GWO based SFCM has better segmentation results compared to SFCM and GASFCM. It can be concluded from this study that GWO is computationally fast and a very effective algorithm. Further the algorithm can be tested on other images and the performance in a corrupted image can also be considered for robustness.

REFERENCES

[1] Rafael C. Gonzalez, Richard E. Woods, "Digital Image Processing, Pearson Education", Second Edition, ISBN 81-7758-168-6, 2005.

[2] Bezdek, J. C., "Pattern Recognition with Fuzzy Objective Function Algorithms", Plenum, NY, 1981.

[3] Keh-Shih Chuang, Hong-Long Tzeng, Sharon Chen, Jay Wu, Tzong-Jer Chen, "Fuzzy c-means clustering with spatial information for image segmentation", Computerized Medical Imaging and Graphics, Volume 30, Issue 1, January 2006, pp. 9-15.

[4] Seyedali Mirjalili, Seyed Mohammad Mirjalili, Andrew Lewis, "Grey Wolf Optimizer", Advances in Engineering Software, Volume 69, March 2014, pp. 46-61

[5] C. Bezdek, L.O. Hall, L. P. Clarke, "Review of MR image segmentation techniques using pattern recognition", Med. Phys., vol. 20, No. 4, pp.1033-1048, 1993.

[6] Ivana Despotović, Bart Goossens, and Wilfried Philips, "MRI Segmentation of the Human Brain: Challenges, Methods, and Applications", Computational and Mathematical Methods in Medicine, 2015.

[7] Balafar M. A., "Fuzzy c -means based brain MRI segmentation algorithms", Artificial intelligence review, Springer Netherlands,2012.

[8] Bing Nan Li, Chee Kong Chui, Stephen Chang, S.H. Ong, "Integrating spatial fuzzy clustering with level set methods for automated medical image segmentation", Computers in Biology and Medicine, Volume 41, Issue 1, January 2011, pp. 1-10.

[9] Eman Abdel-Maksoud, Mohammed Elmogy, Rashid Al-Awadi, "Brain tumor segmentation based on a hybrid clustering technique", Egyptian Informatics Journal, Volume 16, Issue 1, March 2015, pp.71-81.

[10] Yingjie Wang, "Fuzzy Clustering Analysis Using Genetic Algorithm", and ICIC International @ 2008 ISSN 1881-803 X, pp: 331—337.

[11] Y. Gao, S. Wang and S. Liu. Automatic Clustering Based on GA-FCM for Pattern Recognition, "Computational Intelligence and Design", ISCID '09. Second International Symposium on, Changsha, 2009, pp. 146-149.

[12] A.Halder, S.Pramanik, A.Kar, "Dynamic Image Segmentation using Fuzzy C-Means based Genetic Algorithm", International Journal of Computer Applications (0975 – 88 87) Volume 28– No.6, August 2011, pp.: 15 – 20.

[13] Romesh Laishram, W.Kanan Kumar Singh, N.Ajit Kumar, Robindro.K, S.Jimriff, "MRI Brain Edge Detection Using GAFCM Segmentation and Canny Algorithm", International Journal of Advances in Electronics Engineering, Volume 2: Issue 3 ISSN 2278 - 215X, 2012.

[14] Laishram, R.; Kumar, W.K.; Gupta, A.; Prakash, K.V., "A Novel MRI Brain Edge Detection Using PSOFCM Segmentation and Canny Algorithm", IEEE International Conference on Electronic Systems, Signal Processing and Computing Technologies (ICESC), 2014, vol., no., pp.398-401.

[15] Kamalam Balasubramani, Dr. Karnan Marcus, "Artificial Bee Colony Algorithm to improve brain MR image segmentation", International Journal on Computer Science and Engineering (IJCSE), 2013.

[16] Thiyam Ibungomacha Singh, Romesh Laishram, Sudipta Roy, "Medical Image Segmentation Using Fuzzy C Means Clustering with Optimization using Artificial Bee Colony Algorithm", Advanced Research in Electrical and Electronic Engineering, p-ISSN: 2349-5804; e-ISSN: 2349-5812 Volume 2, Issue 12 July-September (2015) pp. 35-40.

[17] Bezdek JC., "Cluster validity with fuzzy sets", J. Cybern. 1974; 3:58-73.

[18] Bezdek JC., "Mathematical models for systematic and taxonomy", proceedings of 8th international conference on numerical taxonomy, San Francisco; 1975, pp. 143-66.

[19] Xie Xl, Beni GA., "Validity measure for fuzzy clustering", IEEE Trans on Pattern Anal. Mach. Intell. 1991;3:841-6.

Denoising of MRI Images Using Curvelet Transform

Ranjit Biswas, Debraj Purkayastha and Sudipta Roy

Abstract Most of the medical images are usually affected by different types of noises during acquisition, storage, and transmission. These images need to be free from noise for better diagnosis, decision, and results. Thus, denoising technique plays an important role in medical image analysis. This paper presents a method of noise removal for brain magnetic resonance imaging (MRI) image using curvelet transform thresholding technique combined with the Wiener filter and compares the result with the curvelet and wavelet-based denoising techniques. To assess the quality of denoised image, the values of peak signal-to-noise ratio (PSNR), mean square error (MSE), and structural similarity index measure (SSIM) are considered. The experimental results show that curvelet denoising method depicts better result than wavelet denoising method, but the combined method of curvelet with Wiener filtering technique is more effective than the wavelet- and curvelet-based denoising method in terms of PSNR, MSE, and SSIM.

Keywords Wiener filter · Wavelet transform · Curvelet transform · Denoising

1 Introduction

Medical images are having an important role for diagnosis of diseases. These images are obtained from various methods such as MRI, CT, and X-ray imaging. Nowadays, these images are captured using digitized systems. During the

R. Biswas (✉)
Department of Information Technology, Ramkrishna Mahavidyalaya, Kailashahar, Tripura 799277, India
e-mail: ranjit_tb@yahoo.co.in

D. Purkayastha · S. Roy
Department of Computer Science & Engineering, Assam University, Silchar 788011, India
e-mail: cyberdebraj@gmail.com

S. Roy
e-mail: sudipta.it@gmail.com

A. Konkani et al. (eds.), *Advances in Systems, Control and Automation*,
Lecture Notes in Electrical Engineering 442, https://doi.org/10.1007/978-981-10-4762-6_55

acquisition process, the images may be corrupted by different types of noise and it is very important to remove the noise to get better interpretation. Removal of noise from digital images is a big challenge for the researchers. Huang et al. [1] proposed a type of median filtering technique which is much faster and was implemented in 2D. Later, Ney [2] implemented a technique of dynamic programming for implementing nonlinear smoothing filters, which gives a good result in removing noise but keeps much more information around the curves by penalizing when there is large difference in two consecutive samples and rewarding when these are close. Saluja et al. [3] proposed an adaptive Wiener filter based on wavelet transform to calculate coefficients of weighted high-pass filtering. Boulfelfel et al. [4] investigated the usage of Wiener filter and PSE filter in CT images and developed a 3D filter that performs better than 2D filters.

The transform domain filtering contains wavelet transform, ridgelet transform, and curvelet transform. Lang et al. [5] used wavelet analysis of undecimated wavelet transform on unidimensional signals to remove noise which was one of the earlier implementations of wavelet in noise removal. To remove noise and to compress image, Chang et al. [6] used adaptive wavelet soft threshold using data-driven method called as Bayes Shrink method for threshold estimation. Mojsilovic et al. [7] classified the stages of liver disease using wavelet transform. One of the important thresholding techniques—Visu Shrink developed by Donoho et al. [8, 9] using wavelet shrinkage. Another technique called SURE (Stein's Unbiased Risk Estimator) shrink also developed by Donoho et al. [10], which is based on SURE estimator developed by Steinin [11]. Stein name it as Unbiased Risk Estimator. SURE estimator estimates mean of random normal variable which is independent. Zhang [12] proposed and implemented diffusion in image domain and also in wavelet domain.

Candes and Donoho [13] showed ridgelet transform of images. Based on ridgelets, curvelet transform came into existence. The disadvantage of wavelet denoising is that it does not perform well while denoising in the curves in an image and results in loss of details. Starck and Candes in [14] proposed a curvelet transform based on Candes's ridgelet technique. This technique can efficiently represent a curve because it has ability to select and identify curves along with time and frequency relations. This technique also uses wavelet shrinkage for thresholding. Ulfarsson et al. [15] removed speckle noise efficiently from SAR images using curvelet domain transform. Liu et al. [16] studied and analysed the curvelet based on ridgelet. Ali et al. [17] developed a method to fuse CT image and MR image, and the fusion is done in curvelet domain.

2 Denoising Techniques

There are two fundamental approaches to image denoising, viz. spatial domain filtering and transform domain filtering methods.

2.1 Wavelet Transform

Wavelet is very useful for nonlinear representation of signals. Wavelet basically decomposes the image into its time and frequency relation components. Thus, the image is transformed into frequencies rather than pixel. In the wavelet domain, the noisy image is decomposed into four subsamples according to their low (L) and high (H) frequency bands called LL, LH, HL, and HH. The LL subsample is again decomposed into four subsamples at level two [3] and so on as per the requirement of the computation.

2.2 Curvelet Transform

Stark and Candes [14] solved the problem of wavelet transform by proposing curvelet transform based on ridgelet transform. Ridgelet implementation was done by converting it into radon transform. In the ridgelet transform, support interval or the scaling is done by anisotropy scaling relationship, denoted by Eq. (1).

$$\text{width} = \text{length}^2 \tag{1}$$

This was done in the first generation of curvelet transform using multiscaling ridgelet where the curve is divided into blocks and the subblocks are approximated into a straight line and ridgelet analysis is done upon it. The basic curvelet decomposition steps are given as follows.

The subband decomposition is done by Eq. (2).

$$f \mapsto (P_0 f, \Delta_1 f, \Delta_2 f, \ldots) \tag{2}$$

where P_0 are subband filters, and $\Delta_s, s \geq 0$, and subbands $\Delta_s f$ contain details about 2^{-2s} wide. The smooth windows are $w_Q(x_1, x_2)$ which are localized in diadic squares and which is defined by Eq. (3).

$$Q = [k_1/2^s, (k_1+1)/2^s] \times [k_2/2^s, (k_2+1)/2^s] \tag{3}$$

Then, the resulting square is renormalized to unit scale, which is represented by Eq. (4).

$$g_Q = T_Q^{-1}(w_Q \Delta_S f), \quad Q \in Q_S \tag{4}$$

where $(T_Q f)(x_1, x_2) = 2^s f(2^s x_1 - k_1, 2^s x_2 - k_2)$ is a renormalization operator.

After the renormalization, the ridgelet transform is done by Eq. (5).

$$\alpha_{\mu} = \langle g_Q, p_{\lambda} \rangle \tag{5}$$

3 Thresholding Technique

Thresholding in transform domain is achieved by hard thresholding and soft thresholding to remove unwanted noise signals. Hard thresholding removes all the value after a certain limit, and soft thresholding lowers the intensity of noise towards zero values, which is defined by Eqs. (6) and (7).

$$y(t)_{\text{Hard}} = \begin{cases} x(t) & |x(t)| \geq T \\ 0 & |x(t)| < T \end{cases} \tag{6}$$

$$y(t)_{\text{Soft}} = \begin{cases} \text{sign}(x(t)) \cdot (|x(t)| - T) & |x(t)| \geq T \\ 0 & |x(t)| < T \end{cases} \tag{7}$$

where T is threshold value, and x and y are input and output coefficients in the respective transform domain.

The threshold value in wavelet domain is calculated by Donoho et al. [10], using Visu Shrink method. Visu Shrink is based on universal thresholding as explained in the following Eq. (8).

$$T_w = \sigma\sqrt{\log(N)} \tag{8}$$

where T is the threshold value, N is the size of image, and ∂ is the noise variance.

The threshold value in curvelet transform is calculated by value of 3*sigma and 4*sigma [18] used for the coarse-scale and fine-scale elements (9).

$$T_c = 3 * \text{sigma} + \text{sigma} * (s == \text{length}(C)) \tag{9}$$

where C is the size of decomposed images, and s = 2 to length of C.

4 Proposed Technique

A new technique is proposed here using curvelet transform thresholding technique combined with the Wiener filter. The curvelet transform helps to overcome the problem of wavelet transform, and noise is removed using it first, and then, the Wiener filter is used to remove the residual noise.

5 Parameter Estimations

To evaluate the performance of the techniques, we have considered the values of peak signal-to-noise ratio (PSNR), mean square error (MSE), and structural similarity index measure (SSIM), which are defined by Eqs. (10), (11), and (12).

$$\text{PSNR} = 10 \cdot \log_{10}\left(\frac{\text{MAX}_I^2}{\text{MSE}}\right) \tag{10}$$

$$\text{MSE} = \frac{1}{mn}\sum_{i=0}^{m-1}\sum_{j=0}^{n-1}[f(i,j) - g(i,j)]^2 \tag{11}$$

where mn is size of image, MAX_I is maximum probable pixel value of the image, $f(i, j)$ is the noisy image, and $g(i, j)$ is denoised image.

$$\text{SSIM}(x, y) = \frac{(2\mu_x\mu_y + C_1)(2\sigma_{xy} + C_2)}{(\mu_x^2 + \mu_y^2 + C_1)(\sigma_x^2 + \sigma_y^2 + C_2)} \tag{12}$$

where μ_x, μ_y are local means, σ_x, σ_y are standard deviations, and σ_{xy} is cross-covariance for images x, y.

6 Experimentation

In this work, the proposed technique along with other existing techniques is experimented on MRI images of brain. The experiments are performed using MATLAB on MRI images of size 256 × 256 following the wrapping technique on curvelet software package. White Gaussian noise is added in MRI images with different sigma, i.e., σ = 10, 20, 30, 40, 50, 60, 70. Then, the various types of denoising techniques were implemented, viz. Wiener filter, wavelet thresholding, curvelet thresholding, and curvelet thresholding, with Wiener filter.

7 Results and Discussion

After applying different denoising methods to noisy MRI brain image, results were compared visually and using quality metrics values of PSNR, MSE, and SSIM. The experimental results show that the proposed combined method of curvelet with Wiener filter-based image denoising is performed more effectively compared to other methods. Tables 1, 2 and 3 show the PSNR, MSE, and SSIM values obtained by each method for MRI brain image with different sigma, i.e., σ = 10, 20, 30, 40,

Table 1 Comparison of PSNR values for brain MRI image

Sigma σ	Wiener	Wavelet hard	Wavelet soft	Curvelet hard	Curvelet soft	Combined
10	31.452	29.198	28.154	30.351	28.153	42.179
20	26.611	23.952	23.529	24.336	23.011	43.364
30	23.708	20.875	20.686	20.932	20.050	44.630
40	23.708	18.743	18.660	18.608	17.978	45.943
50	19.849	17.064	17.037	16.829	16.400	47.543
60	18.456	15.729	15.718	15.462	15.133	48.500
70	17.297	14.590	14.583	14.318	14.057	50.421

Table 2 Comparison of MSE values for brain MRI image

Sigma σ	Wiener	Wavelet hard	Wavelet soft	Curvelet hard	Curvelet soft	Combined
10	46.550	78.219	99.460	59.973	99.496	3.937
20	141.890	261.756	288.531	239.570	325.069	2.997
30	276.860	531.575	555.183	524.607	642.812	2.239
40	276.860	868.621	885.359	895.977	1035.770	1.655
50	673.310	1278.371	1286.375	1349.516	1489.665	1.145
60	927.760	1738.323	1742.991	1848.875	1994.280	0.918
70	1211.600	2260.087	2263.393	2405.855	2554.956	0.590

Table 3 Comparison of SSIM values for brain MRI image

Sigma σ	Wiener	Wavelet hard	Wavelet soft	Curvelet hard	Curvelet soft	Combined
10	0.729	0.672	0.657	0.688	0.634	0.988
20	0.556	0.409	0.400	0.401	0.345	0.989
30	0.503	0.281	0.276	0.253	0.204	0.990
40	0.503	0.216	0.213	0.170	0.131	0.991
50	0.471	0.177	0.176	0.119	0.088	0.994
60	0.471	0.149	0.148	0.087	0.062	0.995
70	0.470	0.131	0.131	0.064	0.045	0.996

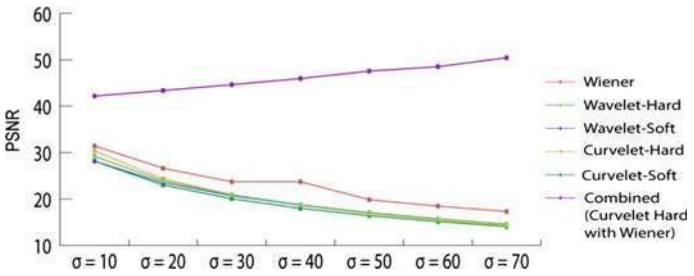

Fig. 1 PSNR values of MRI brain image

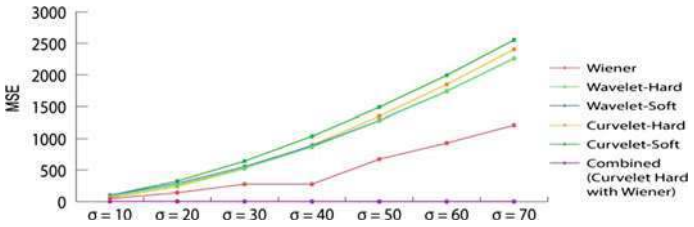

Fig. 2 MSE values of MRI brain image

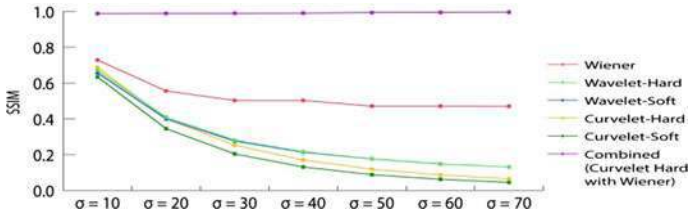

Fig. 3 SSIM values of MRI brain image

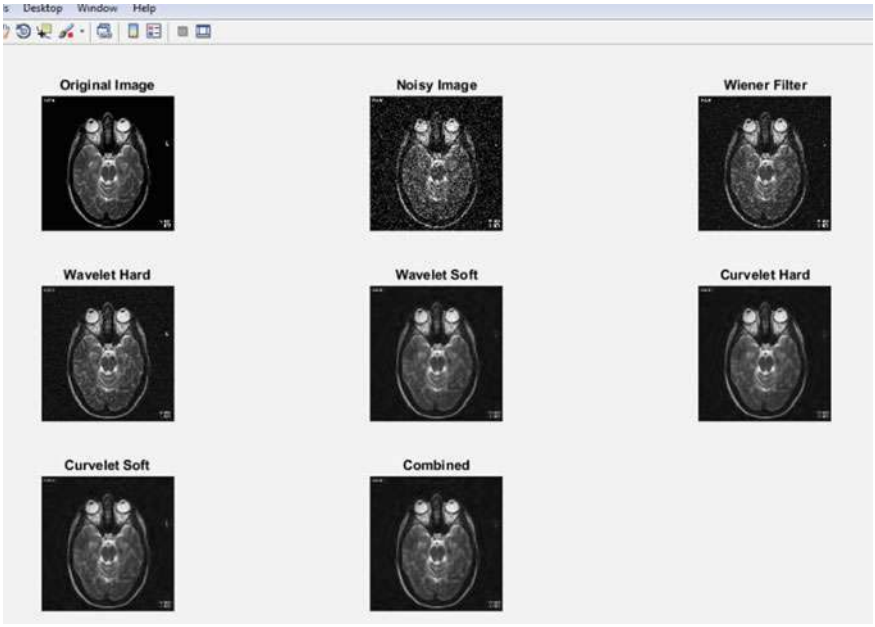

Fig. 4 Experimental results of MRI brain image denoising (where $\sigma = 40$)

50, 60, 70. The noise level of the image gradually comes down for the high PSNR value and the low MSE value. We have analysed that the combined method of curvelet with Weiner filter gives the higher PSNR and SSIM value and lower MSE value compared to other techniques. These are represented graphically in Figs. 1, 2, and 3, whereas in Fig. 4, the noisy image and resulting images of different methods corrupted by Gaussian noise with $\sigma = 40$ are shown. The visual quality of the image also becomes better in this combined curvelet with Wiener filter technique.

8 Conclusion

In this paper, we have studied wavelet, curvelet, and proposed filtering method and their effect in terms of the considered assessment parameters. The experimental results show that curvelet based approach performs better than the wavelet-based method. It also clearly indicates that curvelet with Wiener filter method outperforms compared to the other denoising methods, i.e., Wiener, wavelet, and curvelet. Also, the combined method does a very good job even when the noise is high as revealed from the experimental results. The curvelet denoising method removes the noise mostly lying in low frequency subbands, but some of the white Gaussian noise is spread in high frequency subbands also. So Weiner filter combined with curvelet transform is used here to remove that residual noise to some extent and the results were satisfactory.

References

1. Huang, T., Yang, G., Tang, G.: A fast two-dimensional median filtering algorithm. IEEE Trans. Acoust. Speech Signal Process. **27**(1), 13–18 (1979)
2. Ney, H.: A dynamic programming technique for nonlinear smoothing. In: IEEE International Conference on ICASSP, pp. 62–65 (1981)
3. Saluja, R., Boyat, A.: Wavelet based image denoising using weighted highpass filtering coefficients and adaptive wiener filter. In IEEE International Conference on Computer, Communication and Control (IC4-2015) (2015)
4. Boulfelfel, D., Rangayyan, R.M., Hahn, L.J., Kloiber, R.: Three dimensional restoration of single photon emission computed tomography images. IEEE Trans. Nucl. Sci. **41**(5), 1746–1754 (1994)
5. Lang, M., Guo, H., Odegard, J.E.: Noise reduction using an undecimated discrete wavelet transform. IEEE Signal Process. Lett. **3**, 10–12 (1995)
6. Chang, S.G., Yu, B., Vetterli, M.: Adaptive wavelet thresholding for image denoising and compression. IEEE Trans. Image Process **9**, 1532–1546 (2000)
7. Mojsilovic, A., Popovic, M., Sevic, D.: Classification of the ultrasound liver images with the 2nx1-d wavelet transform. In: Proceedings of IEEE International Conference Image Proceedings, vol. 1, pp. 367–370 (1996)
8. Donoho, D.L., Johnstone, I.M.: Ideal spatial adaptation via wavelet shrinkage. Biomefrika **81**, 425–455 (1994)
9. Donoho, D.L.: De-noising by soft thresholding. IEEE Trans. Inf. Theory **41**(3), 613–627 (1995)

10. Donoho, D.L., Johnstone, I.M.: Adapting to unknown smoothness via wavelet shrinkage. J. Am. Stat. Assoc. **90**, 1200–1224 (1995)
11. Stein, C.M.: Estimation of mean of a multivariate normal distribution. Ann. Stat. **9**, 1135–1151 (1981)
12. Zhang, X.: A denoising approach via wavelet domain diffusion and image domain diffusion. Multimedia Tools Appl. 1–17 (2016)
13. Candes, E.J., Donoho, D.L.: Ridgelets: a key to higher-dimensional intermittency? Phil. Trans. R. Soc. Lond. A **357**, 2495–2509 (1999)
14. Starck, J.L., Candes, E.J., Donoho, D.L.: The curvelet transform for image denoising. IEEE Trans. Image Process. **11**, 670–684 (2002)
15. Ulfarsson, M.O., Sveinsson, J.R., Benediktsson, J.A.: Speckle reduction of SAR images in the curvelet domain. In: Proceeding of the International Geoscience and Remote Sensing (IGARSS), vol. 1, pp. 315–317 (2002)
16. Liu, Y., Liu, Y.: Study on the basic principle and image denoising realization method of curvelet transform. In: International Conference on Multimedia Technology, pp. 1–4 (2010)
17. Ali, F.E., El-Dokany, I.M., Saad, A.A., El-Samie, F.E.A.: Fusion of MR and CT images using the curvelet transform. In: National Radio Science Conference, pp. 1–8 (2008). doi:10.1109/NRSC.2008.4542354
18. Candes, E.J., Demanet L., Donoho D.L., Ying, L. http://www.curvelet.org/